

2008201162

J.G.E.M. Fraaije

# INTERFACIAL THERMODYNAMICS AND ELECTROCHEMISTRY OF PROTEIN PARTITIONING IN TWO-PHASE SYSTEMS

Proefschrift  
ter verkrijging van de graad van  
doctor in de landbouwwetenschappen,  
op gezag van de rector magnificus,  
dr. C.C. Oosterlee,  
in het openbaar te verdedigen  
op dinsdag 6 oktober 1987  
des namiddags te vier uur in de aula  
van de Landbouwuniversiteit te Wageningen

1217246504

**BIBLIOTHEEK  
LANDBOUWUNIVERSITEIT  
WAGENINGEN**

**STELLINGEN****I**

Een fenomenologische analyse van de ion herverdeling bij de verdeling van eiwit over twee-fase systemen, waarbij de ene fase bestaat uit een waterige oplossing en de andere uit een oppervlak of een apolaire vloeistof, is mogelijk zonder dat men de moleculaire samenstelling van de tweede fase kent.

Dit proefschrift, hoofdstuk 3.

**II**

Discrete ladingseffecten bepalen in belangrijke mate de electrochemische wisselwerking tussen twee geaguleerde colloïdale deeltjes. Gemiddeld veld benaderingen zijn dan ontoereikend.

Dit proefschrift, hoofdstuk 4.

**III**

De elektrische capaciteit van een oppervlak, bedekt met een compacte geadsorbeerde eiwit laag, wordt in sterkere mate bepaald door het intrinsiek electrochemisch aanpassingsvermogen van de geadsorbeerde eiwitmoleculen dan door die elektrische afscherming.

Dit proefschrift, hoofdstuk 5

**IV**

De snelheid van eiwit adsorptie is, in tegenstelling tot de evenwichtsligging, niet eenduidig gerelateerd aan de stochiometrie van de ion co-adsorptie.

## V

Indien bij de overgang van een geadsorbeerde chromofoor van de grondtoestand naar een aangeslagen toestand slechts één overgangsmoment is betrokken, kan de oriëntatieverdeling van de chromofoor ten opzichte van de normaal van het oppervlak eenduidig worden bepaald met behulp van Totale Interne Reflectie Fluorescentie (1). Echter, zijn er bij de excitatie meerdere overgangsmomenten betrokken die onderling verschillen in richting, dan is dit alleen mogelijk als de snelheid van (foto)tautomerisatie veel groter is dan de vervalsnelheid van de aangeslagen toestand. Dit doet zich wellicht voor bij excitatie van geadsorbeerd vrije base porphyrine.

Is aan bovenstaande eis voor een samengestelde overgang niet voldaan, dan moet men zijn toevlucht nemen tot Totale Interne Reflectie Absorptie (2).

(1) N.L. Thompson, H.M. McConnel, T.P. Burghardt (1984) *Biophys. J.* 46, 739

(2) M. van der Graaf (1987), doctoraalverslag landbouwniversiteit, Wageningen

## VI

De randhoek van een druppel op een oppervlak met eindstandig verankerde polymeerketens verandert sterk bij de  $\Theta$ -temperatuur van het polymeer. Indien de ketens voldoende lang zijn, is dit een entropisch gedreven eerste orde overgang.

## VII

De verstoring van de perikinetische vlokking van kolloïdale deeltjes door de afschuifkrachten in een Single Particle Optical Sizer kan alleen worden vastgesteld als de gemeten deeltjesgrootteverdeling afhankelijk is van de stroomsnelheid in het instrument.

(1) H. Gedan, H. Lichtenfeld, H. Sonntag, H.-J. Krug (1984)

*Colloids Surfaces* 11, 199

(2) E. Pelssers (1988), proefschrift landbouwniversiteit, Wageningen

VIII

Het verschil tussen de eindwaarde van de oppervlaktespanning gemeten bij de adsorptie van (bio)polymeren aan het lucht-water grensvlak en de laagst mogelijke vrije oppervlakte energie kan worden toegeschreven aan het visko-elastisch gedrag van de geadsorbeerde laag (1,2).

(1) E. Keupink (1987), doctoraalverslag landbouwuniversiteit, Wageningen

(2) J.-W. Brouwer (1987), doctoraalverslag landbouwuniversiteit, Wageningen

IX

Zowel in de wetenschap als de kunst nemen de intensiteit en zeggingskracht van de gerealiseerde projecten toe indien de beoefenaars werken vanuit respect voor de traditie.

X

De geestelijke en lichamelijke gedrevenheid die ten grondslag ligt aan het scheppen van een kunstwerk is identiek aan de geestelijke en lichamelijke gedrevenheid die ten grondslag ligt aan het creëren van een wetenschappelijke probleemstelling.

Wetenschappelijk onderzoek wordt ondermijnd door een emotionele routinematige en gewisse beantwoording van problemen. Ik pleit dan ook voor een wetenschappelijke vorming die recht doet aan de zin voor het avontuur en het verlangen naar het onzekere.

Proefschrift J.G.E.M. Fraaije  
Interfacial Thermodynamics and Electrochemistry of  
Protein Partitioning in Two-Phase Systems  
Wageningen, 6 oktober 1987

**CONTENTS**

|   |    |
|---|----|
| <b>1. GENERAL INTRODUCTION</b>  | 1  |
| 1.1 OUTLINE OF THE THESIS   | 1  |
| 1.2 REFERENCES  | 3  |
| <b>2. CHEMICAL POTENTIAL OF PROTEIN IN SOLUTION</b>                           | 4  |
| 2.1 INTRODUCTION  | 4  |
| 2.2 DERIVATION OF A PHENOMENOLOGICAL EXPRESSION FOR THE<br>CHEMICAL POTENTIAL | 4  |
| 2.3 ESIN-MARKOV ANALYSIS  | 9  |
| 2.4 COMPARISON WITH THE POLYNOME METHOD                                       | 14 |
| 2.5 EXAMPLE: ANALYSIS OF BSA PROTON TITRATION CURVES                          | 16 |
| 2.6 REFERENCES  | 21 |
| <b>3. PROTEIN PARTITION AND ION CO-PARTITION IN TWO-PHASE SYSTEMS</b>         | 22 |
| 3.1 INTRODUCTION  | 22 |
| 3.2 SURFACE-LIQUID SYSTEMS  | 22 |
| 3.2.1 GIBBS CO-ADSORPTION EQUATION  | 22 |
| 3.2.2 EXAMPLE: AGI TITRATION OF ADSORBED BSA                                  | 28 |
| 3.2.3 EXAMPLE: CHROMATOGRAPHY OF BSA  | 30 |
| 3.2.4 EXAMPLE: ADSORPTION OF HPA ON POLYSTYRENE LATICES                       | 35 |
| 3.3 LIQUID-LIQUID SYSTEMS   | 36 |
| 3.3.1 GIBBS CO-PARTITION EQUATION   | 36 |
| 3.3.2 EXAMPLE: SOLUBILIZATION OF CYTOCHROME C                                 | 42 |
| 3.4 REFERENCES  | 47 |
| <b>4. CO-PARTITION MODEL</b>  | 48 |
| 4.1 INTRODUCTION  | 48 |
| 4.2 ELECTROCHEMISTRY OF FREE SURFACES   | 49 |
| 4.2.1 THE ELECTRICAL DOUBLE LAYER   | 49 |
| 4.2.2 CONSIDERATIONS ON THE EXCESS FREE ENTHALPY                              | 51 |
| 4.2.3 ION ADSORPTION ISOTHERMS  | 54 |
| 4.2.4 THERMODYNAMIC CONSISTENCY   | 55 |
| 4.3 ELECTROCHEMISTRY OF INTERACTING SURFACES                                  | 57 |
| 4.3.1 THE ELECTRICAL DOUBLE LAYER   | 57 |
| 4.3.2 THE EXCESS FREE ENTHALPY  | 59 |

|   |            |
|---|------------|
| 4.3.3 ION ADSORPTION ISOTHERMS                      | 60         |
| 4.3.4 THERMODYNAMIC CONSISTENCY                     | 60         |
| 4.4 NET FREE ENTHALPY OF INTERACTION                | 61         |
| 4.5 CALCULATIONS                                    | 62         |
| 4.5.1 DETAILS OF THE SITE BINDING MODEL             | 62         |
| 4.5.2 EXPLICIT EXPRESSIONS                          | 62         |
| 4.5.3 CALCULATION PROCEDURE                         | 66         |
| 4.5.4 RESULTS                                       | 66         |
| 4.6 REFERENCES                                      | 79         |
| <b>5. CHARGE REGULATION IN PROTEIN ADSORPTION</b>   | <b>80</b>  |
| 5.1 INTRODUCTION                                    | 80         |
| 5.1.1 GENERAL                                       | 80         |
| 5.1.2 PROPERTIES OF AGI                             | 80         |
| 5.1.3 PROPERTIES OF BOVINE SERUM ALBUMIN            | 82         |
| 5.2 EXPERIMENTAL                                    | 83         |
| 5.2.1 PREPARATION OF AGI AND BSA                    | 83         |
| 5.2.2 ADSORPTION ISOTHERMS AND EXCHANGE EXPERIMENTS | 84         |
| 5.2.3 TITRATION EXPERIMENTS                         | 85         |
| 5.3 RESULTS   | 89         |
| 5.3.1 ADSORPTION AND EXCHANGE EXPERIMENTS           | 89         |
| 5.3.2 TITRATION EXPERIMENTS                         | 95         |
| 5.4 DISCUSSION                                      | 106        |
| 5.4.1 THERMODYNAMIC ANALYSIS                        | 106        |
| 5.4.2 MODEL ANALYSIS                                | 112        |
| 5.5 REFERENCES                                      | 122        |
| <b>SUMMARY</b>                                      | <b>124</b> |
| <b>SAMENVATTING</b>                                 | <b>126</b> |
| <b>LEVENSLLOOP</b>                                  | <b>129</b> |
| <b>DANKWOORD</b>                                    | <b>130</b> |

## CHAPTER 1

## GENERAL INTRODUCTION

## 1.1 OUTLINE OF THE THESIS

Distribution of proteins between two phases is a frequent phenomenon in systems of both natural and man-made origin. In a living cell many enzymes reversibly attach to membranes, and the transcription and replication of the genetic code is dramatically linked to the dissociation of the complexes between the histone proteins and the polynucleic acids. In biotechnology, many purification methods are based on the preferential partition of protein between two liquid phases (1,2), between a surface and a liquid phase (3,4,5) or between a precipitate and a liquid phase (6,7). There are also cases where the accumulation of protein in one phase has an adverse effect. In the medical sciences, strong adsorption of (blood) proteins on artificial implants and medical equipment is considered a dangerous and expensive nuisance. Ways are sought to develop materials that neither adsorb proteins readily, nor become passivated by the preferential adsorption of some protein (8).

In the past decade, considerable insight has been gained in the physical principles underlying protein adsorption (9,10). Nevertheless, we know of only a few articles (11,12) in recent literature where a general thermodynamic theory of the protein partitioning process is presented. The lack of theoretical descriptions is perhaps due to the complexity of the systems under study, which commonly contain many interacting components. However, in this thesis we shall show that it is possible to derive generally applicable expressions without invoking serious approximations.

The central idea which we want to convey is the following. Whenever a protein molecule passes the boundary between two phases, the two phases will adjust their composition in order to maintain equilibrium, reflecting the different electrostatic and non-electrostatic interactions of the protein with its surroundings in the two phases. In other words, re-distribution of the protein is accompanied by a co-distribution of all kinds of molecules, including small ions. There must be a theory that can phenomenologically

interrelate these re- and co-distributions. Such a formalism can indeed be derived, through the Gibbs method for relating the excess Gibbs energy of the system to the amount of matter distributed and to the chemical potentials of the various substances present.

In chapters 2 and 3 we elaborate on the Gibbs excess formalism in a general way so that the outcome is applicable to a wide variety of systems. Some of the conclusions we reach can be intuitively understood, and are in fact already partly reported in literature (11). One of them is the notion that an increase of the salt concentration promotes the interaction between a protein and a second particle if, upon interaction, they take up salt. If salt is expelled, an increase of the salt concentration weakens the interaction. Similarly, if the extent of the interaction is maximal or minimal at a certain pH, then the proton exchange should be zero at this pH. Both examples are manifestations of Le Chatelier's principle for chemical equilibria. If a reaction product is withdrawn from a reaction vessel, the equilibrium shifts to the product side. On the other hand, the addition of a reaction product shifts the equilibrium to the substrate side. If a substance is neither produced nor consumed in the reaction, its addition will have no effect.

The phenomenological Gibbs analysis is completely general and independent of any molecular or mechanistic model. For the molecular interpretation of experimental results we do need such a model. A simple but effective one is presented in chapter 4.

Throughout the discussions in the theoretical chapters we will give examples to illustrate the method of analysis. The examples include proton titration curves, ion exchange chromatography, adsorption on colloidal particles and solubilization in reverse micelles. The necessary data are taken either from literature or the experimental chapter 5 of this thesis.

Chapter 5 contains a study of the charge regulation effects in protein adsorption. The experimental model system consists of particles of the insoluble salt silver iodide as the adsorbent and the protein Bovine Serum Albumin as the adsorbate. It allows for independent control of the charge of the precipitate and charge of the adsorbed protein. The results corroborate many of the theoretical predictions.

## 1.2 REFERENCES

1. M.R. Kula (1979) Appl. Biochem. Bioeng. 2,71
2. P.Albertson (1970) Advan. Protein Chem. 24,309
3. W. Kopaciewicz, F.E. Regnier (1983) Anal. Biochem. 133,251
4. J.Ungelstad, L. Söderberg, A. Berge, J. Bergström (1983) Nature 303,95
5. W. Kopaciewicz, M.A. Rounds, J. Fausnaugh, F.E. Regnier (1983) J. Chrom. 266,3
6. A.A. Green, W.L. Hughes (1955) Meth. Enzym. 1,67
7. M. Dixon, E.C. Webb (1961) Advan. Protein Chem. 16,197
8. J. N. Mulvihill, J-.P. Cazenave, A. Schmitt, P. Maisonneuve, C. Pusineri (1985) Colloids Surfaces 14, 317
9. W. Norde (1986) Advan. Colloid Interface Sci. 25,267
10. W. Norde, J.G.E.M. Fraaye, J. Lyklema (1987) ACS Symposium Series,accepted
11. M.T. Record Jr., C.F. Anderson, T.M. Lohman (1978) Quart. Rev. Biophys. 11(2),103
12. J. Wyman (1984) Quart. Rev. Biophys. 17(4),453

## CHAPTER 2

## CHEMICAL POTENTIAL OF PROTEIN IN SOLUTION

## 2.1 INTRODUCTION

A phenomenological description of the protein distribution between two phases requires an expression for the chemical potential  $\mu_p$  of protein in solution. The formula must describe how  $\mu_p$  depends on the number of small ligands (such as ions) bound by the protein and on the protein concentration. Several expressions already exist for the chemical potential of a protein. The more realistic ones are based on the binding polynome method (1-6), introduced by Wyman (2,3). The method presupposes site-bound ligands which are in direct contact with the protein. In addition to the ligand binding an activity coefficient of the protein is introduced, usually based on some extension of the Debye-Hückel theory. The approach is in principle incorrect because by doing so ions adsorbed in the diffuse part of the electrical double layer are not considered as being bound phenomenologically. Furthermore, the results are usually presented in the form of an integrated algebraic equation, and therefore the information contained in the differential dependence of  $\mu_p$  on the chemical potentials of the small ligands is lost.

## 2.2 DERIVATION OF A PHENOMENOLOGICAL EXPRESSION FOR THE CHEMICAL POTENTIAL

Before starting our alternative and more general approach, it is convenient to realize the following features.

First, like any electrolyte solution, solutions containing proteins and small ions are electroneutral. So are the protein molecules including their envelope of positively and negatively adsorbed ions. By consequence, it must be possible to formulate general phenomenological expressions in terms of chemical potentials of electroneutral species only.

Secondly, the binding of any component by the protein must be defined with respect to a reference. The zeroth principle of thermodynamics tells us that if two phases are each in equilibrium with a third phase they are also in

mutual equilibrium. We introduce as our reference R a solution with which the protein solution L is in membrane equilibrium but which contains no protein (see fig. 2.1). The total system R+L is fully characterised by the mole fractions  $x_i$  of all permeable components, the mole fraction of the protein  $x_p$ , the temperature T and the pressure P.

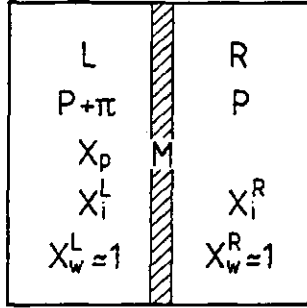


FIGURE 2.1. The protein solution L and the reference R connected by a dialysis membrane M which is permeable to all components except the protein. P is the pressure, T the temperature,  $\pi$  the osmotic pressure,  $x_i$ ,  $x_w$  and  $x_p$  are the mole fractions of component  $i$ , water and the protein respectively

In our analysis the partial volumina are independent of the protein concentration and the outer pressure (P) and temperature are constant. Furthermore the sum of the molar fractions of all components other than water is negligible compared to  $x_w$  ( $\approx 1$ ).

If we apply the Gibbs-Duhem relation to the protein solution we have at fixed P and T

$$x_p d\mu_p = - \sum x_i^{\circ L} d\mu_i^L \quad [1]$$

where  $\mu_i^L$  is the chemical potential of component  $i$  in the protein solution. The superscript  $\circ$  indicates that the protein is not counted in the sum. As we consider electroneutral components only, eq.[1] does not contain electrical terms and there is no need for an additional expression to account for electroneutrality. The electroneutral components  $i$  usually refer to

electroneutral combinations of charged ions.

In general, the chemical potential of any component is a function of the composition, the temperature and the pressure. Following Guggenheim (7) we write for the differential of the chemical potential of component  $i$

$$d\mu_i = -\bar{s}_i dT + \bar{v}_i dP + D\mu_i \quad [2]$$

where  $\bar{s}_i$  and  $\bar{v}_i$  are the partial molar entropy and partial molar volume of component  $i$  respectively.  $D\mu_i$  is the variation in the chemical potential of  $i$  at constant pressure and temperature. Per definition it is only dependent on the mole fractions of the components present

$$D\mu_i = \sum_j \left( \frac{\delta\mu_i}{\delta x_j} \right)_{P, T, x_{k \neq j}} dx_j \quad [3]$$

As in equilibrium the chemical potentials of all permeable components are the same everywhere, we have

$$D\mu_i^L + \bar{v}_i d\pi = D\mu_i^R \equiv D\mu_i \quad i \neq p \quad [4]$$

where  $\pi$  is the osmotic pressure ( $\pi \equiv P^L - P$ ). For the protein we have (from eqs. [1]-[4]),

$$x_p d\mu_p = - \sum_i^{\circ} x_i^L D\mu_i + \bar{v}_w d\pi \quad [5]$$

where  $\bar{v}_w$  is the partial molar volume of water.

The differentials of the chemical potentials in the reference vessel are related by a second Gibbs-Duhem relation, from which

$$D\mu_w = - \sum_i^{\circ} x_i^R D\mu_i \quad [6]$$

The dash at the summation sign means that water is not counted in the sum.

If we combine eqs. [5]-[6] we obtain the following expression for the chemical potential of the protein as a function of the composition of the reference solution and the osmotic pressure

$$d\mu_p = - \sum_i^{\circ} r_i D\mu_i + \frac{\bar{v}_w d\pi}{x_p} \quad [7]$$

where  $r_i$  is defined through

$$r_i = \frac{x_i^L - x_i^R}{x_p} = \frac{\Delta x_i}{x_p} \quad [8]$$

and may be interpreted as the number of molecules of component  $i$  bound by one protein molecule.

The ratio  $r_i$  is an important parameter. Imagine adding protein to the L solution while keeping the chemical potentials of all components other than water constant. This requires addition or withdrawal of the specified amounts of the various components other than water or the protein. Phenomenologically these amounts are interpreted as bound or repelled by the protein.

Upon the addition of the protein, the osmotic pressure will increase. Therefore the next step is to express the differential of the osmotic pressure in terms of the protein concentration and the chemical potentials of the other components. After having done so and with some rearrangement we find

$$d\mu_p = -f_i^{\text{O}'} \left[ r_i + \left( \frac{\delta r_i}{\delta \ln x_p} \right)_{P,T,x_i^R} \right] D\mu_i + fRT d \ln x_p \quad [9]$$

The factor  $f$  will be termed the valency factor and is defined by

$$f = \frac{\bar{v}_w}{RT} \left( \frac{\delta \pi}{\delta x_p} \right)_{P,T,x_i^R} \quad [10]$$

Before we continue the thermodynamic treatment we will digress a little on the valency factor. Suppose salt free protein is dissolved in water without the addition of salt. The base and acid groups of the protein molecules then partly dissociate and give rise to a protein valency of  $z_p$ . Under these circumstances the protons constitute the sole countercharges of the protein molecules. Phenomenologically they are still fully bound by the protein, but nevertheless they contribute to some extent to the osmotic pressure. The total mole fraction of osmotically active particles is therefore about  $(1+z_p)x_p$  and the valency factor equals about  $(1+z_p)$ . Now suppose protein is added to a concentrated electrolyte solution. In this case, the ions of the swamping electrolyte constitute the countercharges, the protons (together with negative ions from the salt) are free to diffuse to the reference vessel and consequently the total mole fraction of osmotically active particles is much smaller than it was before. If the electrolyte concentration is high enough, half of the (non-diffusible) charge of the protein is compensated by an excess

of (diffuse) counter-ions and the other half by a shortage of (diffuse) cations (8). The protein molecules then behave with respect to the osmotic pressure as if they were uncharged: the valency factor attains the value one.

Although the above considerations are fairly general, it is impossible to derive an explicit expression for the valency factor without the help of a mechanistic model. Therefore precise values cannot be given. From the Donnan theory (8) we derive the following approximate expression for a protein solution containing an (1-1) electrolyte

$$f = 1 + \frac{z_p^2 c_p}{\sqrt{(z_p^2 c_p^2 + 4c_s^2)}} \quad [11]$$

The valency factor  $f$  is plotted in fig.2.2 for various values of the valency  $z_p$  of the protein as a function of the ratio of half the protein concentration to the electrolyte concentration in the reference solution. In the derivation of formula [11] the assumptions are made that the electrolyte ions do not bind specifically to the protein (so  $z_p$  is to be understood as the net number of protons bound) and that the proton and hydroxyl ion concentration are negligible compared to  $c_s$ .

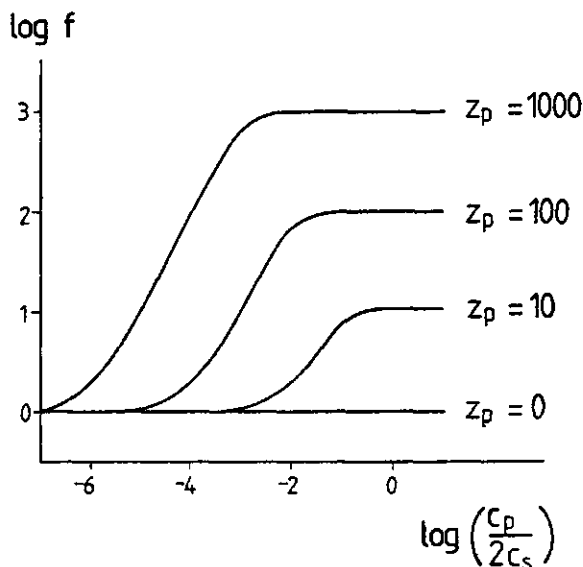


FIGURE 2.2. The valency factor  $f$  as function of the ratio of the protein concentration  $c_p$  (M) to salt concentration  $c_s$  (M) (1-1 electrolyte) for different valencies  $z_p$  of the protein.

In the above analysis we did not use a specific protein property, nor a typical property of macromolecules except for their ability of carrying a charge. So the expressions should apply equally well to, say, a solution of acetic acid in the absence of an electrolyte, as well as for, say, a solution of oligomethacrylic acid in the presence of an excess of an electrolyte. In the former example  $f=1+z_p=1+\alpha$  where  $\alpha$  is the degree of dissociation, and in the latter case  $f=1$ . The valency factor attains higher values for solutions of the larger polyelectrolytes (see fig 2.2). For instance, sodium polystyrene sulfonate with a M.W. of  $10^6$  and a concentration of  $1 \mu\text{M}$  in a  $0.1 \text{ M}$  ( $1-1$ ) electrolyte solution requires a valency factor of about 120 according to eq.[11].

It is highly questionable if the Donnan theory can be applied in the above form to solutions of the larger polyelectrolytes because many of the counterions form non-diffuse complexes with the charged groups of the polyelectrolyte. The non-diffusely bound electrolyte ions cannot contribute significantly to the osmotic pressure, but they reduce the diffuse charge of the polyelectrolyte and therefore the effective polyelectrolyte valency is smaller than  $z_p$ . In those cases, we would need very complicated models to make some estimate of  $f$ . Fortunately things are easier for proteins. By inspection of eq.[11] it follows that the valency factor for a typical protein in a typical protein solution (with  $z_p$  between  $-100$  and  $+100$ ,  $c_p = 1 \mu\text{M}$ ,  $c_s = 0.1 \text{ M}$ ) hardly exceeds unity. Therefore, we can safely neglect the Donnan effect and set  $f=1$ .

Furthermore, we will only analyse solutions dilute enough in protein to render protein-protein interactions negligible. As a consequence,  $r_i$  becomes independent of the protein concentration and hence the term containing  $(\delta r_i / \delta \ln x_p)$  in eq.[9] vanishes. The final equation for the differential of the chemical potential of a protein we use is, all things combined, the following

$$d\mu_p = -\sum_i^{\circ} r_i D\mu_i + RT d \ln x_p \quad [12]$$

### 2.3 ESIN-MARKOV ANALYSIS

The chemical potential of a protein is a function of state so that by cross-differentiation in the right hand side of the eq. [12] new relationships can

be derived. The same applies to combinations of chemical potentials, a useful one is defined through

$$d(\mu_p + r_1 \mu_1) = - \sum_{i>1}^{\infty} r_i D\mu_i + \mu_1 dr_1 + RT d \ln x_p \quad [13]$$

After cross-differentiation in eq.[13] we immediately obtain (also see table 2.1),

$$\left(\frac{\delta r_1}{\delta r_j}\right)_{P,T,x_p,\mu_{k \neq j}} = - \left(\frac{\delta \mu_1}{\delta \mu_j}\right)_{P,T,x_p,r_1,\mu_{k \neq 1,j}} \quad [14]$$

This equality is important because it allows calculation of the binding of component 1 (which may be difficult to measure directly), by relating it to the binding of component j (which may be easy to measure) provided the latter is known as a function of the chemical potentials 1 and j. An example of such a relation is that between the binding of salt and acid or base by proteins. The binding of acids and bases can be measured by proton titration, from which that of salt can be calculated from the salt strength dependence of the proton titration curve.

---

TABLE 2.1: Some useful Maxwell relations

---

$$\left(\frac{\delta r_i}{\delta \mu_j}\right)_{P,T,\mu_{k \neq j},x_p} = \left(\frac{\delta r_j}{\delta \mu_i}\right)_{P,T,\mu_{k \neq i},x_p} \quad [2.1.1]$$

$$\left(\frac{\delta r_i}{\delta r_j}\right)_{P,T,\mu_{k \neq j},x_p} = - \left(\frac{\delta \mu_i}{\delta \mu_j}\right)_{P,T,\mu_{k \neq i,j},r_j,x_p} \quad [2.1.2]$$


---

Equation [14] applies to electroneutral combinations of electrolytes and that is what is phenomenologically operational. However, for interpretational purposes it is possible to identify the various binding ratios as individual ionic contributions, as will now be illustrated by an example. Suppose a protein is titrated with the strong base MOH and the strong acid HX in the presence of excess salt MX, so that besides the protein there are  $\text{OH}^-$ ,  $\text{H}^+$ ,  $\text{M}^+$ , and  $\text{X}^-$  ions present in the system. First the differentials of the chemical potentials of the neutral components are expressed in terms of the measurable differentials of the pH and the salt activity  $a_s$

$$\mu_{\text{MOH}} + \mu_{\text{HX}} = \mu_{\text{MX}} + \mu_{\text{w}} \quad d\mu_{\text{w}} \approx 0 \quad [15]$$

$$D\mu_{\text{MX}} = 4.606 RT d\log a_s \quad D\mu_{\text{HX}} = 2.303 RT (d\log a_s - dpH)$$

The binding ratios of the individual ionic species are identified as

$$r_{\text{H}} \equiv r_{\text{HX}} - r_{\text{MOH}} \quad [16]$$

$$r_{\text{M}} \equiv r_{\text{MX}} + r_{\text{MOH}}$$

$$r_{\text{X}} \equiv r_{\text{MX}} + r_{\text{HX}}$$

Note that we cannot discriminate between proton binding and hydroxyl release or conversely. For example, a release of a proton by an acid residue is phenomenologically undistinguishable from an association of an hydroxyl ion with the same residue. Therefore, where we write  $r_{\text{H}}$  this must, in principle, be read as  $(r_{\text{H}} - r_{\text{OH}})$ .

Finally [15] and [16] are combined with [14] to give the desired differential

$$\left(\frac{\delta r_{\text{M}}}{\delta r_{\text{H}}}\right)_{\text{P,T,a}_s,\text{x}_p} = \frac{1}{2}(\beta-1) \quad [17]$$

$$\beta = \left(-\frac{\delta pH}{\delta \log a_s}\right)_{\text{P,T},r_{\text{H}},\text{x}_p} = \left(\frac{\delta r_{\text{M}} + \delta r_{\text{X}}}{\delta r_{\text{H}}}\right)_{\text{P,T,a}_s,\text{x}_p}$$

where  $\beta$  is a so called Esin-Markov coefficient (10), its value is fairly easy to calculate from the salt strength dependence of a protein titration curve.

After integration of [17] we obtain

$$r_{\text{M}}^{\text{II}} = r_{\text{M}}^{\text{I}} + \int^{\text{II}} \frac{1}{2}(\beta-1) dr_{\text{H}} \quad [18]$$

As we see, non-thermodynamic model assumptions have to be made about the value of the integration constant  $r_{\text{M}}^{\text{I}}$ .

In connection with eq.[17], the following remarks can be made regarding the compensation of the protein charge by positive adsorption of counter-ions versus negative adsorption of co-ions. Some of the ions will bind directly to

the protein itself, especially the protons, but many ions of the supporting electrolyte will bind in the diffuse part of the electrical double layer. If we denote the ions bound in the diffuse and non-diffuse parts of the electrical double layer by the superfices  $d$  and  $nd$  respectively, we can write

$$r_H = r_H^d + r_H^{nd} \approx r_H^{nd} \quad [19]$$

$$r_M = r_M^d + r_M^{nd}$$

$$r_X = r_X^d + r_X^{nd}$$

The  $r_i^d$ 's ( $i = M, X$ ) are related to the potentials in the diffuse part of the electrical double layer by the integrals

$$r_M^d = c_s \int_V (\exp(-F\psi/RT) - 1) dv \quad [20]$$

$$r_X^d = c_s \int_V (\exp(F\psi/RT) - 1) dv$$

where the integration should be carried out over the volume ( $V$ ) around a free, isolated protein molecule. Now, if the diffuse layer potential of a protein is lower than about 30 mV, we may use the Debye-Hückel approximation ( $\exp(\pm F\psi/RT) = 1 \pm F\psi/RT$ ) in the calculation of the integrals, and we find

$$r_M^d \approx - c_s \int_V F\psi/RT dv \approx - r_X^d \quad [21]$$

Hence, in this limit compensation of the non-diffuse charge by the binding of the diffuse counter-ions is equal to that due to the expulsion of the diffuse co-ions. Note that this is true whatever the shape or conformation of the protein.

The zeta-potential of a protein (determined in an electrophoresis experiment) is a good measure of its diffuse double layer potential. Zeta-potentials of proteins are often lower than 30 mV in a wide pH range. For example, the zeta-potential of Human Plasma Albumin varies from 5.5 mV at pH 4 to -27.4 mV at pH 8, that of Ribonuclease varies between 21.0 mV at pH 4 to -19.8 mV at pH 11 (measurements in 0.05 M Veronal-Acetate-KNO<sub>3</sub> buffer, see ref. 18). The low values of the zeta-potentials are probably due to the small radii of proteins (typically less than a few nanometer). The concomitant rapid

decay of the potential profile has two closely related consequences. First, the electrical capacitance of a surface increases with increasing curvature of the surface, because of this, the diffuse potential of a (very) small colloidal particle is lower than that of a (very) large particle if they have the same surface charge. Secondly, the Debye-Hückel approximation becomes better if the potential profile falls off more rapidly with distance. Both effects will diminish the difference in the contributions of the diffuse co- and counter-ions to the compensation of the surface charge. As a consequence, the Esin-Markov coefficients of proteins must be relatively small, at least smaller than the Esin-Markov coefficients of many bigger colloids. Therefore we expect a proton titration curve of a protein to be less dependent on the salt strength, and if this is not true for a part of the curve, then in that region the diffuse layer potential is higher than 30 mV ( $r_M^d \neq -r_X^d$ ) and/or there is a specific interaction between the ions of the supporting electrolyte and the protein ( $r_M^{nd} \neq 0$  and/or  $r_X^{nd} \neq 0$ ). Many of the published titration curves confirm our expectation (9).

Although the above Esin-Markov analysis to study the coupled binding of salt and acid or base resembles the analysis by Lyklema of titration curves of insoluble metal-oxide sols and AgI precipitates (10,11), it has remained unnoticed in the Biophysical and Biochemical literature, and as far as we know up to date no titration curves of proteins have been studied along these lines.

An Esin-Markov type of analysis might be well applicable for all kind of ligands, not necessarily inorganic ions. Of course, the analysis will only be fruitful if the bound ligands in some way or the other shift the acid/base equilibria, such that the differential  $(\delta r_L / \delta r_H)_{\mu_i \neq L}$  (where L denotes the ligand) is not zero. Possible mechanisms for such an interaction are: (i) ion exchange, (ii) a change in the electrical capacitance and/or (iii) an alteration of dipole orientations in and around the protein body. Charged polar ligands will predominantly interact via (i), uncharged apolar ligands via (ii) and (iii).

Many experimental techniques that are now in use for the direct determination of the binding of some substance other than acid or base suffer from lack of sensitivity (for example if ion selective electrodes are employed), or, especially when spectroscopic technique are applied, require a detailed model of the interaction of a (spectroscopic active) probe with its surroundings. In contrast, proton titration curves can be measured with great

precision and may be interpreted unambiguously with thermodynamics.

#### 2.4. COMPARISON WITH THE POLYNOME METHOD

As mentioned in the introduction, another approach would be to start from the definition of  $\mu_p$  based on the polynome method introduced by Wyman (2,3). Especially Schellman (5) has reviewed this approach critically. We will use his results (and his notation) to demonstrate the shortcomings of the polynome method by way of an illustrative example. In fact, the following is a slight modification of the first example given by Schellman in his article (5).

Consider a protein P with N identical base sites, so that there are N+1 possible species  $PH_n$  ( $n=0, \dots, N$ ), in abbreviated notation denoted by  $P_i$ .  $P_0$  stands for the species to which no protons are bound,  $P_N$  is fully saturated with protons. The concentration of each species (denoted by brackets) is governed by an equilibrium expression of the form

$$\langle P_n \rangle = \langle P_0 \rangle K_n a_H^n \quad (n = 1, \dots, N) \quad [22]$$

where  $a_H$  is the activity of the proton and  $K_n$  the nth "phenomenological association constant". The chemical potentials of the various species are then given by

$$\mu_n = \mu_n^0 + RT \ln \langle P_n \rangle \quad (i = 0, \dots, N) \quad [23]$$

$$\mu_H = \mu_H^0 + RT \ln a_H$$

The total concentration of protein (P) is related to the concentration of the uncharged protein ( $P_0$ ) by a polynome

$$\langle P \rangle = \sum_0^N \langle P_n \rangle = \langle P_0 \rangle B \quad [24]$$

$$B \equiv \sum_0^N K_n a_H^n$$

where B is defined as the "binding polynomial" (in the article of Schellman B is denoted as  $\Sigma$ ). The fraction of the macromolecules in a given state of

binding ( $f_n$ ) is given by

$$f_n = \frac{(P_n)}{(P)} = \frac{K_n a_H^n}{B} \quad [25]$$

For the sake of simplicity, suppose that the system contains one mole of protein. Prior to the interaction reaction, (P) equals  $(P_0)$  and the free enthalpy is then written as

$$G_I = \mu_0^0 + RT \ln(P) + n_b (\mu_H^0 + RT \ln a_H) + G_{\text{other}} \quad [26]$$

where  $n_b$  is the number of moles of protons which will bind at equilibrium ( $n_b = \sum_0^N n f_n$ ).  $G_{\text{other}}$  is the free enthalpy of those components which do not react with the protein (e.g. excess ligand, solvent). After the interaction, the free enthalpy will be given by

$$\begin{aligned} G_{II} &= f_0 [\mu_0^0 + RT \ln(P_0)] + \sum_1^N f_n [\mu_n^0 + RT \ln(P_n)] + G_{\text{other}} \quad [27] \\ &= \mu_0^0 + RT \ln(P_0) + \sum_1^N f_n [\mu_n^0 + RT \ln(P_n) - \mu_0^0 - RT \ln(P_0)] + G_{\text{other}} \end{aligned}$$

Subtracting eq.[27] from [26], and after some rewriting (taking into account the equilibrium relations [22]), we obtain for the chemical potential of the protein

$$\mu_p = \mu_0^0 + RT \ln(P) + G_{II} - G_I = \mu_0^0 + RT \ln(P) - RT \ln B \quad [28]$$

Now, how does this formula compare to ours? Let us first differentiate eq.[28] with respect to the chemical potential of the protons (in this case, we must consider individual ion chemical potentials). We find

$$\left( \frac{\delta \mu_p}{\delta \mu_H} \right)_{a_s} = - \left( \frac{\delta \ln B}{\delta \ln a_H} \right)_{a_s} = - \frac{\sum_1^N n K_n a_H^n}{B} = - \bar{n} = - n_b \quad [29]$$

So, the differential quotient is equal to the mean number of protons bound per molecule, a result which is similar to ours. Next we would like to take the derivatives with respect to the electrolyte concentration. Here we encounter a problem. It is easy to see that the differential of B with respect to the salt concentration is zero if we assume that the phenomenological association

constants are independent of the salt concentration. Clearly, in order to obtain a result which is comparable to ours, we must introduce activity coefficients for the macromolecular species (reflecting the charge-charge interactions on the protein surface), and they must be incorporated in the  $K_n$ .

In the above example, where we have excluded specific interactions of electrolyte ions with the base groups, the derivative of  $\mu_p$  with respect to the salt concentration should have yielded the sum of the diffusely bound anions and cations. In our opinion it would be very involved, and require a detailed model of the shape and conformation of the protein, to improve the parameters  $K_n$  in such a way that this result would also have been obtained with the polynome method. We conclude that even if the polynome method is proven to be consistent with thermodynamics for some cases, it can never be as generally applicable as the reference method we have introduced.

The above comment does not mean that a model analysis based on site-binding should always be hampered with inconsistencies. In chapter 4, where we introduce a model for the co-partition of ions based on a combination of a site-binding and a electrical double layer model, we will show that, if proper care is taken of the various types of binding, results are obtained which are consistent with thermodynamics.

## 2.5 EXAMPLE: ANALYSIS OF BSA PROTON TITRATION CURVES

As a concrete experimental example which serves to demonstrate the range of our thermodynamic method we re-analyse proton titration curves of Bovine Serum Albumine (BSA) obtained more than thirty years ago by Tanford et.al.(12,13). They titrated BSA with HCl and KOH in solutions of various KCl concentrations. Two of their curves ( $c_s$  0.03 and 0.15 M KCl) are plotted in fig.2.3. In order to fix the vertical positions of the titration curves we assumed the proton binding to be zero at the isoionic point ( $pH_{iip} = 5.6$ ) for both concentrations.

The binding ratios are calculated for a mean titration curve defined as the curve for the (logarithmic) mean salt concentration 0.07 M. The  $\bar{pH}$  of the mean curve is obtained from

$$\bar{pH} = \frac{1}{2} [pH(c_s = 0.03) + pH(c_s = 0.15)]_{r_h} \quad [30]$$

The Esin-Markov coefficients of the mean curve (fig. 2.3 insert) are

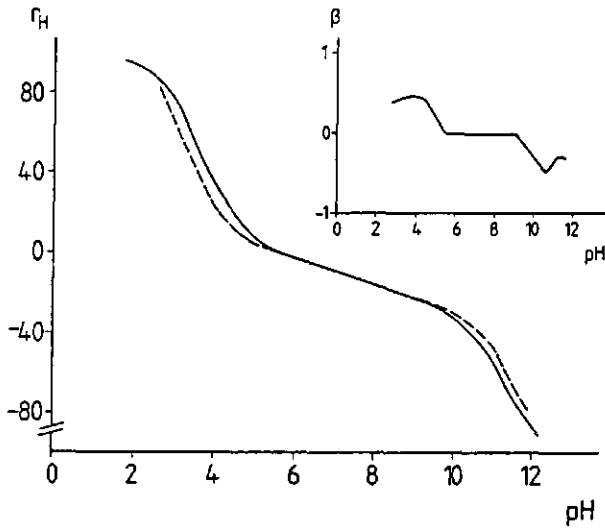


FIGURE 2.3. Proton binding characteristics of Bovine Serum Albumin. Data taken from Tanford et al. (12). Titration curves for  $c_{KCl}$  0.03 M (dotted curve) and 0.15 M (drawn curve). Insert: Esin-Markov coefficients for the mean titration curve in 0.07 M KCl.

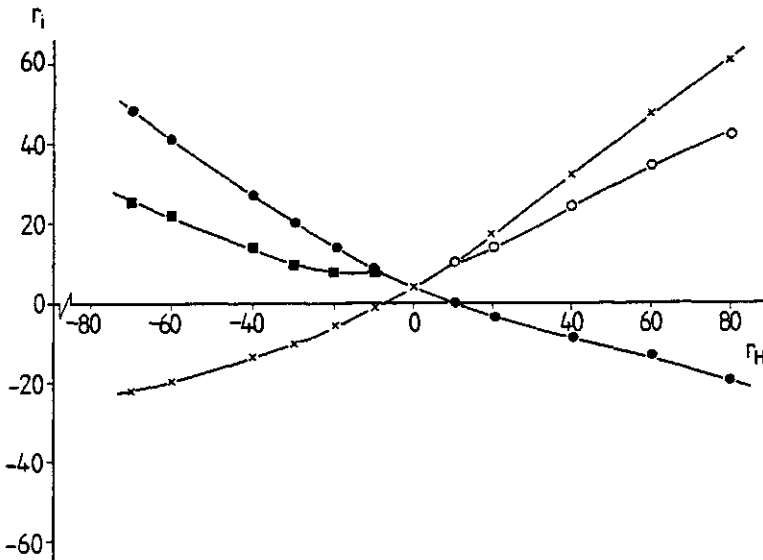


FIGURE 2.4. Binding of potassium and chloride ions to Bovine Serum Albumin according to the Esin-Markov analysis.  $c_{KCl} = 0.07$  M. Points calculated from fig. 2.3 using eqs. [32]-[35]

$r_K$  ( $\bullet$ );  $r_K^{nd}$  ( $\blacksquare$ );  $r_{Cl}$  ( $\times$ );  $r_{Cl}^{nd}$  ( $\circ$ ).

calculated with

$$\beta(\bar{pH}) = 1.59 [\text{pH}(c_s = 0.15) - \text{pH}(c_s = 0.03)] r_h \quad [31]$$

The factor 1.59 arises from the difference in the electrolyte activities of the two curves. In order to calculate the binding ratios of both the K and Cl ions absolutely we have to make a model assumption. As the isoelectric point of the protein ( $\text{pH}_{iep} = 4.7$ ) is somewhat lower than the isoionic point it seems reasonable to neglect the specific interactions of the potassium ions with the protein below pH 5. The binding ratio of the potassium ions is then calculated with

$$r_K(\bar{pH}) = \frac{r_H(\bar{pH})}{r_H(\bar{pH}=4.7)} \int_{r_H(\bar{pH}=4.7)}^{r_H(\bar{pH})} \frac{1}{2}(\beta-1) dr_H \quad [32]$$

and the binding ratio of the chloride ions is obtained from

$$r_{Cl} = r_H + r_K \quad [33]$$

If we assume furthermore that the Deby-Hückel approximation for the diffuse part of the electrical double layer holds over the entire pH range and that the specific binding of the chloride ions can be neglected in the alkaline region above pH 7, the binding ratios of the diffusely and non-diffusely bound ions can also be estimated from,

below pH 5,

$$r_K^{nd} = 0 \quad [34]$$

$$r_{Cl}^d = -r_K^d = -r_K$$

$$r_{Cl}^{nd} = r_H + 2 r_K$$

and above pH 7,

$$r_{Cl}^{nd} = 0 \quad [35]$$

$$r_K^d = -r_{Cl}^d = -r_{Cl}$$

$$r_K^{nd} \approx -r_H + 2 r_{Cl}$$

The calculated binding ratios are plotted in fig.2.4. Although we will not discuss the results in detail we note the strong specific interaction of both the chloride and potassium ions with the protein. In their original (mechanistic) analysis of these same titration curves, Tanford et.al. used chloride ion binding data obtained by Scatchard et al. (14) in order to calculate the net charge of the protein as a function of pH. However, according to our thermodynamic analysis the titration curves contained (almost) all the necessary information to do so.

A comparison of the results of our analysis with data on chloride and potassium (or sodium) ion binding by albumin obtained by direct determination is not easy because most of the literature on this subject is rather old and defective. In the course of time techniques and the preparation of materials have changed considerably. As early as 1953 Carr (15) determined the binding of chloride ions to BSA in a NaCl solution of approximately 0.1 M by using equilibrium dialysis and a conductance method. Some "binding numbers" he found are (they are calculated by us from one of his figures):  $\sim 60$  (pH 3),  $\sim 33$  (pH 4) and  $\sim 16$  (pH 5). If we interpret these numbers as (phenomenological) binding ratios we find that our results ( $r_{Cl} = \sim 54$  (pH 3),  $\sim 25$  (pH 4),  $\sim 8$  (pH 5)) are in fair agreement with those of Carr. Carr himself, as well as all the other authors who have written on this subject, did not realize that many of the ions bind in the diffuse part of the double layer while only a portion is directly associated with the protein. In a following experiment Carr (16) used ion selective membranes to determine the binding ratios of potassium ions. In a 0.03 M KCl solution at pH 10.8 his results seem to indicate that about 7 potassium ions bind to one BSA molecule. The binding ratio  $r_K$  we determined at pH 10.8 is  $\sim 30$ , which is higher than the number of Carr by a factor of about 4. Perhaps the discrepancy is due to the low accuracy of the ion selective electrode technique Carr used. Scatchard et al. (14) determined the binding of chloride and sodium ions to isoionic BSA ( $r_H=0$ ) by using ion selective electrodes. At 0.071 M NaCl they found that about 7 chloride ions bind to BSA and also that the binding of sodium ions is negligible. Our results are at  $r_H=0$ :  $r_{Cl} = r_K = 4$ . The results of Scatchard et al. are in our opinion inconsistent. If  $r_H$  remains zero (as was the case in their experiments), the binding ratios of the sodium and chloride ions must be the same in order to maintain electroneutrality. More recently, Hall et al. (17)

studied the binding of  $^{35}\text{Cl}$  ions to Human Plasma Albumin by employing a "nuclear magnetic quadrupole relaxation enhancement" technique. Although their results did not enable them to calculate the exact number of chloride ions associated with the protein, they conclude from rather indirect evidence that at neutral pH approximately 7 bound chloride ions provide eighty percent of the observed excess relaxation rate.

## 2.6 REFERENCES

1. M.T. Record Jr., C.F. Anderson. T.M. Lohman (1978)  
Quart. Rev. Biophys. 11(2), 101
2. J. Wyman (1964) Advan. Protein Chem. 19, 223
3. J. Wyman (1984) Quart. Rev. Biophys. 17(4), 453
4. G. Weber (1975) Advan. Protein Chem. 17, 69
5. J. Scheilman (1975) Biopolymers 14, 999
6. C. Tanford (1969) J. Mol. Biol. 39, 539
7. E. A. Guggenheim (1950) "Thermodynamics, an advanced treatment for chemists and physics", North-Holland Publishing Company, Amsterdam
8. J.Th.G. Overbeek (1956) Progr. Biophys. Biophysic. Chem. 6, 57
9. J. Steinhardt, S. Beychock (1964) in "The Proteins,II" , ch. 8  
ed. H. Neurath, Academic Press, New York, London
10. J. Lyklema (1972) J. Electroanal. Chem. Interf. Electrochem. 37, 53
11. B.H. Bijsterbosch, J. Lyklema (1978) Advan. Colloid Interface Sci. 9, 147
12. C. Tanford, S. A. Swanson, W.S. Shore (1955) J. Am. Chem. Soc. 77, 6421
13. C. Tanford (1962) Advan. Prot. Chem. 17, 69
14. G. Scatchard, I.H. Scheinberg, S. H. Armstrong Jr. (1950)  
J. Am. Chem. Soc. 72, 535
15. C. W. Carr (1953) Arch. Biochem. Biophys. 46, 417, 424
16. C. W. Carr (1956) Arch. Biochem. Biophys. 62, 476
17. B. Hall, B. Lindman (1978) Biochem. 17(8), 3775
18. W. Norde, J. Lyklema (1978) J. Colloid Interface Sci. 66, 277

## CHAPTER 3

## PROTEIN PARTITION AND ION CO-PARTITION IN TWO-PHASE SYSTEMS

## 3.1 INTRODUCTION

In this chapter we elaborate on phenomenological relations between the extent of the protein partition and the concomitant ion co-partition in two-phase systems. As in the previous chapter, we use the Gibbs excess formalism to derive the sought expressions.

We discuss the closely related surface-liquid and liquid-liquid systems. Examples of the former can be found in the adsorption of proteins from solution on a flat impenetrable surface, the attachment of proteins to nucleic acids or to membranes. Examples of the latter can be found in the partition of proteins between a water phase and an apolar oil phase either or not containing reverse micelles or between the two phases of a phase-separated (synthetic) polymer solution.

## 3.2 SURFACE-LIQUID SYSTEMS

## 3.2.1 GIBBS CO-ADSORPTION EQUATION

The thermodynamic analysis of the surface-liquid systems proceeds from the Gibbs adsorption equation. The Gibbs equation relates the surface tension  $\gamma$  to the chemical potentials and adsorbed amounts. As we are especially interested in the relations between the co-adsorptions of the small ions and the adsorption of the protein itself, we will again use the reference vessel of chapter 2. The membrane now extends through both phases, see fig.3.1.

The adsorption of protein leads to a difference in the adsorption of the small components on the L surface (the surface in the protein solution) with respect to the adsorption of the same small components on the R surface. In other words, there is a co-adsorption of the small components. The co-adsorption may be negative (less adsorption on the L surface than on the R surface) or positive (more adsorption on the L surface than on the R surface).

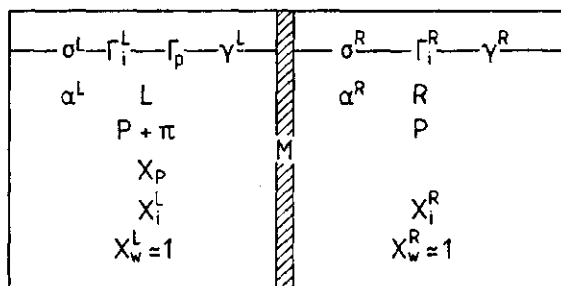


FIGURE 3.1. The surface-liquid system with the dialysis membrane  $M$  extending through the bulk  $\alpha$  and surface  $\sigma$  phases of the protein solution  $L$  and the reference solution  $R$ .  $P$  is the pressure,  $T$  the temperature (both constant in our analysis).  $x_i$ ,  $x_w$  and  $x_p$  are the mole fractions of all the permeable components, water and protein respectively.  $\gamma$  is the surface tension.

A more precise definition of co-adsorption is the following. Imagine adding protein to a solution, containing a surface, while keeping the chemical potentials of the components other than water constant. This requires addition or withdrawal of those components. The ensuing change in the adsorption of a certain component  $i$  on the  $L$  surface (the adsorption on the  $R$  surface is constant), divided by the adsorption of the protein, is defined as the binding ratio of that component in the surface phase ( $r_i^\sigma$ ). The co-adsorption ratio  $\Delta r_i$  is then defined as the difference between the binding ratio in the surface phase and the binding ratio in the liquid phase  $r_i^\alpha$ ,

$$r_i^\sigma \equiv \frac{\Gamma_i^L - \Gamma_i^R}{\Gamma_p} = \frac{\Delta \Gamma_i}{\Gamma_p} \quad [1]$$

$$\Delta r_i \equiv r_i^\sigma - r_i^\alpha$$

We assume, as in chapter 2, that the molar fraction of water is approximately unity. At constant pressure and temperature the Gibbs adsorption equations for the protein solution and the reference solution are then given by (1),

$$d\gamma^L = - \sum \Gamma_i^L D\mu_i - \Gamma_p d\mu_p \quad [2]$$

$$d\gamma^R = - \sum \Gamma_i^R D\mu_i$$

where  $\gamma^L$  and  $\gamma^R$  are the surface tensions of the protein and reference solution respectively. A convenient expression which relates the co-adsorption ratios to the adsorption of the protein is obtained by subtracting  $d\gamma^R$  from  $d\gamma^L$ , using the relation for the chemical potential of the protein we have derived in the previous chapter (eq.[12], chapter 2). We obtain

$$d(\gamma^L - \gamma^R) = -\Gamma_p \left[ \sum_i^{0'} \Delta r_i D\mu_i + RT d \ln x_p \right] \quad [3]$$

Given the restrictions of constant pressure, temperature and a low protein concentration (such that the valency factor is unity and protein-protein interactions in the solution can be neglected, see section 2.2) this Gibbs "co-adsorption equation" is fairly general. It describes the entire adsorption isotherm, whether the adsorbed amount is low, as in the linear initial part of the isotherm, or high as in the plateau.

Because  $\gamma^R$  and  $\gamma^L$  are both functions of state, their difference must also be a function of state. Therefore Maxwell relations between the variables of eq.[3] can be deduced from transformations and cross-differentiations. It somewhat depends on the actual system under study which relations are useful and which are not. Some generally important relations are listed in table 3.1

In the limiting case of adsorbed protein molecules interacting only with the surface and not with each other, some simple equations can be derived. The protein adsorption is then, by definition, linearly dependent on the protein concentration, the ratio of adsorbed amount to concentration being defined (apart from a constant) as the Henry constant H,

$$H = \lim_{\frac{x_p}{x_p} \rightarrow 0} \left( \frac{\Gamma_p A \bar{v}_w}{x_p V} \right) \quad [4]$$

where A and V are the total surface and total volume of the protein solution respectively. The dependence of the Henry constant on the chemical potentials of the small molecules can be derived from eq.[3] with the result

$$RT d \ln H = \sum_i^{0'} \Delta r_i^\ddagger D\mu_i \equiv -d\Delta G_{ads}^\ddagger \quad [5]$$

$$\Delta r_i^\ddagger = \lim_{\frac{x_p}{x_p} \rightarrow 0} \Delta r_i = RT \left( \frac{\delta \ln H}{\delta \mu_i} \right)_{T, \mu_{j \neq i}} = - \left( \frac{\delta \Delta G_{ads}^\ddagger}{\delta \mu_i} \right)_{T, \mu_{j \neq i}}$$

where  $\Delta r_i^\ddagger$  is the initial (or limiting) co-adsorption ratio of component i

TABLE 3.1: Some useful Maxwell relations

From the Gibbs co-adsorption equation (eq.[3]):

$$\left(\frac{\delta \gamma}{\delta \ln x_p}\right)_{P, T, \mu_i} = -RT \Gamma_p \quad [3.1.1]$$

$$\left(\frac{\delta \Delta r_i^{\Gamma_p}}{\delta \ln x_p}\right)_{P, T, \mu_i} = RT \left(\frac{\delta \Gamma_p}{\delta \mu_i}\right)_{P, T, \mu_{j \neq i}, x_p} \quad [3.1.2]$$

$$\left(\frac{\delta \Delta r_i^{\Gamma_p}}{\delta \mu_j}\right)_{P, T, \mu_{k \neq j}, x_p} = \left(\frac{\delta \Delta r_j^{\Gamma_p}}{\delta \mu_i}\right)_{P, T, \mu_{k \neq i}, x_p} \quad [3.1.3]$$

$$\left(\frac{\delta \Delta r_i^{\Gamma_p}}{\delta \mu_j}\right)_{P, T, \mu_{k \neq j}, \Gamma_p} = \left(\frac{\delta \Delta r_j^{\Gamma_p}}{\delta \mu_i}\right)_{P, T, \mu_{k \neq i}, \Gamma_p} \quad [3.1.4]$$

$$\left(\frac{\delta \Delta r_i^{\Gamma_p}}{\delta \Delta r_j^{\Gamma_p}}\right)_{P, T, \mu_{k \neq j}, \Gamma_p} = - \left(\frac{\delta \mu_j}{\delta \mu_i}\right)_{P, T, \mu_{k \neq i}, j, \Delta r_j^{\Gamma_p}} \quad [3.1.5]$$

In the Henry region of adsorption (eq.[5]):

$$\Delta r_i^{\ddagger} = RT \left(\frac{\delta \ln H}{\delta \mu_i}\right)_{P, T, \mu_{j \neq i}} \quad [3.1.6]$$

For the analysis of protein partition in a liquid-liquid system equations [3.1.1 - 3.1.6] can be used after replacing  $\gamma$  by  $\xi$ ,  $\Gamma_p$  by  $c_p^a$  and  $H$  (the Henry constant) by  $K$  (the partition constant) (compare eqs.[34], [36]).

and  $\Delta G_{\text{ads}}^{\ddagger}$  is the Gibbs energy of adsorption.

In section 2.3 we discussed the relatively small influence of the diffusely bound ions on the proton binding by the protein. A similar effect may be noted about the co-adsorption ratios. Suppose the salt  $\text{MX}$  is the supporting electrolyte and further the system contains  $\text{MOH}$  and  $\text{HX}$  in a ratio determined by the pH. The co-adsorption ratio of the salt can then be written as,

$$\Delta r_{\text{MX}} = \Delta r_{\text{M}}^{\text{d}} + \Delta r_{\text{X}}^{\text{d}} + \Delta r_{\text{M}}^{\text{nd}} + \Delta r_{\text{X}}^{\text{nd}} \quad [6]$$

where the superscripts d and nd denote the co-adsorption ratios due to the diffusely and non-diffusely bound ions respectively. Dissolved proteins bind approximately as much diffuse counter-ions as they expel diffuse co-ions

(section 2.3). When this is also true for adsorbed protein, the diffuse parts of the co-adsorption ratios cancel upon adsorption. Of course, if the diffuse layer potential of the surface prior to the protein adsorption (that is, the diffuse layer potential of the reference surface) is high, the compensation by diffuse ions is smaller. In view of the above, we note that if for some reason the re-distribution of the non-diffuse ions is nil, the adsorption (in the Henry region) will not depend much on the salt strength.

It is often stated (2,3) that the interaction of a protein molecule with its surroundings obeys Le Chatelier's principle for chemical equilibria (chapter 1). In the case of protein adsorption in the Henry region (eq. [5]) it is indeed true that adsorption is promoted or inhibited upon the increase of the chemical potential of any component  $i$ , if upon the adsorption substance  $i$  is co-adsorbed, respectively co-desorbed. However, if protein adsorption is accompanied by protein-protein interactions on the surface, eq. [5] no longer holds. Instead, we must use the more general eq. [3.1.2] (table 3.1). Slightly rewritten this expression reads

$$\left[ \Delta r_i + \left( \frac{\delta \Delta r_i}{\delta \ln \Gamma_p} \right)_{P,T,\mu_i} \right] \cdot \left( \frac{\delta \Gamma_p}{\delta \ln x_p} \right)_{P,T,\mu_i} = RT \left( \frac{\delta \Gamma_p}{\delta \mu_i} \right)_{P,T,\mu_{j \neq i}, x_p} \quad [7]$$

Surprisingly, we find that (in rare situations) it is possible that Le Chatelier's principle is not obeyed. Suppose for example that at a certain adsorbed amount of protein, the co-adsorption ratio changes due to increasing protein-protein interactions on the surface. If then the relative change in the co-adsorption ratio of a component with respect to the adsorbed amount ( $\delta \Delta r_i / \delta \ln \Gamma_p$ ) is larger in magnitude and opposite in sign as compared with the net co-adsorption ratio  $\Delta r_i$ , we observe a dependence of  $\Gamma_p$  on  $\mu_i$  contradictory to that predicted by Le Chatelier's principle.

The polynome method of Wyman (4,5) has also been used to analyse the interactions of proteins with other colloidal particles (2,3,6). In chapter 2 we discussed the shortcomings of this method. The arguments we gave there apply here a forte. Let us consider, for example, a protein P with N base sites reacting with a small portion of a surface S, containing M base sites, neglecting protein-protein interactions. In the spirit of the polynome method the equilibrium interaction is written as



where  $\Delta n$  is the number of co-adsorbed protons. In addition to the chemical potential of the protein ( $\mu_p$ ), chemical potentials are introduced for the portion of the surface it reacts with ( $\mu_s$ ), and for the combined complex P-S ( $\mu_{ps}$ ), according to (see chapter 2)

$$\mu_p = \mu_{p,0}^0 + RT \ln(P) - \ln B_p \quad [9]$$

$$\mu_s = \mu_{s,0}^0 + RT \ln(S) - RT \ln B_s$$

$$\mu_{ps} = \mu_{ps,0}^0 + RT \ln(P-S) - RT \ln B_{ps}$$

where the brackets indicate concentrations, so (S) is the "free equilibrium concentration" of surface, (P) that of protein and (P-S) stands for the concentration of the complex. The factors B are the binding polynomials, defined as

$$B_p \equiv \sum_0^N K_{p,n} a_H^n \quad [10]$$

$$B_s \equiv \sum_0^M K_{p,n} a_H^n$$

$$B_{ps} = \sum_0^N K_{ps,n} a_H^n + \sum_0^M K_{ps,n} a_H^n$$

The quantities  $K_n$  are termed "phenomenological association constants" (3),  $a_H$  is the activity of the protons. Perhaps it is a matter of taste, but in our view any definition of "chemical potentials" of surfaces or protein-surface complexes would be unrealistic. Anyway, the next step is to write the equilibrium constant  $K_{int.}$  for reaction [8] in terms of the binding polynomials,

$$RT \ln K_{int.} = - (\mu_{ps,0}^0 - \mu_{p,0}^0 - \mu_{s,0}^0) + RT \ln \frac{B_{ps}}{B_p \cdot B_s} \quad [11]$$

If we take the derivative of  $\ln K_{int.}$  with respect to the proton chemical potential we obtain (assuming the association constants  $K_n$  to be independent of the proton concentration)

$$RT \left( \frac{\delta \ln K_{int.}}{\delta \mu_H} \right)_{a_s} = (\bar{n}_{ps} - \bar{n}_p - \bar{n}_s) = \Delta n \quad [12]$$

where  $a_s$  is the activity of salt. This result is comparable to ours: the derivative of the Henry constant with respect to the chemical potentials of acid or base at constant salt strength yields  $\Delta r_H$ . But if we now try to take the derivative of  $\ln K_{int}$  with respect to the salt strength at constant pH, we encounter difficulties. Obviously, in order to obtain a finite value of the electrolyte co-adsorption (which certainly will occur as we have two particles with the same sign of charge interacting), we must introduce some kind of activity coefficients for the protein, surface and combined complex, reflecting the charge-charge interactions. As we have stated in chapter 2, it would be virtually impossible to do so in a general way. For example, what kind of activity coefficients must be used for the interacting charges of the protein and the surface? Whatever solution is found for this problem, the answer will always be of limited validity because it will be highly dependent on the type of interaction model that is used.

### 3.2.2 EXAMPLE: AGI TITRATION OF ADSORBED BSA

The first experimental example to illustrate the thermodynamic analysis of surface-liquid systems anticipates chapter 5 of this thesis. The example concerns the charge-charge interactions between Bovine Serum Albumin (BSA) and the surface of a precipitate of the insoluble salt AgI. A typical experiment was done as follows. Colloidal AgI particles (radii a few micron) were first partially coated with the protein and then titrated with KI while keeping the pH constant. The Galvani potential of the AgI surface  $\Delta\phi$  was monitored with an AgI electrode. The iodide ions specifically adsorbed on the AgI surface and not on the (adsorbed) protein. Furthermore, protons did not adsorb on the (bare) AgI surface. The titration technique allowed for straightforward calculation of the co-adsorption ratio of  $I^-$  minus that of  $Ag^+$ ,  $\Delta r_I$ , and proton co-adsorption ratio  $\Delta r_H$ . In fig 3.2 the ratios are plotted as functions of the surface Galvani potential  $\Delta\phi$ .

The general appearance of the curves conforms to our expectations. Indeed we would expect an adsorbed protein molecule to bind extra protons when the surface potential is more negative, and indeed we would expect the adsorption of the iodide ions (or expulsion of silver ions) to be promoted at pH values lower than the isoelectric point of the protein ( $pH_{iep} = 4.7$ ) and inhibited at pH values higher than the i.e.p. However, some aspects are not immediately obvious, for example why  $\Delta r_I$  in the pH 4 curves changes sign at a certain

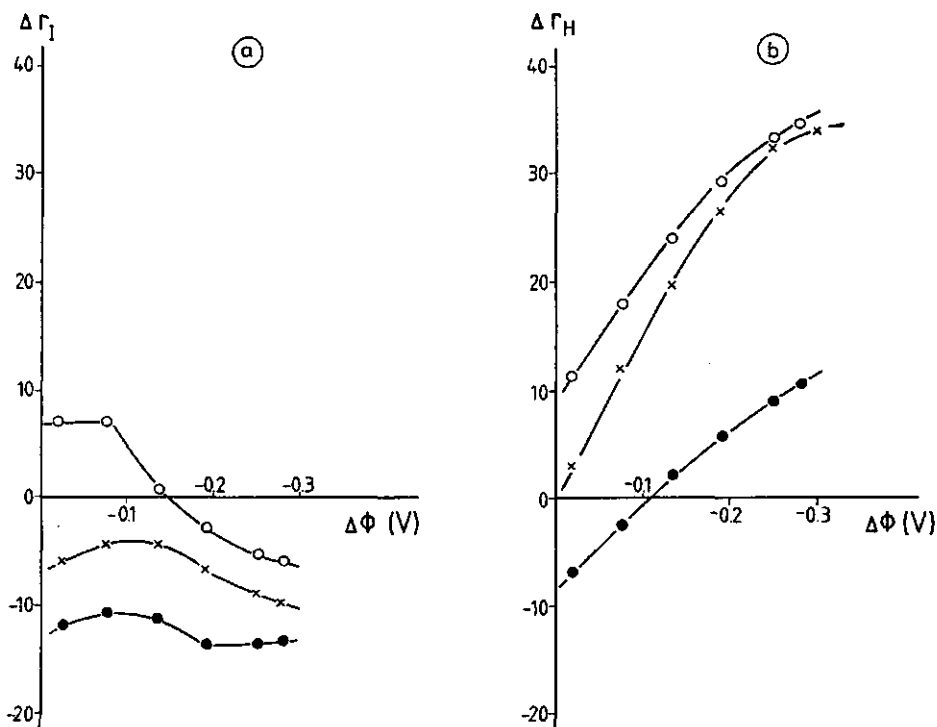


FIGURE 3.2. Co-adsorption of ions in Bovine Serum Albumin adsorption on AgI crystals. Final Adsorbed amount of BSA about  $1 \text{ mg/m}^2$ ,  $c_{\text{KNO}_3} = 0.1 \text{ M}$ .

pH 4 (○) ; pH 5 (×) ; pH 6 (●)

a) co-adsorption of  $\text{I}^-$  minus co-adsorption of  $\text{Ag}^+$ .

b) co-adsorption of protons

negative surface potential. For a full discussion of these and other effects the reader is referred to chapter 5.

The thermodynamic analysis of this system centers around eq.[3.1.5] of table 3.1. In terms of the observable quantities this Maxwell relation is written as

$$g = \left( \frac{\delta\Delta r_H}{\delta\Delta r_I} \right)_{P,T,a_s,pH,\Gamma_{\text{BSA}}} \cdot \left( \frac{\delta p_H}{\delta p_I} \right)_{P,T,a_s,\Delta r_I,\Gamma_{\text{BSA}}} = -1 \quad [13]$$

where the  $pI$  is defined as  $-\log a_I$  and  $a_s$  is the activity of the supporting electrolyte  $\text{KNO}_3$ . With our titration technique both differential coefficients of eq.[13] can be measured independently so that the theoretically derived relation can be verified. As such a (Gibbs) check put a heavy demand on the

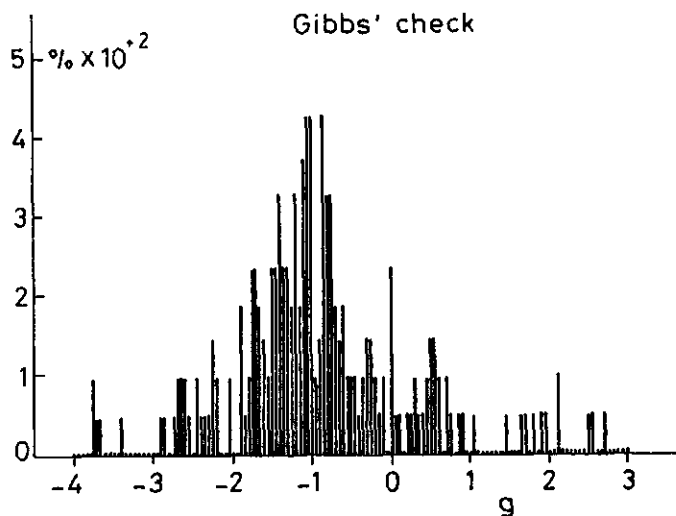


FIGURE 3.3. Histogram of the Gibbs ratio  $g$ .

accuracy of the measurements it was necessary to repeat it several times in order to obtain statistically significant results. The frequency distribution of  $g$ , based on more than 200 observations, is represented in fig.3.3. The histogram shows a clear optimum around  $-1$ , as it should.

### 3.2.3 EXAMPLE: CHROMATOGRAPHY OF BSA

The second experimental example to illustrate the use of the Gibbs co-adsorption equation concerns the interactions of BSA with the charged groups of a commercial HPLC anion exchanger. The interactions are studied by monitoring the pH and salt strength dependence of the retention volume while the column is operated in the isocratic mode. In figure 3.4 some typical results are shown (see ref. 7 for details on the experimental conditions). The results are readily understandable. The protein is washed out of the column at a salt concentration higher than a certain critical value, but retention is promoted at a lower salt concentration. The higher the pH, the higher the critical value. These results can also be analysed with our thermodynamic relations. When we use eq.[3.1.6] of table 3.1., expressed in the ionic composition of the chromatographic system (compare eq.[15] of chapter 2), we have,

$$\Delta r_H^\ddagger = - \left( \frac{\delta \log H}{\delta \text{pH}} \right)_{P,T,a_s} \quad [14]$$

$$\Delta r_{Na}^\ddagger = \frac{1}{2} \left\{ \left( \frac{\delta \log H}{\delta \text{pH}} \right)_{P,T,a_s} + \left( \frac{\delta \log H}{\delta \log a_s} \right)_{P,T,\text{pH}} \right\}$$

$$\Delta r_{Cl}^\ddagger = \frac{1}{2} \left\{ - \left( \frac{\delta \log H}{\delta \text{pH}} \right)_{P,T,a_s} + \left( \frac{\delta \log H}{\delta \log a_s} \right)_{P,T,\text{pH}} \right\}$$

where  $\Delta r_{Na}^\ddagger$  and  $\Delta r_{Cl}^\ddagger$  are the initial co-adsorption ratios of the Na and the Cl ions, and  $a_s$  is the activity of the electrolyte NaCl (the buffer concentrations are so low that co-adsorption of the buffer can be neglected). Some calculated ion co-adsorption ratios are plotted in fig 3.5. We find that the interaction of the protein with the anion exchanger gives rise to almost as much cation as anion expulsion! Furthermore the Na and Cl co-adsorption ratios are more negative than the proton co-adsorption ratio, but rise to less negative values at the isoelectric point of the protein.

A more detailed analysis of these results requires a model for the titration behaviour of: (i) the protein prior to adsorption, (ii) the reference surface and (iii) the adsorbed protein. By way of illustration we will now try to interpret the measured co-adsorption ratios at pH 9.5,  $c_{NaCl} = 0.2$  M, using a very simple titration model. From a thermodynamic analysis of the titration characteristics of BSA, we have deduced (chapter 2) that at pH 9.5,  $c_{KCl} = 0.07$  M, the binding ratios of the protons, potassium, and chloride ions for dissolved BSA are,  $r_H = -27$ ,  $r_K = 18$  ( $r_K^{nd} = r_K^d = 9$ ),  $r_{Cl} = -9$  ( $r_{Cl}^{nd} = 0$ ). For sake of argument, we will assume that the same numbers apply to the binding ratios in a solution of 0.2 M NaCl, with sodium ions replacing the potassium ions. Now, only a fraction of the total number of acid/base residues of the protein will make direct contact with the surface of the anion exchanger. Suppose that this fraction equals 1/3 (in chapter 5 we will estimate the area an adsorbed BSA molecule occupies on a AgI surface as 30-50 nm<sup>2</sup>, whereas the total outer surface of a native BSA molecule is between 100 and 150 nm<sup>2</sup>), then for the interacting side of the protein molecule the charge balance prior to adsorption is given by,  $r_H = -9$ ,  $r_{Na} = 6$  ( $r_{Na}^d = r_{Na}^{nd} = 3$ ) and  $r_{Cl} = -3$  ( $r_{Cl}^{nd} = 0$ ). Next suppose that the surface of the anion exchanger is densely covered with strong base groups (B), with which chloride ions form complexes to such an extent that the diffuse charge is negligible. Finally, assume that the 9 acid residues of the protein which are dissociated in excess, and one extra acid residue (priorly to adsorption undissociated, it could be a tyrosine residue), form ion pairs with the strong base groups on

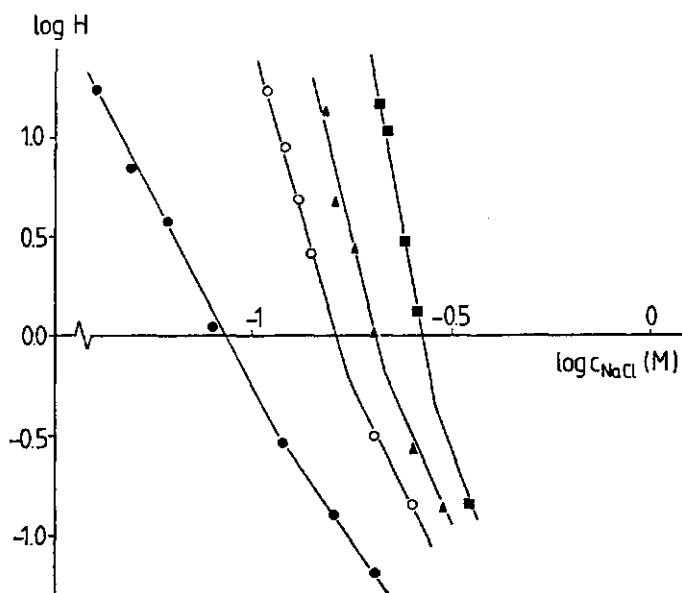


FIGURE 3.4. Henry constant  $H$  for the adsorption of Bovine Serum Albumin on a Pharmacia MonoQ anion exchanger. Buffer concentration 10 mM, Piperazine.HCl (pH 5.5), bis-Tris.HCl (pH 6.5), Tris.HCl (pH 7.5), Piperazine.HCl (pH 9.5). Flow 1 ml/min, void volume 1 ml.

pH = 5.5 (●) ; 6.5 (○) ; 7.5 (▲) ; 9.5 (■)

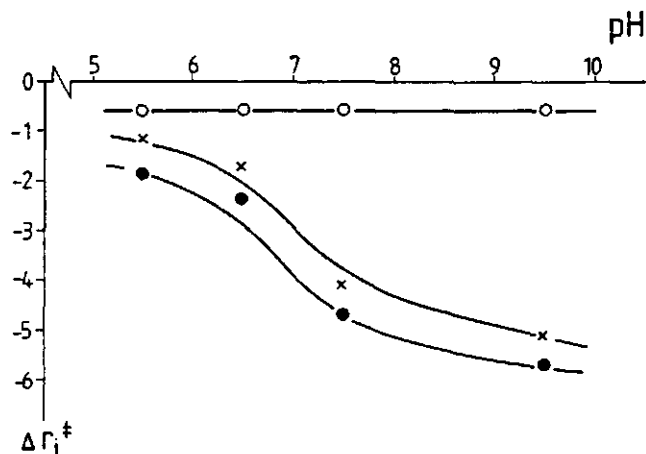
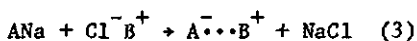


FIGURE 3.5. Limiting co-adsorption of Na, Cl and H ions in the chromatography of BSA on the Mono Q anion exchanger,  $c_{NaCl} = 0.2$  M. Points calculated from fig. 3.4 using eq. [8].  $\Delta\Gamma_H^{\ddagger}$  (○) ;  $\Delta\Gamma_{Na}^{\ddagger}$  (x) ;  $\Delta\Gamma_{Cl}^{\ddagger}$  (●)

the surface. The ion redistributions are then governed by three types of ion exchange reactions:



The numbers in the brackets give the frequencies of occurrence of the reactions. As a result of the ion pair formation, 10 chloride ions are effectively removed from the anion exchanger surface. Because 3 chloride ions are used to compensate the deficit of diffusely bound chloride ions, the net co-adsorption ratio of chloride ions is then -7. One acid residue is extra titrated, so the co-adsorption ratio of the protons is -1. The sodium ion co-adsorption ratio equals -6 (three ions are removed from the protein through the third reaction, three were diffusely bound to the protein prior to adsorption and of course also expelled upon adsorption). The measured co-adsorption ratios at pH 9.5 are,  $\Delta r_H = -0.6$ ,  $\Delta r_{Na} = -5.1$ ,  $\Delta r_{Cl} = -5.7$ . The agreement between experiment and prediction is satisfactory, considering the large number of assumptions. But, to be sure, the above is only meant as an illustration of the use of the phenomenological relations, not as a rigorous analysis.

In the literature on the (ion exchange) chromatography of proteins (or polyelectrolytes), retention data are often analysed with a model proposed by Kopaciewicz et al. (8) and Rounds et al. (9), based on an older model by Boardman et al. (10). In order to make clear what the difference is between their approach and ours, we cite from one of their articles (8) the following derivation of a relation between the capacity factor of the column and the salt concentration:

"...A non-mechanistic model for the ion exchange proces is given by the equilibrium expression



The symbol  $D_b$  represents the concentration of displacing ions associated

with the surface and is in direct proportion to the ion-exchange stationary phase density (i.e. ligand density) in moles/m<sup>2</sup>.  $P \cdot C_i$  is the concentration (moles/l) of protein in solution above the surface with accompanying counter-ion concentration ( $C_i$ ).  $P_b$  signifies the protein concentration on the ion-exchange column in moles/m<sup>2</sup>, while  $D_0$  is the displacing ion concentration of the mobile phase in moles/l. It is known, however, that the displacing power of an ion is proportional to its ionic strength, and that the constants  $a$  and  $b$  are needed to adjust for valency, activity coefficient and relative displacing power differences between ions. The  $Z$  term in the formula is the number of charges that are associated with the adsorption-desorption process.

The equilibrium constant for the ion-exchange process may be expressed as

$$K_b = \frac{(P_b)(aD_0)^Z (bC_i)^Z}{(P \cdot C_i)(D_b)^Z} \quad [C2]$$

where  $K_b$  is a binding constant....".

Next Kopaciewicz et. al. assume that the fraction of the surface covered with protein is very small in a chromatography experiment, after some algebraic manipulations they then obtain an expression for the capacity factor  $k'$ ,

$$k' = K_z / [(D_0) (C_i)]^Z \quad [C3]$$

where  $K_z$  is a constant depending on  $(D_0)$ ,  $a$ ,  $b$ , the available surface area and the mobile phase volume. We proceed the quotation:

"....expression [C3] relates retention of a solute to the displacing agent concentration of the mobile phase, and the number of charged groups involved in the adsorption-desorption process. When sodium chloride is used as a displacing agent, it is assumed that  $(D_0)$  equals  $(C_i)$  and that eq. [C3] is further reduced to

$$k' = K_z / [NaCl]^{2Z} \quad [C4]$$

Graphical evaluation of  $Z$  is simplified by expressing eq. [C4] in the log

form

$$\log k' = -2Z \log[\text{NaCl}] + \log K_z \quad [C5]$$

where  $Z$  is the slope and  $\log K_z$  the intercept of  $\log k'$  versus  $-\log[\text{NaCl}] \dots$ .

In our opinion, the above derivation is in principle incorrect. To give a few arguments, (i) if  $Z$  ion-exchanging groups on the surface react with the protein simultaneously they will not react independently of each other as is implicitly assumed by using the power term  $(D_b)^Z$ , (ii) the redistribution of the co-ions as well as that of the protons is completely neglected, (iii) there is no a priori justification for the interpretation of  $Z$  as the "number of charges associated with the adsorption-desorption process". According to our reference approach, the conclusion they draw is also incorrect. The proper interpretation of the slope of the  $\log k'$  curve (or  $\log H$ , the Henry constant is equal to the capacity factor) must be

$$\left( \frac{\delta \log H}{\delta \log a_s} \right)_{\text{pH}} = \Delta r_{\text{Na}} + \Delta r_{\text{Cl}} \quad [16]$$

which is not the same as twice the number of exchanging groups (compare the simple model analysis we gave in the beginning of this section).

#### 3.2.4 EXAMPLE: ADSORPTION OF HPA ON POLYSTYRENE LATICES

As a third example we analyse the data obtained by Norde and Lyklema (11,12) on the adsorption of Human Plasma Albumin (HPA) on polystyrene latices some ten years ago. They determined adsorption isotherms of HPA as a function of pH and salt strength ( $\text{KNO}_3$ ) (11) and, independently, proton titration curves of the adsorbed protein (12). Prior to the titrations the latex surface was completely saturated with protein.

Some of their results are listed in table 3.2. The underlying adsorption isotherms all have the same shape with a well defined linear part of the isotherms extending almost up to the plateau level. As a function of pH, the plateau value of adsorption is a maximum at pH 4.7. In principle the listed results would allow us to verify integral expressions of Maxwell relation [3.1.2] of table 3.1. The relevant expression is,

TABLE 3.2: Adsorption of Human Plasma Albumin on polystyrene latex (8,9)

$$c_{KNO_3} = 0.05 \text{ M}$$

| pH  | $\Delta r_H$<br>[-] | $\Gamma_{HPA}^{max}$<br>[nmol/m <sup>2</sup> ] | H    |
|-----|---------------------|--|------|
| 4.0 | 17.2                | 24   | 12.2 |
| 4.7 | 9.5                 | 30   | 6.7  |
| 7.0 | 0.6                 | 16   | 8.9  |

$$\Delta r_H = \frac{1}{\Gamma_p} \int_0^{x_p} \left( -\frac{\delta \Gamma_p}{\delta \text{pH}} \right)_{P,T,a_s} d \log x_p \quad [17]$$

By inspection of table 3.2. it is immediately clear that the experimental results are inconsistent with the thermodynamic analysis. According to the right hand side of eq.[17] at pH = 4.7 the proton co-adsorption ratio (in the plateau) should approximately be zero as both the Henry constant and the plateau attain extremal values at this pH, whereas according to the titrations the proton co-adsorption ratio is extremely large.

This example shows caution must be taken in using the thermodynamic relations. From the onset of our analysis we have tacitly assumed the system under study to be in equilibrium. However, especially when the surface coverage is high and shear forces in the solution are low or absent, protein adsorption may attain equilibrium slowly. Under these circumstances it is very dangerous to combine different kinds of experiments using thermodynamics.

### 3.3 LIQUID-LIQUID SYSTEMS

#### 3.3.1 GIBBS CO-PARTITION EQUATION

One elegant way to purify proteins is to extract them from a compound aqueous solution through preferent solubilization in a second liquid phase. An older method was to create an aqueous two-phase system through the addition of polymers (13). Recently, it was discovered that under proper conditions,

water-immiscible apolar solvents containing aggregates of surfactant molecules which are insoluble in water are also capable of such a preferent solubilization (14-18). The (co-) surfactant molecules are thought to form reverse micelles which may serve as a host for protein molecules in an otherwise protein-hostile environment (19,20).

It is frequently observed that the partition coefficients of the proteins are strongly dependent on the ionic composition of the water phase (14-19). In our view, this would already indicate substantial co-partitioning of small ions, reflecting the difference in charge-charge interactions of the protein with its surroundings in the two phases. As before, it must be possible to relate the dependencies of the partition coefficients on, for example the salt strength or the pH, to the co-partitioning of the small ions. As far as we are aware, a (phenomenological) theory for this process has not been presented yet.

In the following we will restrict our analysis to those cases where the second phase consists of an apolar solvent. Extension to aqueous two-phase systems would be straightforward but outside the scope of the present study.

There are at least three different ways to proceed the analysis:

(1) We could start from the assumption that all the surfactant molecules form reverse micelles of fixed composition. This would be equivalent to the assumption that all the reverse micelles are colloidal particles with constant surface area, embedded in an inert matrix which does not affect the partitioning process. We then could use the Gibbs co-adsorption equation without any adaptations. Obviously, such an analysis would be limited in perspective: in many cases a reverse micelle containing a protein molecule will have a shape and composition different from the "empty" micelles.

(2) A second approach is to use the expression for the chemical potential for the protein (eq. [12], chapter 2) in the aqueous as well as in the apolar phase. In doing so we assume a priori that in the apolar phase (i) the protein concentration is so low that protein-protein interactions may be neglected, (ii) the valency factor is unity and (iii) the mole fraction of the bulk component (for example isooctane) is close to unity. We then have

$$d\mu_p^w = - \sum_i^0 r_i^w D\mu_i + RT d \ln x_p^w \quad (\text{for the water phase}) \quad [19]$$

$$d\mu_p^a = -\sum_i^0 r_i^a D\mu_i^a + RTd\ln x_p^a \quad (\text{for the apolar phase})$$

where the superscripts <sup>a</sup> and <sup>w</sup> denote water and apolar phase respectively. The dot <sup>0</sup> indicates that the bulk component in the apolar phase is not counted in the sum. The next step is to realize that the chemical potentials must be the same everywhere in equilibrium. Equating the differentials of eq.[19] gives

$$RTd\ln(x_p^a/x_p^w) = \sum_i^0 [r_i^a - r_i^w] D\mu_i \quad [20]$$

if we then define the co-partition ratio  $\Delta r_i$  of component  $i$

$$\Delta r_i \equiv r_i^a - r_i^w \quad [21]$$

and the partition coefficient  $K$  as

$$K = x_p^a / x_p^w \quad [22]$$

eq. [20] is written as

$$RT\ln K = \sum_i^0 \Delta r_i D\mu_i \equiv -d\Delta G_{\text{par}}^\ddagger \quad [23]$$

where  $\Delta G_{\text{par}}^\ddagger$  is the Gibbs energy of partition.

Now, eq. [23] looks simple, but for two reasons its practical use will be limited.

The first reason is that the summation must take into account all the components, whether they are preferentially dissolved in the water phase (for example the salt) or in the apolar phase (the surfactant). In doing so eq.[20] indeed includes the possibility of alteration of shape and composition of the reverse micelles upon the addition of protein, an advantage with respect to the first method of analysis. However, as a consequence we require some model which allows us to relate the chemical potential of the surfactant to the ionic composition and the surfactant concentration. Especially in the case of charged surfactants (which are more commonly used) such a model would be very involved.

The second reason is that it is not at all obvious if the Donnan effect in the apolar phase may be neglected. In chapter 2, we showed that the value for the valency factor ( $f$ ) in the water phase is highly dependent on the charge of

the protein and the electrolyte concentration. An estimate for  $f$  was given, using the original Donnan theory. We concluded that when  $z_p c_p \ll c_s$  (where  $z_p$  is the valency and  $c_p$  the protein concentration) we indeed may neglect the Donnan effect. In order to make a similar estimate for the apolar phase we would again require a model as to how the reverse micelles look like. A number of questions can then be put forward which are difficult to answer. For example, does charged surfactant contribute to the ionic strength?, do the solubilized substances (which reside predominantly in the water cores of the reverse micelles) add to the osmotic pressure?, etc., etc.

(3) The third method circumvents all the problems associated with the first two methods. It is based on three minor assumptions which will generally be fulfilled, viz. (i) the surfactant and co-surfactant reside only in the apolar phase, (ii) the apolar solvent is ideally immiscible with water and (iii) the volumina of the two phases are not affected by the partition of protein.

With these assumptions, the derivation of a Gibbs (co-) partition equation similar to the Gibbs (co-) adsorption equation is an easy task.

Suppose we have the apolar phase in equilibrium with the water phase. The energy ( $U$ ) of the total system (water phase+apolar phase) is then given by

$$dU = TdS + \sum_i \mu_i d(N_i^a + N_i^w) + \sum_j \mu_j^* dN_j^* \quad [24]$$

where  $S$  stands for the total entropy. The quantities  $N$  denote numbers, the first sum includes those components which are soluble in both the apolar and water phase, the second sum refers to the components which are assumed not to dissolve in water (denoted by the asterix), so  $N_j^* = N_j^a$ . As the volume of the apolar phase is not influenced by the partitioning process, we have the additional relation

$$dN_j^* = c_j^* dV^a \quad [25]$$

where  $V_a$  is the volume of the apolar phase. Combination of eqs. [24] and [25] yields

$$dU = TdS + \sum_i \mu_i d(N_i^a + N_i^w) + \xi dV^a \quad [26]$$

$$\xi \equiv \sum_j \mu_j^* c_j^*$$

Anticipating the discussion below, the quantity  $\xi$  (dimension  $J/m^3$ ) may be termed the "volume tension" of the apolar phase, it plays the same role in the resulting (co-) partition equation as the surface tension  $\gamma$  in the (co-) adsorption equation.

The energy of the water phase,  $U^W$ , is given by

$$dU^W = TdS^W + \sum_i \mu_i dN_i^W \quad [27]$$

The next step is to subtract  $dU^W$  from  $dU$ , which results in

$$d(U - U^W) = Td(S - S^W) + \sum_i \mu_i dN_i^a + \xi dV^a \quad [28]$$

The energies are homogeneous functions of the extensive variables, so an alternative expression for the difference  $(U-U^W)$  can be obtained by integration and subsequent differentiation of eq.[28], yielding

$$d(U - U^W) = Td(S - S^W) + (S - S^W) dT + \sum_i \mu_i dN_i^a + \sum_i N_i^a d\mu_i + \xi dV^a + V^a d\xi \quad [29]$$

After subtracting eq.[29] from [28] and a little re-writting we obtain (for constant temperature and pressure)

$$d\xi = - \sum_i c_i^a D\mu_i \quad [30]$$

The chemical potential of water is related to those of the other water-soluble components through the Gibbs-Duhem relation in the water phase,

$$x_w^W D\mu_w = - \sum_i x_i^W D\mu_i \quad [31]$$

Combination of eqs.[30] and [31] gives

$$d\xi = - \sum_i \left[ c_i^a - \left( \frac{x_i^W}{x_w^W} \right) \cdot c_w^a \right] D\mu_i \quad [32]$$

If we then assume, as before, that the molar fraction of water in the aqueous phase is approximately unity, we finally obtain the sought Gibbs partition equation

$$d\xi = - \sum_i c_i^a D\mu_i \quad [33]$$

As this equation is morphologically identical to the Gibbs adsorption formula, everything that has been said in section 3.2.1 applies here as well. So the "excess" volume tension ( $\xi^L - \xi^R$ ), that is, the extra increase or decrease of  $\xi$  of the system containing protein (L) with respect to a reference system devoid of protein (R), is given by (compare eq.[3])

$$d(\xi^L - \xi^R) = - c_p^a [ \sum_i \Delta r_i D\mu_i + RT \ln x_p^w ] \quad [34]$$

where  $\Delta r_i$  is the co-partition ratio of component i, defined as

$$\Delta r_i \equiv r_i^a - r_i^w \quad [35]$$

$$r_i^a \equiv \frac{c_i^{a,L} - c_i^{a,R}}{c_p^a} = \Delta c_i^a / c_p^a$$

Note that these definitions are different from the ones according to the second method.

The Maxwell relations of table [3.1] now apply (with minor alterations) for the water-apolar two-phase system as well.

In the case of partition in the Henry region the protein concentration in the apolar phase is linearly related to the protein concentration in the water phase, the partition constant K is simply defined as

$$K \equiv \lim_{x_p^w \rightarrow 0} \left( \frac{c_p^a v_p^a}{x_p^w v_p^w} \right) \quad [36]$$

$$RT \ln K = \sum_i \Delta r_i^\ddagger D\mu_i \equiv -d\Delta G_{\text{par}}^\ddagger$$

where  $\Delta r_i^\ddagger$  is the limiting co-partition ratio of component i and  $\Delta G_{\text{par}}^\ddagger$  is the Gibbs energy of partition.

In comparison with the first two methods, the third method of analysis does not require a model for the properties of the reverse micelles. In fact, the apolar phase is treated as a "black box" of which we do not need to know what is going on inside: the relation between the partition of the protein and the

co-partition of the ions is fully determined through their chemical potentials in the water phase. Of course, the advantage is also a disadvantage as we are now unable to obtain information on size and conformation of the micelles. If we then try to analyse the dependency of the protein partition on the salt strength and pH through a model, we must realize that any change in the aggregates resulting from the solubilization of protein may in principle also affect the charge-charge interactions and hence the co-adsorption ratios.

### 3.3.2 EXAMPLE: SOLUBILIZATION OF CYTOCHROME C

This example concerns the interactions of ferri cytochrome C with reverse micelles of TOMAC (trioctylmethylammonium chloride). The interactions are studied by analysing the partition of the protein between an aqueous and an isooctane phase (see ref. (21) for details on the experimental conditions). The water phase contains EDA buffer (ethylene diamine,  $pK_1 = 7$ ,  $pK_2 = 10$ ), NaCl and a negligible amount of the water-insoluble TOMAC and octanol. The isooctane phase contains reverse micelles of TOMAC, octanol (necessary for the stabilisation of the micelles) and a small amount of solubilized water, EDA and NaCl.

Some of the observed dependencies of the ratio  $x_p^a/x_p^w$  with the pH and salt concentration are plotted in fig.3.6. The curves show a pronounced salt and pH effect indicating substantial acid and salt co-partition. Significant solubilization of the protein by the apolar phase occurs only over a small pH interval around the isoionic point of the protein ( $pH_{iip} = 10.2$ , see ref.(22)). To the left and to the right of the pH optimum the addition of even a small amount of salt inhibits respectively promotes the solubilization strongly. Similar results were obtained for various buffer concentrations.

We will now analyse these results in terms of the co-adsorption ratios according to the third method of analysis as presented in section 3.3.1. According to this method, the ratio of the molar fractions must be multiplied with a constant in order to calculate the partition constant. But as we are only interested in relative changes of  $\log K$ , we only need the ratio of the molar fractions.

The chemical potentials of the acid and base are expressed in the salt concentration and pH according to eq.[15] of chapter 2. As the concentration of the buffer is high compared to that of the salt, its co-partition cannot be neglected a priori.

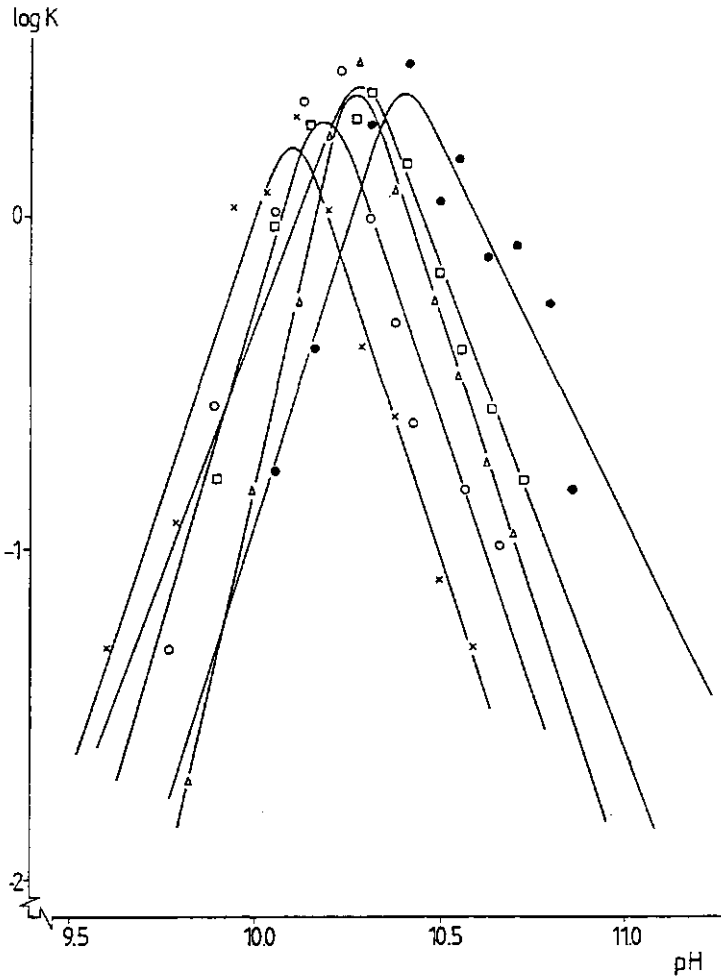


FIGURE 3.6 Partition ratio  $x_p^a/x_p^w$  for the distribution of ferri cytochrome C between an isooctane and a water phase. Volume water phase = volume isooctane phase = 2 ml. TOMAC concentration 10 mM, 1-octanol concentration 0.1%, both in the isooctane phase. Initial protein concentration in the water phase 4.5  $\mu$ M. Equilibration time 2 min.

$$c_{EDA}^w = 0.02 \text{ M,}$$

$$c_{NaCl}^w \text{ (M) = 0 (x) ; 0.005 (o) ; 0.0075 (\Delta) ; 0.01 (\square) ; 0.0125 (\bullet)}$$

For the chemical potential of the buffer we have

$$d\mu_{\text{EDA}} \approx 2.303 RT(d\log c_e + \alpha dpH) \quad [37]$$

where  $c_e$  is the total concentration of the buffer in the water phase and  $\alpha$  is the degree of protonation (neglecting the second association step at pH 7). The co-partition ratios are calculated through

$$\Delta r_{\text{H}}^{\ddagger} = \frac{(1+F_s)}{2} \left\{ -\left(\frac{\delta \log K}{\delta pH}\right) - \frac{F_e \alpha}{(1+F_s)} \left(\frac{\delta \log K}{\delta \log c_s}\right) + \alpha \left(\frac{\delta \log K}{\delta \log c_e}\right) \right\} \quad [38]$$

$$\Delta r_{\text{Na}}^{\ddagger} = \frac{(1+F_e \alpha)}{2} \left\{ \frac{F_s}{(1+F_e \alpha)} \left(\frac{\delta \log K}{\delta pH}\right) + \left(\frac{\delta \log K}{\delta \log c_s}\right) - \frac{F_s \alpha}{(1+F_e \alpha)} \left(\frac{\delta \log K}{\delta \log c_e}\right) \right\}$$

$$\Delta r_{\text{E}}^{\ddagger} = \frac{F_e \alpha}{2} \left(\frac{\delta \log K}{\delta pH}\right) - \frac{F_e \alpha}{2} \left(\frac{\delta \log K}{\delta \log c_s}\right) + \left(1 - \frac{F_e \alpha}{2}\right) \left(\frac{\delta \log K}{\delta \log c_e}\right)$$

$$\Delta r_{\text{Cl}}^{\ddagger} = \frac{1}{2} \left\{ -\left(\frac{\delta \log K}{\delta pH}\right) + \left(\frac{\delta \log K}{\delta \log c_s}\right) + \alpha \left(\frac{\delta \log K}{\delta \log c_e}\right) \right\}$$

where  $c_s$  is the concentration of the salt in the water phase (at low salt strength equal to the electrolyte activity). The coefficients  $F_s$  and  $F_e$  are defined as

$$F_e = \frac{c_e}{(\alpha c_e + c_s)} \quad [39]$$

$$F_s = \frac{c_s}{(\alpha c_e + c_s)}$$

In the limiting cases where buffer is absent,  $F_e = 0$ ,  $F_s = 1$ ,  $\Delta r_{\text{E}}^{\ddagger} = 0$  and eq.[39] transforms to the eq.[14] we used for the analysis of the ion exchange chromatography of BSA (section 3.2.3).

In fig.3.7 the calculated co-partition ratios are plotted. We observe a small co-partitioning of the buffer and, as expected, a high partitioning of the acid, base and salt. There seems to be an almost one to one correlation between the co-partition ratios of the protons and the chloride ions; below the isoionic point approximately 4 protons and 4 chloride ions are ejected in the water phase upon the partition of protein, above the isoionic point

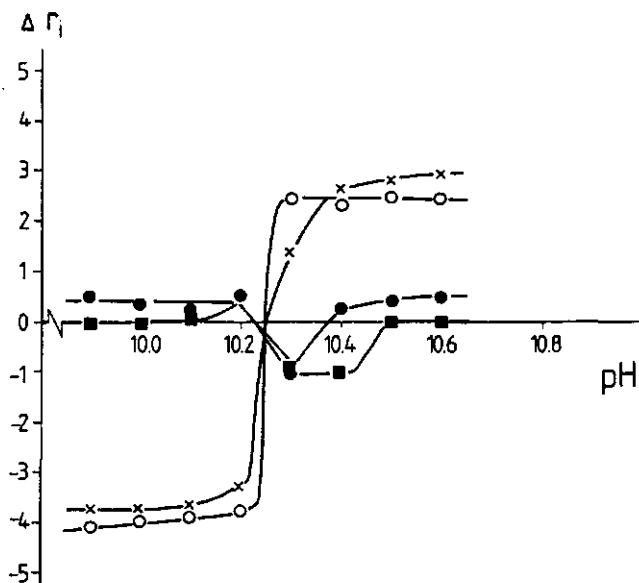


FIGURE 3.7. Limiting co-partition of EDA, Na, Cl and H in the partition of ferri cytochrome C between an iso-octane and a water phase. Points calculated from fig.3.6 using eq. [13].  $c_{NaCl}^w = 0.0075$  M.  
 $\Delta r_H^\ddagger$  (○);  $\Delta r_{Cl}^\ddagger$  (×);  $\Delta r_{Na}^\ddagger$  (●);  $\Delta r_E^\ddagger$  (■)

roughly 3 protons and 3 chloride ions co-partition. The sodium ions behave rather indifferently; their co-partition ratio is close to zero over the entire pH range.

A full explanation of these effects is not so easy as we do not know how the reverse micelles, either or not containing protein, look like. Nevertheless, some deductions can be made.

It is logical to assume that most TOMAC molecules in an "empty" reverse micelle form complexes with chloride ions because of the confinement of the strong basic head groups in a small volume. The diffuse co-ion charge of the reverse micelles due to the expulsion of sodium ions will therefore be very small. Now, from the titration curve of cytochrome C (in 0.15 M KCl, see ref. (22)) it appears that the proton binding ratio in the water phase varies from approximately +1 at pH 10 to -1 at pH 10.5. As a result, the sodium binding ratio in the water phase varies from roughly -0.5 at pH 10 to +0.5 at pH 10.6. These numbers (referring to the contribution of the sodium ions to the diffuse charge) were calculated assuming that the specific interactions of the sodium

and chloride ions and EDA buffer with the protein are negligible - we do not have sufficient data to make a more accurate estimate. Anyway, as little sodium is bound to the protein in the water phase and to the "empty" reverse micelles in the apolar phase, the net co-partition ratio  $\Delta r_{Na}^{\ddagger}$  must also be small.

A second deduction is closely connected to the first. Below the isoionic point protons are ejected into the water phase. In principle they could either originate from an extra titration of the lysine residues (of which ferri cytochrome C has 19) or from the four tyrosyl residues (of which three have a pK of 12.7, and one a pK of 10.7 (22)). Dissociated tyrosyl acid residues are capable of forming favourable ion pairs with the strong basic head groups, which indeed would result in an approximately one to one ion correlation between the co-partition ratios of the protons and the chloride ions. The possibility of ion pair formation between de-protonated lysine groups and the TOMAC molecules seems unlikely.

The decrease of the protein partition above the isoionic point is peculiar. Intuitively we would expect that since the charge contrast between the reverse micelles and the protein increases with increasing pH, the protein would have a larger affinity for the micelles at higher pH than at lower pH. One possible explanation might be the following. In the next chapter we will show that in some cases an increasing charge-contrast between two surfaces results in a decrease of the interaction energy. This happens when the charge of the one surface is more negative than the charge of the other surface is positive. Admittedly, this explanation is difficult to reconcile with the low charge density of the protein, especially since the highest partition coefficients are found very close to the isoionic point.

## 3.4 REFERENCES

1. A.W. Adamson (1967) "Physical Chemistry of Surfaces", 2<sup>nd</sup> ed. Interscience Publishers, New York, London, Sydney
2. M.T. Record Jr. C.F. Anderson, T.M. Lohman (1978) Quart. Rev. Biophys. 11(2), 103
3. J. Schellman (1975) Biopolymers 14, 999
4. J. Wyman (1964) Advan. Protein Chem. 19, 223
5. J. Wyman (1984) Quart. Rev. Biophys. 17(4), 453
6. G. Weber (1975) Adva. Protein Chem. 17, 69
7. R. Murriss (1986) M.Sc thesis, Agricultural University, Wageningen
8. W. Kopaciewicz, M.A. Rounds, J. Fausnach, F.E Regnier (1983) J. Chromatogr. 266, 3
9. M.A. Rounds, F.E. Regnier (1984) J. Chromatogr. 283, 37
10. N.K. Boardman, S.M. Partridge (1955) Biochem. J. 59, 543
11. W. Norde, J. Lyklema (1978) J. Colloid Interface Sci. 66, 257
12. W. Norde, J. Lyklema (1978) J. Colloid Interface Sci. 66, 266
13. P. Albertson (1970) Advan. Protein Chem. 24, 309
14. M. Dekker, K. Van't Riet, S.R. Weijers, J.W.A. Baltussen, C. Laane, B.H. Bijsterbosch (1986) Chem. Eng. J. 33, B27
15. M.E. Leser, G. Wei, P.L. Luisi, M. Maestro Biochem. Biophys. Res. Commun. 135(2), 629
16. K.L. Kadam (1986) Enzyme Microb. Technol. 8, 266
17. K.E. Göcklen, T.A. Hatton (1985) Biotechnol. Progr. 1(1), 69
18. P.L. Luisi, C. Laane (1986) Trends Biotechnol. 4, 153
19. E. Sheu, K. E. Göcklen, T.A. Hatton, S.-H Chen (1986) Biotechnol. Progr. 2(4), 175
20. A.V. Levashov, Y.L. Khmel'nitsky, N.L. Klyachko, V.Y. Chernyak, K. Martinek (1982) J. Colloid Interface Sci. 88(2), 444
21. E.J. Rijniëse (1986) M.Sc thesis, Agricultural University, Wageningen
22. G.E. Marti (1977) Ph.D Thesis, Northwestern University, Evanston, Ill.

## CHAPTER 4

## CO-PARTITION MODEL

## 4.1 INTRODUCTION

In the previous chapter generally valid relations between the protein partition and ion co-partition in two-phase systems have been obtained. The expressions enabled us to "translate" experimental observations in comprehensible molecular quantities.

However, it is beyond thermodynamics to predict a priori the charge regulation mechanism or to give a model interpretation of the net free enthalpy of interaction. To do so, we need a model analysis (such as the one described in this chapter) which explicits the electrochemical behaviour of the protein molecules in the two phases.

The one phase is usually a dilute solution of protein in water, the other may be a surface phase, or an apolar liquid phase, a protein precipitate etc. The first assumption we make is that the properties of the protein in the second phase are determined by its electrostatic interactions with a "particle". The particle may be a reverse micelle, a small area on a surface, a second protein. In the analysis we consider the non-interacting and interacting states of the protein and the second "particle" separately. From a comparison of the charges and potentials between the two states, we obtain information on the charge regulation mechanism.

A second approximation made is that the electrochemistry of both the protein molecule and the second particle in the free and interacting state can be modelled via acid/base equilibria on flat, impermeable, rigid surfaces. In doing so we disregard any effect of conformational changes. As they certainly will occur, we must be very cautious in the generalization of our theory. Nevertheless, we have decided to neglect structural alterations because we want to emphasize the purely electrostatic features.

The present problem is similar to that of two (large and rigid) colloidal particles with different surface properties coagulating reversibly. Healy (1), Parsegian (2,3), Ruckenstein and co-workers (4,5,6) and others (7,9) have

incorporated charge regulation in the classical DLVO theory (8) for colloid stability. These theories are capable of predicting the extent of the charge regulation in hetero-coagulation as a function of the distance between the two particles. However, the (modified or not) DLVO theory is a stability theory, as such it does not need to describe the final state after coagulation in great precision. In fact, in the original DLVO theory the depth of the primary minimum is assumed infinite. As a consequence, DLVO based theories are ill-suited for the description of the electrochemical behaviour of two contacting particles.

Opposed to the above mentioned theories, in our analysis we focus on the difference between the electrochemical properties of two charged surfaces at infinite separation (the free state) and those of the surfaces in close proximity (the interacting state). The distance dependency of the charge-regulation is not considered.

## 4.2 ELECTROCHEMISTRY OF FREE SURFACES

### 4.2.1 THE ELECTRICAL DOUBLE LAYER

In this sub-section we briefly discuss the electrical double layer on a flat surface, in (10) a more complete description of similar double layer models is given. The surface is in contact with a salt solution of composition:  $M^+$  (electrolyte cations),  $X^-$  (electrolyte anions),  $H^+$  (protons) and  $OH^-$  (hydroxyl ions). The proton concentration  $x_H$  (= mole fraction) or hydroxyl concentration  $x_{OH}$  is much lower than the salt concentration:  $x_M = x_X = x_S$  where  $x_S$  stands for the mole fraction of the salt. We assume that the solution behaves ideal so that we may write for any of the ion chemical potentials  $\mu_k = \mu_k^0 + RT \ln x_k$ ,  $k = H, OH, M, X$ .

In our analysis we make an explicit distinction between the adsorption of the ions in the diffuse part of the double layer, and the adsorption of the ions on acid or base sites on the surface. The fractional occupancy of a site with an ion is quantified by a "degree of titration" (e.g.  $\alpha_{AH}$  or  $\alpha_{BHX}$  where A denotes acid and B base). We assume that the surface charges are separated from the diffuse part of the double layer by a charge free Stern layer.

Our analysis is not restricted to a particular kind of site binding, as long as the assumption that all non-diffusely bound ions adsorb in one plane (resulting in a charge free Stern layer) is valid. Therefore, in order to keep

the discussion as general as possible, we will postpone a detailed description of the allowed ion configurations on the sites until section 4.5 which contains results of calculations. Two additional minor assumptions concerning the site binding are (i) that the surface charge is linearly related to degrees of site titration (for example via  $\sigma_0 = F\Gamma_{BH} = F\Gamma_B^m \alpha_{BH}$  where  $\Gamma_B^m$  denotes the surface density of a base site) and (ii) that the sites do not interact in any other way than through the mean electrostatic field of the double layer.

The Stern potential  $\psi_S$  is related to the surface charge  $\sigma_0$  and surface potential  $\psi_0$  through the Stern capacitance  $K_S$  via

$$\sigma_0 = K_S(\psi_0 - \psi_S) \quad [1]$$

The diffuse charge density  $\sigma_d$  (which cancels the surface charge density exactly as the Stern layer is devoid of charge) is related to the Stern potential via the capacitance relation for the diffuse part of the double layer

$$\sigma_d = -2K/\beta \sinh(\beta\psi_S/2) \quad [2]$$

where  $\beta$  is the constant  $F/RT$ .  $K$  is defined as

$$K \equiv \epsilon\kappa \quad [3]$$

$$\kappa \equiv (2F\beta 55.56 \cdot 10^3 / \epsilon)^{\frac{1}{2}} \cdot x_S^{\frac{1}{2}} \quad (\text{m}^{-1})$$

where  $\epsilon$  is the dielectric constant of the solution and  $\kappa$  the reciprocal double layer thickness.

Combination of eqs. [1] and [2] yields an integral capacitance relation between the surface charge and surface potential

$$\sigma_0 = 2K/\beta \sinh\{\beta(\psi_0 - \sigma_0/K_S)/2\} \quad [4]$$

The functionality of  $\sigma_0$  in terms of  $\psi_0$  and  $x_S$  (which is implicit in eq.[4]) is briefly written as

$$\sigma_0^{DL} = \sigma_0^{DL}(\psi_0, x_S) \quad (\text{from double layer properties}) \quad [5]$$

As the capacitance relation [4] is derived from Gouy-Chapman-Stern double layer properties only,  $\sigma_0^{DL}$  does not contain information on the titration of the various surface sites. In section 4.2.3 we show there is a second functionality of  $\sigma_0$  in terms of  $\psi_0$ ,  $x_S$ ,  $x_H$  and  $x_{OH}$  (designated  $\sigma_0^{SB}$ ) with the complementary characteristics.

The interfacial ionic components of charge in the non-diffuse part (<sup>nd</sup>) of the double layer are denoted by  $\Gamma_H^{nd}$ ,  $\Gamma_{OH}^{nd}$ ,  $\Gamma_M^{nd}$  and  $\Gamma_X^{nd}$ , so

$$\sigma_0 = F(\Gamma_H^{nd} - \Gamma_{OH}^{nd} + \Gamma_M^{nd} - \Gamma_X^{nd}) \quad [6]$$

The diffusely bound charges are given by

$$\sigma_{d,H} = F\Gamma_H^d = 0 \quad (x_H \ll x_S) \quad [7]$$

$$\sigma_{d,OH} = -F\Gamma_{OH}^{nd} = 0 \quad (x_{OH} \ll x_S)$$

$$\sigma_{d,M} = F\Gamma_M^d = K/\beta \{ \exp(-\beta\psi_S/2) - 1 \}$$

$$\sigma_{d,X} = -F\Gamma_X^d = -K/\beta \{ \exp(\beta\psi_S/2) - 1 \}$$

These equations satisfy the electroneutrality condition of the total double layer (surface charge + diffuse charge),

$$\sigma_{d,M} + \sigma_{d,X} = \sigma_d = -\sigma_0 \quad [8]$$

#### 4.2.2 CONSIDERATIONS ON THE EXCESS FREE ENTHALPY

One of our aims is to study the contribution of charge-regulation to the net excess free enthalpy of interaction  $\Delta G_{int.}$  of variably charged surfaces. To that end, an explicit expression is needed for the excess free enthalpy  $G_E$  of free surfaces:  $\Delta G_{int.}$  is completely determined by the difference between the excess free enthalpies of the surfaces in the interacting and non-interacting state. In literature, relatively little attention is paid to the computation of  $G_E$  for site-binding models. Usually attention is focused on the charge-potential relations (11,12,13). In fact, we know of only one article in modern literature (14) where an explicit expression for the surface grand partition

function is given, but even there numerical results of calculations of  $G_E$  are not presented.

In this sub-section we present an alternative derivation of  $G_E$ . The result will be formally equivalent to that of Healy and White (14), but the method is more easily extended to the case of surfaces in close proximity. In addition, the thermodynamic reference point is explicated by using a modification of the reference approach of chapters 2 and 3.

We are interested in the change of the free enthalpy of the system upon the insertion of a single surface in a solution. As we add only one "particle", the osmotic pressure will not increase significantly if the area to volume ratio is within reasonable limits. Stated otherwise, we may consider the L vessel (see chapters 2 and 3) as the bulk (phase  $\alpha$ ), its bulk properties are identical to those of the R vessel. The volume of the bulk is considered as infinitely large. Hence, any finite change in the set of total number of molecules  $N_i^\alpha$  will not affect the set of mole fractions  $x_i^\alpha$ , and thus the chemical potentials  $\mu_i$  are constant.

The phenomenological analysis of chapters 2 and 3 was based on uncharged components, whereas we are now considering ionic components. Nevertheless we can still use the (modified) reference system by employing a charging process (8,14). If we denote the chemical potentials of the uncharged ions by  $\mu_{i,u}$ , and the contribution of the charging process by  $\mu_{i,el}$  (a similar notation is used for the free enthalpies), we may write

$$\mu_k = \mu_{k,u} + \mu_{k,el} \quad k = H, OH, M, X \quad [9]$$

We will now derive the sought expression for  $G_E$ .

1. In the initial situation (the thermodynamic reference point) we have phase  $\alpha$  separated from the surface  $\sigma$  (not to be confused with surface charge). The total free enthalpy expressed per unit of area of the surface is given by

$$G(1) = G^{\sigma,0} + \sum_k \mu_k \Gamma_k^\alpha \quad [10]$$

where  $G^{\sigma,0}$  is the free enthalpy of the surface in air.

2. The second step involves discharging the ions on the surface and in the bulk. After this step,

$$G(2) = G_u^{\sigma,0} + \sum_k \mu_{k,u} \Gamma_k^\alpha \quad [11]$$

3. Next we add the surface to the solution and let  $\Gamma_k^{nd}$  discharged ions  $k$  bind on the surface sites. Due to the infinite volume of the bulk, all the  $\mu_k$ 's remain constant. We then have,

$$G(3) = G_u^\sigma + \sum_k \mu_{u,k} (\Gamma_k^\alpha - \Gamma_k^{nd}) \quad [12]$$

4. In the fourth step we recharge all the ions, after which

$$G(4) = G_u^\sigma + G_{el}^\sigma + \sum_k \mu_k (\Gamma_k^\alpha - \Gamma_k^{nd}) \quad [13]$$

where  $G_{el}^\sigma$  is the free enthalpy of charging the surface while keeping the quantities  $\Gamma_k^{nd}$  constant.

The excess free enthalpy  $G_E$  is now obtained by subtracting  $G(1)$  from  $G(4)$ .

$$G_E \equiv G(4) - G(1) = G_u^\sigma + G_{el}^\sigma - G^{\sigma,0} - G^\alpha \quad [14]$$

where  $G^\alpha$  (the free enthalpy change of the solution) is defined as

$$G^\alpha \equiv \sum_k \mu_k \Gamma_k^{nd} \quad [15]$$

The free enthalpy of charging the surface can be split into two contributions. One term accounts for the electrostatic self-energies of the adsorbed ions (denoted by  $\mu_{k,el}^{0,\sigma}$ ) and one term accounts for the interionic (double layer) interactions. In the mean field approximation the  $\mu_{k,el}^{0,\sigma}$  do not depend on the surface concentrations and so the double layer free enthalpy can be calculated through

$$G_{el}^\sigma = \int_0^{\sigma_0} \psi d\sigma + \sum_k \mu_{k,el}^{0,\sigma} \Gamma_k^{nd} \quad [16]$$

In the case of flat surfaces an analytical expression for the charging integral is obtained by substituting the implicit capacitance relation [4]. We obtain

$$\int_0^{\sigma_0} \psi d\sigma = \frac{1}{2} \sigma_0^2 / \kappa_B + 4\sigma_0 / \beta \operatorname{arcsinh}(\beta \sigma_0 / \kappa) - 2/\beta^2 (4\kappa^2 + \beta \sigma_0^2)^{\frac{1}{2}} + 4\kappa / \beta^2 \quad [17]$$

We see that both the surface concentration and the ionic composition of the

solution determine the value of the  $G_{e1}^{\sigma}$ .

$G_u^{\sigma}$  depends only on the surface concentrations, but in an intricate way. In the following sections, we will show there are two factors contributing to  $G_u^{\sigma}$  which are related to the degrees of titrations ( $\alpha_i$ ) of the sites. One contribution originates from the specific chemical interactions of the ions with the sites (involving terms of type  $\alpha_i \Delta g_i \Gamma_s^m$  where  $\Gamma_s^m$  is the surface density of a site). The second contribution accounts for the configurational entropy of the ions bound on the sites (e.g.  $RT \Gamma_s^m \{ \alpha_i \ln \alpha_i + (1-\alpha_i) \ln (1-\alpha_i) \}$ ). The exact formula for these two contributions will be given in section 4.5.

$G^{\alpha}$  accounts for the change in free enthalpy of the solution upon the insertion of the surface. Its value depends both on the chemical potentials of the ions and the non-diffusely adsorbed amounts. The expression for  $G^{\alpha}$  can be slightly simplified by considering additional relations between the chemical potentials. We have

$$\mu_H + \mu_{OH} = \mu_{H_2O} = \text{constant} \quad (x_{H_2O} \approx 1) \quad [18]$$

$$\mu_X = \mu_M + \mu_X^0 - \mu_M^0 \quad (x_M = x_S)$$

Hence, we may select the chemical potentials of the protons and the cations as the independent quantities. Combination of eqs. [18] and [15] yields

$$G^{\alpha} = (\Gamma_H^{nd} - \Gamma_{OH}^{nd}) \mu_H + (\Gamma_M^{nd} + \Gamma_X^{nd}) \mu_M + \Gamma_{OH}^{nd} \mu_{H_2O} + \Gamma_X^{nd} (\mu_X^0 - \mu_M^0) \quad [19]$$

#### 4.2.3. ION ADSORPTION ISOTHERMS

When the system (surface + solution) is in equilibrium,  $G_E$  must be minimal and consequently invariant with respect to any infinitesimal change in any of the degrees of titration  $\alpha_i$  of the sites

$$\left( \frac{\delta G_E}{\delta \alpha_i} \right)_{T, \mu_k, \alpha_{j \neq i}} = 0 \quad k = H, M \quad [20]$$

If we next apply the chain rule for differentiation, eq. [20] is written as

$$\left( \frac{\delta G_E}{\delta \alpha_i} \right)_{T, \mu_k, \alpha_{j \neq i}} = \left( \frac{\delta G_E}{\delta \alpha_i} \right)_{T, \mu_k, \alpha_{j \neq i}, \psi_0} + \left( \frac{\delta G_E}{\delta \psi_0} \right)_{T, \mu_k, \alpha_i} \cdot \left( \frac{\delta \psi_0}{\delta \alpha_i} \right)_{T, \mu_k, \alpha_{j \neq i}} \quad [21]$$

In the equilibrium situation the derivatives of  $G_u^\sigma$ ,  $G^0, \sigma$ ,  $G_{e1}^\sigma$  and the bulk term  $G^\alpha$  with respect to the surface potential are zero because all of them can be expressed as a function of the degrees of titration only (the charging term through eq. [17]). Hence, the second term in eq. [21] vanishes. Differentiation of  $G_E$  with respect to the degrees of titration at constant surface potential leads to explicit expressions for the  $\alpha_1$  in terms of the surface potential and the ionic concentrations. Of course, in order to carry out the differentiation we need an explicit expression for  $G_u^\sigma$  in terms of the degrees of titration. However, as stated before, our analysis is not restricted to a particular type of site binding. Therefore, in order to keep the discussion as general as possible, we will postpone presentation of the resulting formula for the  $\alpha_1(\psi_0, x_k)$  to section 4.5, which contains details of a particular set of allowed ionic configurations.

One of our assumptions was that the surface charge is linearly correlated to the degrees of titration (section 4.2.1). Hence, proper summation of the expressions for the  $\alpha_1$  results in a second relation (denoted by  $\sigma_0^{SB}$ ) between the surface charge, the surface potential and the ionic composition of the bulk,

$$\sigma_0^{SB} = \sigma_0^{SB}(\psi_0, x_k) \quad (\text{from site binding}) \quad [22]$$

From the Gouy-Chapman-Stern description of the double layer we derived the relation  $\sigma_0^{DL}(\psi_0, x_S)$  (eq. [5]). As  $\sigma_0^{DL}$  must be equal to  $\sigma_0^{SB}$  in equilibrium, they can be solved for the surface potential. Once the surface potential is known, the degrees of titration and subsequently the excess free enthalpy can be calculated. In section 4.5. we will give more details on the implementation of this procedure (and a similar one for interacting surfaces) in a computer program.

#### 4.2.4 THERMODYNAMIC CONSISTENCY

The proof that our analysis of the electrochemistry of (non-interacting) surfaces is consistent with thermodynamics, involves the re-derivation of the phenomenological Gibbs adsorption equation. To that end, we examine how the total differential of  $G_E$  (at constant temperature) is related to the adsorptions and chemical potentials of the electroneutral species  $HX, MX$  and  $MOH$ .

First, the differential of the excess free enthalpy is written in terms of the ionic chemical potentials of the protons and the cations, according to

$$dG_E = \sum_k \left( \frac{\delta G_E}{\delta \mu_k} \right)_{T, \mu_{s \neq k}} d\mu_k \quad k = H, M \quad [23]$$

By applying the chain rule for differentiation, the differential coefficients of eq. [23] can be written as,

$$\left( \frac{\delta G_E}{\delta \mu_k} \right)_{T, \mu_{s \neq k}} = \left( \frac{\delta G_E}{\delta \mu_k} \right)_{T, \mu_{s \neq k}, \alpha_i} + \sum_i \left( \frac{\delta G_E}{\delta \alpha_i} \right)_{T, \mu_{s \neq k}, \alpha_{j \neq i}} \cdot \left( \frac{\delta \alpha_i}{\delta \mu_k} \right)_{T, \mu_{s \neq k}, \alpha_{j \neq i}} \quad [24]$$

The first terms in the products in the sum are zero in view of the equilibrium condition [20], so

$$\left( \frac{\delta G_E}{\delta \mu_k} \right)_{T, \mu_{s \neq k}} = \left( \frac{\delta G_E}{\delta \mu_k} \right)_{T, \mu_{s \neq k}, \alpha_i} \quad [25]$$

The differential of  $G_E$  is equal to the sum of the differentials of the various contributions to  $G_E$  (see [14])

$$dG_E = dG_u^\sigma + dG_{el}^\sigma - dG^{0, \sigma} - dG^\alpha \quad [26]$$

As the degrees of titration are held constant (right hand side of eq. [25]), the differentials  $G_u^\sigma$  and  $G^{0, \sigma}$  are zero. Differentiating the electric term yields

$$\left( \frac{\delta G_{el}^\sigma}{\delta \mu_H} \right)_{T, \mu_M, \alpha_i} = \left( \frac{\delta G_{el}^\sigma}{\delta \mu_H} \right)_{T, \mu_M, \sigma_0} = 0 \quad [27]$$

$$\left( \frac{\delta G_{el}^\sigma}{\delta \mu_M} \right)_{T, x_H, \alpha_i} = - \frac{2K}{\beta^2 RT} \{ \cosh(\beta \psi_S / 2) - 1 \} = - (\Gamma_M^d + \Gamma_X^d)$$

In the last differentiation use is made of eqs. [4] and [17]. Differentiation of  $G^\alpha$  results in

$$\begin{aligned} \left( \frac{\delta G^\alpha}{\delta \mu_H} \right)_{T, \mu_M, \alpha_i} &= \left( \frac{\delta G^\alpha}{\delta \mu_H} \right)_{T, \mu_M, \Gamma_k^{nd}} = - (\Gamma_H^{nd} - \Gamma_{OH}^{nd}) \\ \left( \frac{\delta G^\alpha}{\delta \mu_M} \right)_{T, x_H, \alpha_i} &= \left( \frac{\delta G^\alpha}{\delta \mu_M} \right)_{T, x_H, \Gamma_k^{nd}} = - (\Gamma_M^{nd} + \Gamma_X^{nd}) \end{aligned} \quad [28]$$

The derivatives of  $G_E$  with respect to  $\mu_M$  and  $\mu_H$  can now be written as

$$\left(\frac{\delta G_E}{\delta \mu_H}\right)_{T, x_M} = -(\Gamma_H - \Gamma_{OH}) \quad [29]$$

$$\left(\frac{\delta G_E}{\delta \mu_M}\right)_{T, x_H} = -(\Gamma_M + \Gamma_X)$$

Next, we identify the adsorptions and the chemical potentials of the ionic components with those of HX, MOH and MX,

$$\Gamma_H - \Gamma_{OH} \equiv \Gamma_{HX} - \Gamma_{MOH} \quad [30]$$

$$\Gamma_M \equiv \Gamma_{MX} + \Gamma_{MOH}$$

$$\Gamma_X \equiv \Gamma_{MX} + \Gamma_{HX}$$

$$d\mu_M = \frac{1}{2}d\mu_{MX}$$

$$d\mu_H = d\mu_{HX} - \frac{1}{2}d\mu_{MX}$$

Finally the differential of  $G_E$  can be written as

$$dG_E = -(\Gamma_{HX} - \Gamma_{MOH})d\mu_{HX} - \Gamma_{MX}d\mu_{MX} \quad [31]$$

which is just the Gibbs adsorption equation. Hence, our analysis is consistent with thermodynamics. Note that we did not need to restrict ourselves to any particular kind of site binding model.

#### 4.3 ELECTROCHEMISTRY OF INTERACTING SURFACES

##### 4.3.1 THE ELECTRICAL DOUBLE LAYER

In this section we discuss the double layer of two contacting surfaces. The distance between two such surfaces is generally so small (a few tenths of a nanometer) that the adsorption of diffuse ions is negligible. Therefore we assume that the Gouy-Chapman layer is absent. The surface charge of the one surface <sup>(1)</sup> then constitutes the counter-charge for the second surface <sup>(2)</sup> and conversely such that  $\sigma_0^1 \equiv -\sigma_0^2$ . The charges are assumed to be separated by a

kind of Stern layer, consisting of a charge-free, thin dielectric sheet.

When the two surfaces are within the range of molecular forces, many ions will be locked in a ion pair as a result of the extremely high micro-potentials which occur when an acid site on the one surface is near a base site on the second surface. Especially when the sites are covalently bound to surface attached oligomers ion pairs are likely to form. Although such ion pairs could also be present on free surfaces (between adjoined acid and base sites), they will generally be more dominant in the case of two interacting surfaces: the surfaces can adjust their lateral positions so to diminish steric constraints in the ion pair formation.

One extra assumption allows us to account for ion pair formation. We realize that under most circumstances it will be very difficult for an ion pair to titrate. Therefore, we assume that the degrees of titration of the acid and base site involved in an ion pair are constant (zero and unity respectively), whatever the value of the surface potential or the ionic concentrations. By doing so, the net charge of an ion pair is zero by definition. As a consequence the ion pair does not contribute to the electrostatic potential in the Stern layer.

The surface charge is now of course only dependent on the surface concentrations of those ions not involved in an ion pair. If we denote the ions involved or not involved in ion pair formation by the superscripts <sup>b</sup> (from "bridge") and <sup>nb</sup> respectively, we have

$$\sigma_0^j = F(\Gamma_H^{jnb} - \Gamma_{OH}^{jnb} + \Gamma_M^{jnb} - \Gamma_X^{jnb}) \quad j = 1, 2 \quad [32]$$

In principle it is impossible to attribute the adsorption of the ion pair forming ions to one of the individual surfaces separately because they adsorb on both surfaces at the same time. The total adsorption of the ions is then given by

$$\Gamma_k = \sum_j \Gamma_k^{jnb} + \Gamma_k^b \quad k = H, OH, M, X \quad [33]$$

The electric capacitance  $K_g$  of the Stern layer (the "gap") is related to the surface charges and surface potentials by two simple double layer capacitance equations (cf. eq.[1]),

$$\sigma_0^1 = K_g(\psi_0^1 - \psi_0^2) \quad [34]$$

$$\sigma_0^2 = K_g (\psi_0^2 - \psi_0^1)$$

It is easy to see that indeed  $\sigma_0^1 = -\sigma_0^2$ , and hence the two interacting surfaces together are always electroneutral.

The functionalities of the surface charges in terms of the surface potentials as given by eq.[34] are denoted by  $\sigma_0^{jdl}$  ( $j=1,2$ ), similar to the case for free surfaces.

$$\sigma_0^{jdl} = \sigma_0^{jdl}(\psi_0^1, \psi_0^2) \quad j=1,2 \quad [35]$$

#### 4.3.2 THE EXCESS FREE ENTHALPY

The derivation of the excess free enthalpy of interacting surfaces  $G_E^i$ , proceeds according to the scheme of section 4.2.2. As the thermodynamic reference we have now the two interacting surfaces, together separated from the bulk. The surfaces are inserted into the solution while keeping their relative positions fixed. We immediately obtain

$$G_E^i \equiv G^i(4) - G^i(1) = G_u^{\sigma i} + G_{el}^{\sigma i} - G^{\sigma, 0i} - G^{\alpha i} \quad [36]$$

By analogy to [16], the electrical term is written as

$$G_{el}^{\sigma i} = \int_0^{\sigma_0^2} (\psi_0^2 - \psi_0^1) d\sigma^2 + \sum_j \sum_k \mu_{k,el}^{0\sigma i} \Gamma_k^{jnb} \quad [37]$$

An analytical expression for the integral is obtained by substituting the double layer capacitance relations (eq. [34])

$$\int_0^{\sigma_0^2} (\psi_0^2 - \psi_0^1) d\sigma = \frac{1}{2} (\sigma_0^2)^2 / K_g = \frac{1}{2} (\sigma_0^1)^2 / K_g \quad [38]$$

$G_u^{\sigma i}$  contains an extra term with respect to the corresponding  $G_u^\sigma$  for a free surface. The additional contribution accounts for the ion pair formation and involves terms of type  $\Delta g_b \Gamma_s^m$ . The expressions for the specific chemical interactions and the configurational entropy of the adsorbed ions are given by the sum of the corresponding expressions for the free surfaces. As stated before, we will give these relations in section 4.5.

### 4.3.3 ION ADSORPTION ISOTHERMS

The excess free enthalpy of interacting surfaces may be split into two independent contributions, one from the ion pairs and the other from the titratable sites

$$G_E^i = G_E^{ib} + G_E^{inb} \quad [39]$$

As the degrees of titration of the ion pair forming sites are constant, in equilibrium  $G_E^i$  must be minimal with respect to the  $\alpha_i^{nb}$  only. If we then apply the same kind of reasoning as we used for the free surfaces (section 4.2.3) we find for the equilibrium condition

$$\left( \frac{\delta G_E^i}{\delta \alpha_i^{nb}} \right)_{\mu_k, \alpha_{n \neq i}^{jnb}, \psi_0^j} = 0 \quad [40]$$

From this equation, expressions for  $\alpha_i^{jnb}(\psi_0^j, x_k)$  can again be derived. In fact they must be morphologically identical to the formulas for the  $\alpha_i(\psi_0, x_k)$  of the free surfaces. Proper summation of the degrees of titration results in an explicit functionality of the surface charges in terms of the surface potentials and the ion concentrations

$$\sigma_0^{jSB} = \sigma_0^{jSB}(\psi_0^j, x_k) \quad (\text{from site binding}) \quad [41]$$

As before, in equilibrium the  $\sigma_0^{jDL}$  must be equal to the  $\sigma_0^{jSB}$ : we have two equations which can be solved for the two unknown surface potentials. Once their values are available, the excess free enthalpy can be calculated. See section 4.5 for details.

### 4.3.4 THERMODYNAMIC CONSISTENCY

In the derivation of the Gibbs adsorption equation for interacting surfaces we follow the reasoning of section 4.2.4. In doing so we encounter a small difficulty due to the ion pair formation, but by considering the differentials of  $G_E^{ib}$  and  $G_E^{inb}$  separately, the problem is solved. The differential of the excess free enthalpy is then written as

$$dG_E^i = dG_E^{inb} + dG_E^{ib} \quad [42]$$

The degrees of titration of the ion pairs are constant, so for the derivatives of  $G_E^{ib}$  we find

$$\left(\frac{\delta G_E^{ib}}{\delta \mu_H}\right)_{T, \mu_M} = \left(\frac{\delta G^{i\alpha b}}{\delta \mu_H}\right)_{T, \mu_M} = -(\Gamma_H^b - \Gamma_{OH}^b) \quad [43]$$

$$\left(\frac{\delta G_E^{ib}}{\delta \mu_M}\right)_{T, \mu_H} = \left(\frac{\delta G^{i\alpha b}}{\delta \mu_M}\right)_{T, \mu_H} = -(\Gamma_M^b + \Gamma_X^b)$$

The derivatives of  $G_E^{inb}$  yield (cf. section 4.2.4)

$$\left(\frac{\delta G_E^{inb}}{\delta \mu_H}\right)_{T, \mu_M} = \left(\frac{\delta G_E^{inb}}{\delta \mu_H}\right)_{T, \mu_M, \alpha_i^{jnb}} = -(\Gamma_H^{nb} - \Gamma_{OH}^{nb}) \quad [44]$$

$$\left(\frac{\delta G_E^{inb}}{\delta \mu_M}\right)_{T, \mu_H} = \left(\frac{\delta G_E^{inb}}{\delta \mu_M}\right)_{T, \mu_H, \alpha_i^{jnb}} = -(\Gamma_M^{nb} + \Gamma_X^{nb})$$

After combination of eqs. [43] and [44] and some rearrangement we again obtain the Gibbs adsorption equation

$$dG_E^i = -(\Gamma_{HX} - \Gamma_{OH})d\mu_{HX} - \Gamma_{MX}d\mu_{MX} \quad [45]$$

#### 4.4 NET FREE ENTHALPY OF INTERACTION

Suppose we would bring the two surfaces in the solution from infinite separation to their final interaction positions while maintaining the ion adsorption equilibrium. Following section 4.2.2., the fourth step of the insertion scheme, the net free enthalpy of interaction is then given by

$$\Delta G_{int.} = \Delta G_u^\sigma + \Delta G_{el}^\sigma - \Delta G^\alpha \quad [46]$$

where  $\Delta G$  stands for  $G(\text{interacting}) - G(\text{free})$ . From a comparison of the expression for  $\Delta G_{int.}$  with the expressions for  $G_E$  (eqs. [14] and [36]) we deduce that the net free enthalpy of interaction is equal to the difference of the excess free enthalpies apart from a constant which does not depend on the degrees of titration or the chemical potentials. This constant virtually acts

as a reference.

By taking the differentials of the net free enthalpy of interaction with respect to the chemical potentials, that is, by combining eqs.[31] and [45], we obtain a Gibbs "co-adsorption" equation

$$d\Delta G_{int.} = -(\Delta\Gamma_{HX} - \Delta\Gamma_{MOH})d\mu_{HX} - \Delta\Gamma_{MX}d\mu_{MX} \quad [47]$$

This co-adsorption equation is identical to the one we derived through pure phenomenological arguments (see chapter 3, eq.[5]), so once again we have proven the thermodynamic consistency of our model analysis.

#### 4.5 CALCULATIONS

##### 4.5.1 DETAILS OF THE SITE BINDING MODEL

We consider acid (A) and base sites (B) with the ion configurations  $A^-$ , AH, AM, B,  $BH^+$ ,  $BM^+$ ,  $BX^-$ , BHX and BMX. The surface densities of the ion configurations are denoted by  $\Gamma_i$  ( $i = AH, BM$  etc.). The degrees of titration of the sites with protons or electrolyte ions are defined as

$$\begin{aligned} \alpha_{AH} &\equiv \Gamma_{AH} / \Gamma_A^m & \alpha_{AM} &\equiv \Gamma_{AM} / \Gamma_A^m & [48] \\ \alpha_{BH} &\equiv \Gamma_{BH} / \Gamma_B^m & \alpha_{BM} &\equiv \Gamma_{BM} / \Gamma_B^m & \alpha_{BX} &\equiv (\Gamma_{BHX} + \Gamma_{BMX} + \Gamma_{BX}) / \Gamma_B^m \end{aligned}$$

In this way we disregard adsorption of the hydroxyl ions. Its inclusion would complicate the analysis without producing more insight. The surfaces of most (bio)organic colloids (e.g. protein molecules, membranes, polystyrene latices) do not contain hydroxyl binding sites anyway.

For the interacting surfaces we also have to consider the ion pairs. In order to simplify matters considerably, we only allow for ion pairs with an interstitial proton between an acid and a base site (AHB), other types of ion pairs are not taken into account.

##### 4.5.2. EXPLICIT EXPRESSIONS

As we are only interested in the electrochemical parts of the free enthalpies, we neglect all the terms independent of the salt and proton

concentration. For the purpose of easy calculation and clear presentation of the results, the expressions for the excess free enthalpies are then slightly re-written as

$$G_E = G_C + G_S^\sigma + G_{el} - G_S^\alpha \quad [49]$$

In  $G_C$  the specific chemical interactions and the electrostatic self-energies of the free and adsorbed ions are lumped together in the parameter  $\Delta g_i$  (e.g.  $\Delta g_{AH} \equiv \mu_{AH}^{0\sigma} - \mu_A^{0\sigma} - \mu_H^{0\alpha}$ ).  $G_S^\sigma$  and  $G_S^\alpha$  account for the mixing entropy of the non-diffusely adsorbed ions on the surface and in the solution respectively. The electrical term contains only the charging integral, the electrostatic self-energies are incorporated in  $G_C$ . In the case of interacting surfaces an extra term is added,  $G_B$ , which quantifies the ion pair formation (through  $\Delta g_{AHB} \equiv \mu_{AHB}^{0\sigma i} - \mu_{AB}^{0\sigma i} - \mu_H^{0\alpha}$ ).

All the explicit expressions are listed in the tables 4.1. and 4.2. on the following pages.

TABLE 4.1: Charge-Potential Relations

|  | ACID  | BASE  |
|--|---|---|
| FREE STATE:  |   |   |
| $\Gamma_H^{nd}$  | $\Gamma_A^m (\alpha_{AH}^{-1})$   | $\Gamma_B^m \alpha_{BH}$  |
| $\Gamma_M^{nd}$  | $\Gamma_A^m \alpha_{AM}$  | $\Gamma_B^m \alpha_{BM}$  |
| $\Gamma_X^{nd}$  | 0   | $\Gamma_B^m \alpha_{BX}$  |
| $\sigma_0$   | $F\Gamma_A^m (\alpha_{AH} + \alpha_{AM}^{-1})$                            | $F\Gamma_B^m (\alpha_{BH} + \alpha_{BM}^{-1} - \alpha_{BX})$  |
| $\alpha_H$   | $A_H / (1 + A_H + A_M)$   | $B_H / (1 + B_H + B_M)$   |
| $\alpha_M$   | $A_M / (1 + A_H + A_M)$   | $B_M / (1 + B_H + B_M)$   |
| $\alpha_X$   | 0   | $B_X / (1 + B_X)$   |
| $A_H : B_H$  | $\exp(-\Delta g_{AH} - \beta\psi_0 + \ln x_H)$                            | $\exp(-\Delta g_{BH} - \beta\psi_0 + \ln x_H)$  |
| $A_M : B_M$  | $\exp(-\Delta g_{AM} - \beta\psi_0 + \ln x_S)$                            | $\exp(-\Delta g_{BM} - \beta\psi_0 + \ln x_S)$  |
| $B_X$  |   | $\exp(-\Delta g_{BX} + \beta\psi_0 + \ln x_S)$  |
| $C_i$  | $F\Gamma_A^m (1 - \alpha_{AH} - \alpha_{AM}) (\alpha_{AH} + \alpha_{AM})$ | $F\Gamma_B^m \{ (1 - \alpha_{BH} - \alpha_{BM}) (\alpha_{BH} + \alpha_{BM}) + (1 - \alpha_{BX}) \alpha_{BX} \}$ |
| $C_{i,H}$  | $F\Gamma_A^m (1 - \alpha_{AH} - \alpha_{AM}) \alpha_{AH}$                 | $F\Gamma_B^m (1 - \alpha_{BM} - \alpha_{BX}) \alpha_{BH}$   |
| INTERACTING STATE:   |   |   |
| as above, but replace $\psi_0$ by $\psi_0^1$ or $\psi_0^2$ and nd by nb. |   |   |
| $\alpha_{AHB} \equiv 1$ if the ion pair is incorporated.                 |   |   |

TABLE 4.2: Free Enthalpies

|  | ACID   | BASE   |
|--|--|--|
| FREE STATE:  |  |  |
| $G_C$  | $\Gamma_A^m (\Delta g_{AH}^{\alpha_{AH}} + \Delta g_{AM}^{\alpha_{AM}})$   | $\Gamma_B^m (\Delta g_{BH}^{\alpha_{BH}} + \Delta g_{BM}^{\alpha_{BM}} + \Delta g_{BX}^{\alpha_{BX}})$   |
| $G_S^{\sigma}$   | $\Gamma_A^m \{ \alpha_{AH} \ln \alpha_{AH} + \alpha_{AM} \ln \alpha_{AM} + (1 - \alpha_{AH} - \alpha_{AM}) \ln (1 - \alpha_{AH} - \alpha_{AM}) \}$ | $\Gamma_B^m \{ \alpha_{BH} \ln \alpha_{BH} + \alpha_{BM} \ln \alpha_{BM} + (1 - \alpha_{BH} - \alpha_{BM}) \ln (1 - \alpha_{BH} - \alpha_{BM}) + \alpha_{BX} \ln \alpha_{BX} + (1 - \alpha_{BX}) \ln (1 - \alpha_{BX}) \}$ |
| $G_{el}^{\sigma}$  | eq.[17]  |  |
| $G^{\alpha}$   | $-\Gamma_H^{nd} \ln x_H - (\Gamma_M^{nd} + \Gamma_X^{nd}) \ln x_S$   |  |
| INTERACTING STATE:   |  |  |
| as above, but replace eq.[17] by eq.[38] and $^{nd}$ by $^{nb}$ (the $\alpha_i$ refer to the titratable sites only). |  |  |
| $G_B$  | $\Delta g_{AHB} \Gamma_{AHB}^m$  |  |

#### 4.5.3 CALCULATION PROCEDURE

The equations for the site binding  $\sigma_0^{SB}$  and double layer  $\sigma_0^{DL}$  charges (see sections 4.2.2 and 4.3.2) were solved for the surface potentials by a Newton iteration procedure, implemented in a Simula program on a DEC-10 mainframe computer. The (absolute) difference in the equilibrium charges ( $\sigma_0^{SB} - \sigma_0^{DL}$ ) was typically less than  $10^{-9}$  C/m<sup>2</sup>. After the iterations the surface potentials and the degrees of titration were available and the free enthalpies could be calculated. For a given set of ion concentrations the CPU time was about 0.3 sec.

#### 4.5.4 RESULTS

The parameters we selected are listed in table 4.3. One surface (denoted 1) is covered with weak acid sites ( $pK_A = 5$ , 2 sites/nm<sup>2</sup>), the second surface (2) with strong base sites ( $pK_B = 12$ , 1 site/nm<sup>2</sup>). The free and interacting states are denoted by ( $\bar{f}$ ) and ( $\bar{1}$ ) respectively.

The values for the Stern capacitances we used (3.54 F/m<sup>2</sup>) are fairly high. For model systems such as the H<sub>g</sub> and AgI solid-liquid interface values for  $K_S$  of about 0.3 F/m<sup>2</sup> (15) have been reported. However, recent results indicate that for (metal)oxide surfaces (16) and polystyrene lattices (1,13,14)  $K_S$  is at least above 2 F/m<sup>2</sup>. In the classical analysis of protein titration curves by Tanford (17) the relative dielectric constant and thickness of the Stern layer are set to 80 and 2-4 nm respectively, which leads to about the same value for  $K_S$  which we use. In addition, from a comparison with the results of simulations performed with a tenfold lower Stern capacitance, we found that the important trends are rather insensitive to the precise values of  $K_S$ . The reason for this effect will be explained shortly.

---

 TABLE 4.3: Parameter values used in the calculations
 

---

*MX concentration 0.1 (M).*

*pH varies from 2 to 10.*

*First surface (index <sup>1</sup>) contains acid sites only, second surface (<sup>2</sup>) base sites.*

*First computation (without ion pairs):*

$$\Gamma_A^m = 2 \text{ sites/nm}^2 = 3.32 \cdot 10^{-6} \text{ (mol/m}^2\text{)}$$

$$\Gamma_B^m = 1 \text{ site/nm}^2 = 1.66 \cdot 10^{-6} \text{ (mol/m}^2\text{)}$$

$$\Delta g_{AH}^f = \Delta g_{AH}^i = -15.52 \text{ RT (} pK_a = 5\text{)} \quad \Delta g_{AM}^f = \Delta g_{AM}^i = 0$$

$$\Delta g_{BH}^f = \Delta g_{BH}^i = -31.65 \text{ RT (} pK_b = 12\text{)} \quad \Delta g_{BM}^f = \Delta g_{BM}^i = \Delta g_{BX}^f = \Delta g_{BX}^i = 0$$

$$K_S^1 = K_S^2 = K_g = 3.54 \text{ (F/m}^2\text{)} \text{ (} \epsilon_S = 80, d_S = 0.2 \text{ nm)}$$

*Second computation (with ion pairs):*

*Ion pairs between all base sites and half of the acid sites.*

$$\Gamma_{AHB}^m = 1 \text{ ion pair/nm}^2 = 1.66 \cdot 10^{-6} \text{ mol/m}^2$$

$$\Delta g_{AHB} = -40 \text{ RT}$$

*Other parameters as in the first computation.*

---

The ways the surface charges, surface potentials and degrees of titration vary with the pH (at 0.1 M of MX) are shown in figs.4.1, 4.2 and 4.3. respectively. The curves are readily understood by considering the intrinsic capacitances ( $C_1$ ) of the surfaces. The  $C_1$  of a surface quantifies the adaptability of the charges on the sites with respect to the surface potential. If it is zero, the surface charge is constant under all circumstances. If it is large, a small increase of the surface potential leads to a large change in charge. The intrinsic capacitances are defined through

Free surfaces:

$$C_1 \equiv - \left( \frac{\delta \sigma_0^{SB}}{\delta \psi_0} \right)_{T, x_S, x_H}$$

$$C_{1,H} \equiv \beta \left( \frac{\delta \sigma_0^{SB}}{\delta \ln x_H} \right)_{T, x_S, \psi_0}$$

Interacting surfaces:

$$C_1^j \equiv - \left( \frac{\delta \sigma_0^{jSB}}{\delta \psi_0^j} \right)_{T, x_S, x_H} \quad [50]$$

$$C_{1,H}^j \equiv \beta \left( \frac{\delta \sigma_0^{jSB}}{\delta \ln x_H} \right)_{T, x_S, \psi_0^j}$$

For the expressions in terms of the degrees of titration, see table 4.1. The values for the intrinsic capacitances (fig.4.4) are, of course, not constant, because they depend on the degrees of titration. From the formulas in table 4.1 it is clear that the values for  $C_1$  may be appreciable, especially when the site density is high and the sites are half titrated. One might say that then the buffering capacity with respect to changes in  $\sigma_0$  is maximal.

Our model method of analysis offers an analytical relation between the intrinsic capacitances and the differential double layer capacitance ( $C_d \equiv (\delta \sigma_0^{DL} / \delta \psi_0)_{T, x_S}$ ) on the one hand and the slopes of the potential-pH and charge-pH curves on the other hand.

For free surfaces we have

$$d\sigma_0^{SB} = -C_1 d\psi_0 + C_{1,H} d \ln x_H / \beta = d\sigma_0^{DL} = C_d d\psi_0 \quad (dx_S = 0) \quad [51]$$

which after a little rearrangement yields

$$\left( \frac{\delta \psi_0}{d\text{pH}} \right)_{T, x_S} = -2.303 N / \beta \quad \left( \frac{d\sigma_0}{d\text{pH}} \right)_{T, x_S} = -2.303 C_d N / \beta \quad [52]$$

$$N \equiv C_{1,H} / (C_1 + C_d)$$

where the Nernst factor  $N$  is unity if the surface obeys Nernst's law. The intrinsic and (differential) double layer capacitances are plotted in fig.4.4.

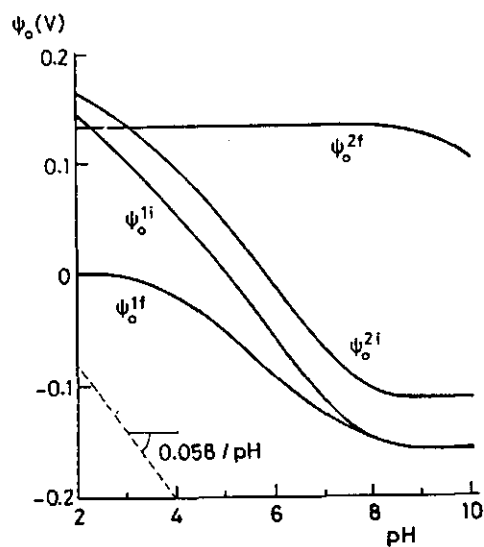


FIGURE 4.1 First computation, surface potentials. Superscripts denote surface and state, for example ( $1^f$ ) is first surface (the acid) in the free state.

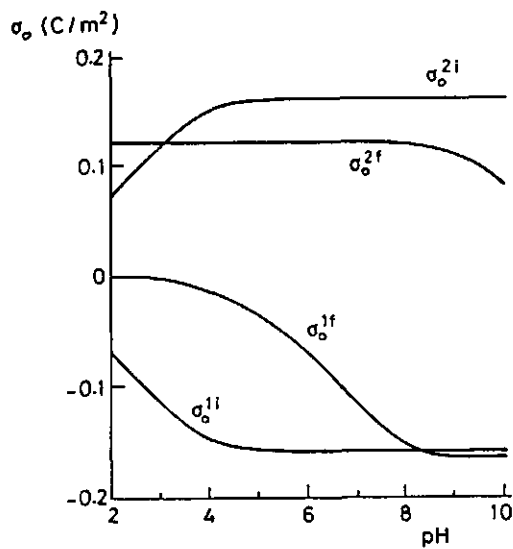


FIGURE 4.2 First computation, surface charges. Superscripts as in fig. 4.1

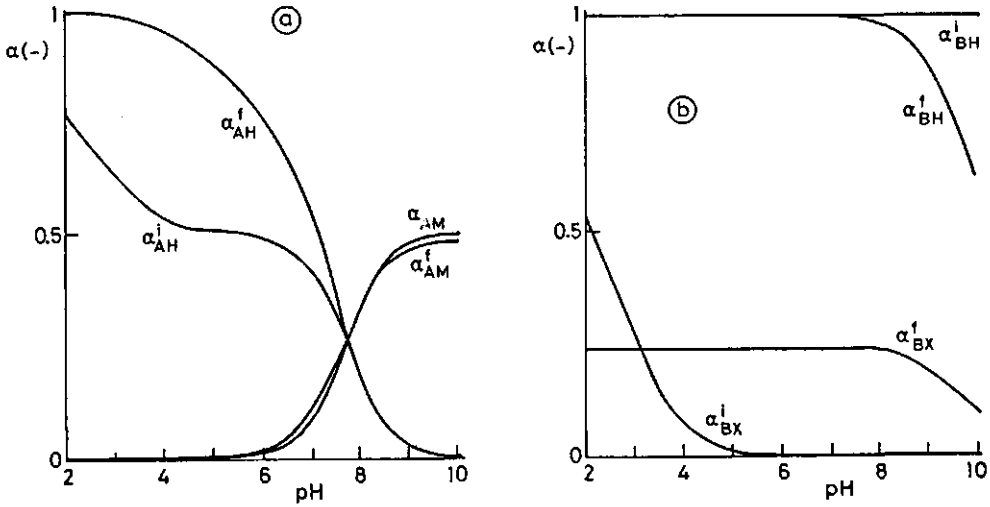


FIGURE 4.3 First computation, degrees of titration. a: acid surface, b: base surface.

Some years ago, Levine and Smith (18) derived equations similar to [52]. They used a more complicated site binding model, including adsorption in the Stern layer and discriminating between macro- and micro-potentials.

Equation [52] tells a simple story. If the surface sites are fully dissociated or associated, so that  $C_{1,H} = 0$ , the surface potential and surface are constant (curves  $\psi_0^{2f}(\text{pH})$  and  $\sigma_0^{2f}(\text{pH})$ ). If the degree of proton diss- or association is half, so that  $C_{1,H}$  is maximal, Nernstian behaviour is still not observed if there is non-diffuse binding of salt and/or  $C_d$  has a high value (curves  $\psi_0^{1f}(\text{pH})$  and  $\sigma_0^{1f}(\text{pH})$ ).

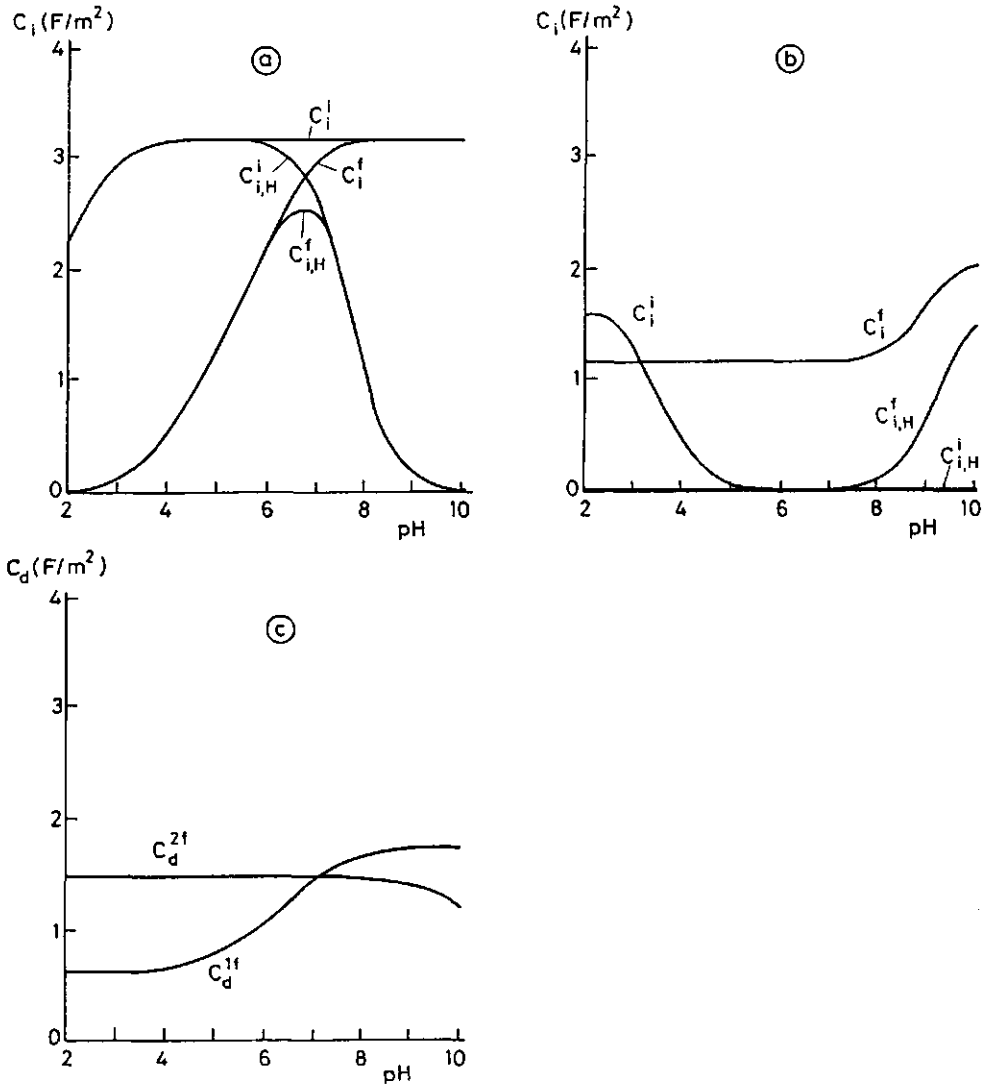


FIGURE 4.4 First computation, capacitances. a: intrinsic capacitances of acid surface, b: intrinsic capacitances of base surface, c: differential double layer capacitances (superscripts as in fig. 4.1)

For surfaces in interaction we have, accordingly

$$d\sigma_0^{1SB} = -C_{i,H}^1 d\psi_0^1 + C_{i,H}^1 d \ln x_H / \beta = d\sigma_0^{1DL} = K_g d\psi_0^1 - K_g d\psi_0^2 \quad [53]$$

$$d\sigma_0^{2SB} = -C_{i,H}^2 d\psi_0^2 + C_{i,H}^2 d \ln x_H / \beta = d\sigma_0^{2DL} = K_g d\psi_0^2 - K_g d\psi_0^1$$

which yields

$$\left(\frac{d\psi_0^1}{d\text{pH}}\right)_{T,x_S} = -2.303 N^1 / \beta \quad \left(\frac{d\psi_0^1}{d\text{pH}}\right)_{T,x_S} = -2.303 K_g N^1 / \beta \quad [54]$$

$$N^1 = \frac{C_{i,H}^1 C_i^2 + K_g (C_{i,H}^1 + C_{i,H}^2)}{C_i^1 C_i^2 + K_g (C_i^1 + C_i^2)}$$

and similar expressions for the second surface. There are two limiting cases which deserve special attention. One extreme situation arises when the site binding of salt is negligible so that  $C_{i,H}^j = C_i^j$ , and thus  $N^1 = N^2 = 1$ . The two surfaces will then always behave Nernstian, even if they can titrate but a little charge. The second extreme situation occurs when the charge of one of the surfaces is constant. If we assume, for example, that this is the case for the second surface, then  $C_{i,H}^2 = C_i^1 = 0$  and thus  $N^1 = N^2 = C_{i,H}^1 / C_i^1$ . In both extreme situations the two surface potentials change in concert. Now consider the slopes of the  $\psi_0^{1f}(\text{pH})$  and  $\psi_0^{2f}(\text{pH})$  curves. In the pH range 3-7, the acid surface does not take up salt ( $C_{i,H}^1 \approx C_i^1$ ) whereas the base surface cannot adjust its proton charge and charge-regulates but a little through the binding of anions ( $C_i^2, C_{i,H}^2 \ll K_g, C_i^1$ ). The result is that in the indicated interval  $N^1 \approx N^2 \approx 1$ .

The shifts in potential between the free and interacting state can also be interpreted in terms of the intrinsic capacitances, via the approximate expression

$$\sigma_0^{j1} - \sigma_0^{jf} = \int_{\psi_0^{jf}}^{\psi_0^{j1}} C_i^{jf} d\psi \approx \frac{1}{2} (C_i^{j1} + C_i^{jf}) (\psi_0^{j1} - \psi_0^{jf}) \quad [55]$$

For the first and second surface the means of the intrinsic capacitances between pH 3 and 8 are 2.4-3.2 F/m<sup>2</sup> and 0.6-1.2 F/m<sup>2</sup> respectively. Hence, in that pH interval the acid surface interacts with more "potential constant" and the base surface with more "charge constant" character.

The curves of the free enthalpies as a function of pH (fig.4.5) have some features in common. In every case  $(\Delta)G_{e1}$  and  $(\Delta)G_S^\sigma$  are relatively small compared to  $(\Delta)G_S^\alpha$  and  $(\Delta)G_C$ . One might think that the electric term is small because of the large values of the Stern capacitances. But if we would have chosen smaller values for  $K_S$ , the surface charges would have decreased due to the poorer electric shielding such that  $\frac{1}{2}\sigma^2/K_S$  would have remained small. That  $G_S^\alpha$  contributes little is easy to understand; the configurational entropy cannot be more than about  $0.7R$  per mole of sites. This means that the restrictions in the allowed ion configurations (section 4.5.1) do not critically influence the results. On the other hand, the chemical interactions on every site can amount to as much as  $-15.5 RT$  or  $-31.65 RT$  for the acid and base respectively, and at  $pH = 7$  the increase in configurational entropy of the bulk is  $20.1R$  per mole of adsorbed proton.

There is a simple relation between the intrinsic capacitances and the curvature of the  $G_E(pH)$  curves. From eq.[29] we have (for the free surfaces)

$$\left(\frac{\delta^2 G_E}{\delta \ln x_H^2}\right)_{T, x_S} = -RT \left(\frac{\delta \Gamma_H}{\delta \ln x_H}\right)_{T, x_S} \quad \rightarrow \quad [56]$$

$$\left(\frac{\delta^2 G_E}{\delta pH^2}\right)_{T, x_S} = -5.308 \frac{C_d N}{\beta^2(1+f_S)}$$

$$f_S \equiv \left(\frac{\delta(\Gamma_M^{nd} - \Gamma_X^{nd})}{\delta \Gamma_H}\right)_{T, x_S}$$

where  $f_S$  is the differential compensation of the proton charge by adsorbed electrolyte. As we have excluded hydroxyl binding, the second derivative of  $G_E$  is always positive. Hence, the curves bend downwards unless  $\Gamma_H$  is constant.

For the free acid surface, till  $pH \approx 5$ ,  $N < 0.6$ ,  $C_d \approx 0.6$  (F/m<sup>2</sup>) and the non-diffuse binding of salt (cations) is zero which results in a relatively small curvature. Between  $pH$  3 and  $pH$  8,  $C_d$  increases threefold due to the increase in surface potential while the Nernst factor remains approximately constant and  $f_S$  is still zero: the curve of  $G_E(pH)$  bends. Above  $pH$  8,  $N$  drops considerably because the acid sites cannot release more protons,  $C_d$  is constant, cations start to adsorb and the curvature is small again. For the base surface a similar argument can be used. In that case the Nernst factor is close to zero in the entire  $pH$  range such that the curvature of the excess free enthalpy is also almost zero.

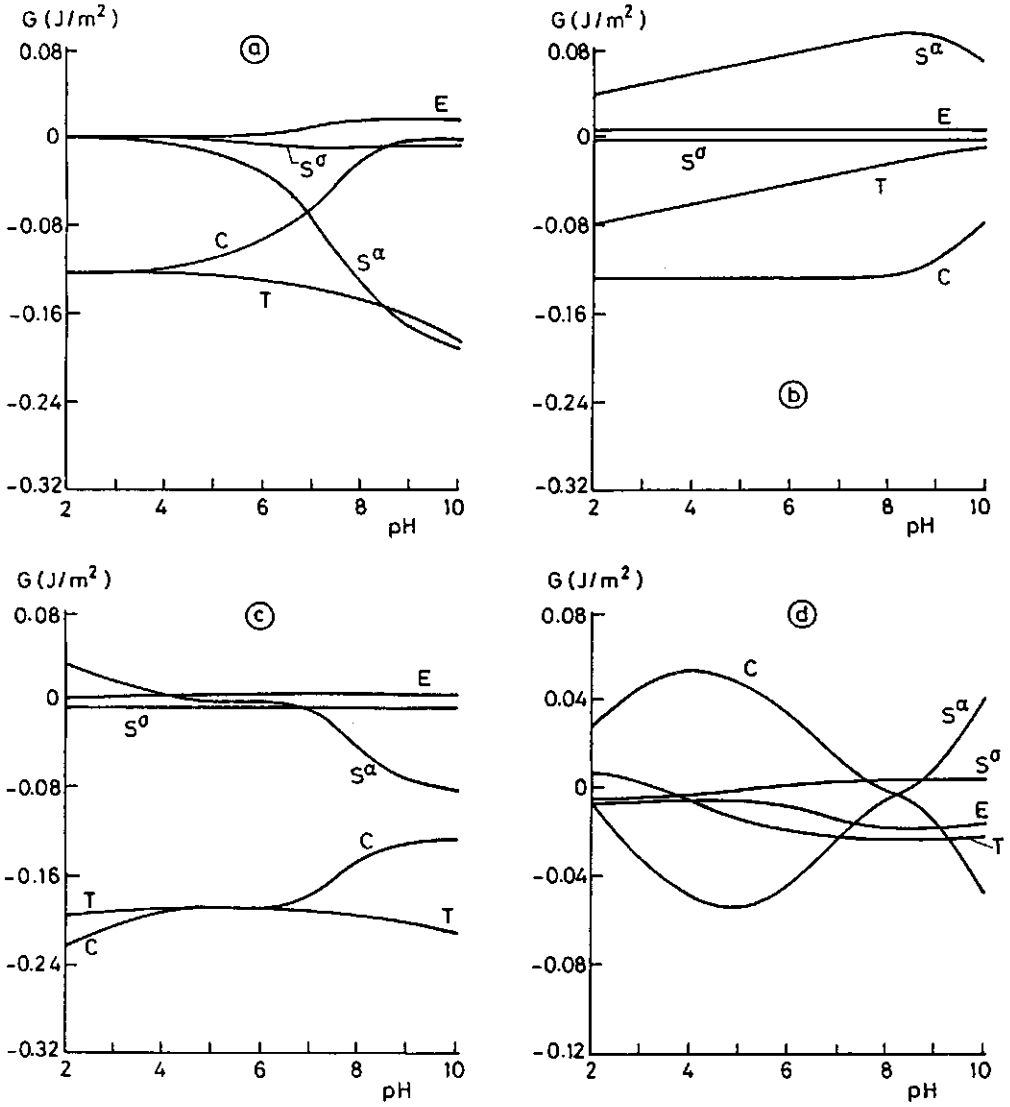


FIGURE 4.5 First computation, free enthalpies. a: excess free enthalpy of acid surface in the free state ( $G_E^1$ ), b: excess free enthalpy of base surface in the free state ( $G_E^2$ ), c: excess free enthalpy of the interacting state ( $G_E^i$ ), d: net free enthalpy of interaction ( $\Delta G_{int}$ ).

In all cases,  $E$  ( $= (\Delta)G_{el}$ ) denotes the charging integral,  $S^\alpha$  ( $= -(\Delta)G_S^\alpha$ ) the contribution of the configurational entropy of the solution,  $S^\alpha$  ( $= (\Delta)G_S^\alpha$ ) the contribution of the configurational entropy on the surface,  $C$  ( $= (\Delta)G_C$ ) the chemical term and  $T$  ( $= (\Delta)G_E$ ) the total. For definitions see section 4.5.2.

For the interacting surfaces we have

$$\left(\frac{\delta^2 G_E}{\delta \ln x_H^2}\right)_{T, x_S} = -RT \left(\frac{\delta \Gamma_H}{\delta \ln x_H}\right)_{T, x_S} \rightarrow \quad [57]$$

$$\left(\frac{\delta^2 G_E}{\delta pH^2}\right)_{T, x_S} = -5.308 \frac{K_g (N^1 - N^2) (f_S^1 - f_S^2)}{\beta^2 (1+f_S^1) (1+f_S^2)}$$

At once we see that because of the (partial) compensation of the proton charge of the one surface by the proton charge of the other surface (expressed by the product of the differences), the second derivative of  $G_E^1$  will typically be smaller than the second derivatives of  $G_E$  of the free surfaces. In the extreme case that salt incorporation is absent, the curvature must be zero (cf. pH 4-7).

The curve for  $\Delta G_{int.}$  has a minimum around pH 8 (fig.4.8a). At that pH the surfaces need not adapt their proton charge, the co-adsorption of protons is zero. Above pH 8 the free acid surface is more negative than the free base surface is positive, so that upon interaction the base surface takes up extra protons while the acid surface maintains its proton charge. Below pH 8 the opposite is true.

A second computation was carried out with ion pairs present between half of the sites of the acid surface and all of the sites of the base surface, setting  $\Delta g_{\text{AHB}} = -40 \text{ RT}$ . The properties of the free surfaces are thus the same as before. In the interacting state, the two surface charges are both zero (all base sites are involved in ion pairs, hence  $\sigma_0^{21} = 0 = \sigma_0^{11}$ ). The surface potentials always must be the same because  $K_g(\psi_0^{11} - \psi_0^{21}) = 0$ . However, they are in principle infinite: the sites of the acid surface not involved in an ion pair must be titrated such that their remaining charge is zero ( $1 - \alpha_{\text{AH}}^{\text{nb}} - \alpha_{\text{AM}}^{\text{nb}} = 0$ ). In the calculations, the tolerance in the residual charge was reached at surface potentials between  $-0.5$  and  $-0.8 \text{ V}$ . The curves for the degrees of titration are given in fig. 4.6. We see that the titratable sites take up about twice as many cations as in the first computation, but as the density of the sites is reduced by a factor of two, the total number of incorporated cations is not changed very much. The intrinsic capacitances are zero over the entire pH range because the surface charge is zero and the proton release is exactly compensated by cation uptake.

The free enthalpies of the interacting state are given in fig. 4.7a. The electrical term is now of course zero because the surface charges are also zero.  $G_S^\sigma$  is even smaller than before as less sites contribute to the configurational entropy. The Nernst factors are undetermined now, we therefore cannot use eq. [57] directly. However if we take the limit  $C_i^j \rightarrow 0$  we obtain the simple formula

$$\left(\frac{\delta^2 G_E}{\delta \text{pH}^2}\right)_{T, x_S} = -5.808 K_g \Gamma_A^m \alpha_{\text{AH}} (1 - \alpha_{\text{AH}}) / \beta^2 \quad [58]$$

It follows that the curvature of  $G_E^i(\text{pH})$  is maximal when  $\alpha_{\text{AH}}^{\text{nb}} = \frac{1}{2}$  (around pH 8, fig 4.7c). Of course, the minimum in the curve of the net free enthalpy of interaction (fig. 4.8b) is still at pH 8: its position is solely determined by the pH dependency of the charges of the free surfaces.

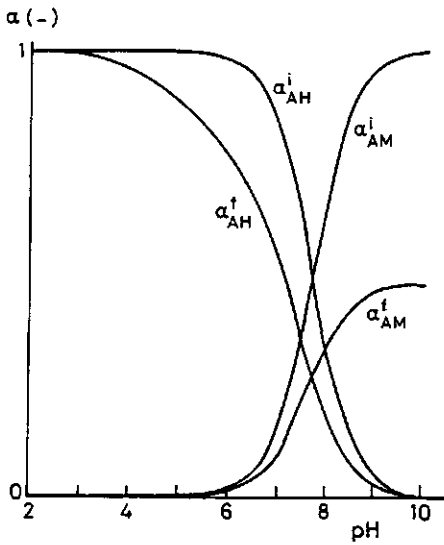


FIGURE 4.6 Second computation, degrees of titration of acid sites not involved in ion pair formation

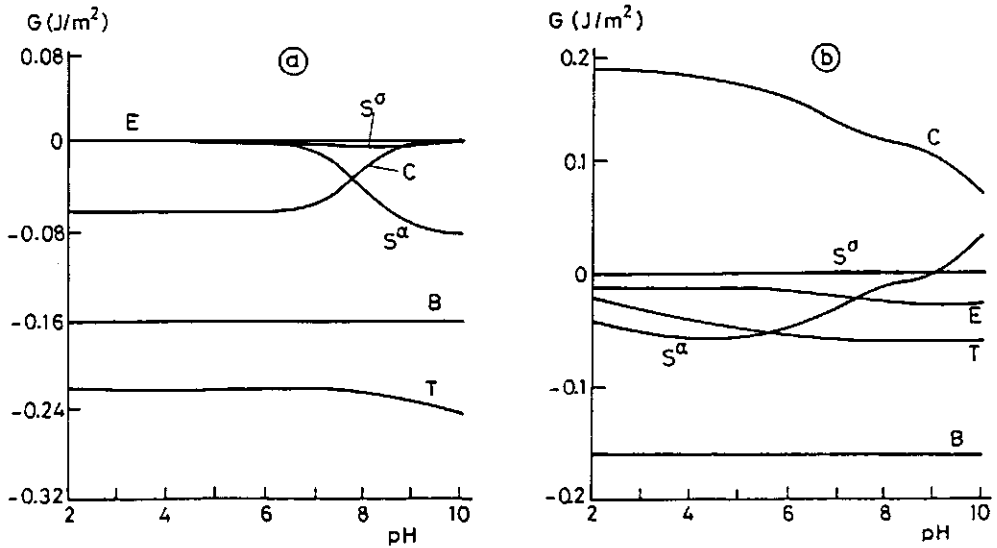


FIGURE 4.7 Second computation, free enthalpies. a: excess free enthalpy of interacting state, b: net free enthalpy of interaction. B (=  $G_B$ ) denotes contribution of ion pair formation. Other symbols as in fig. 4.5.

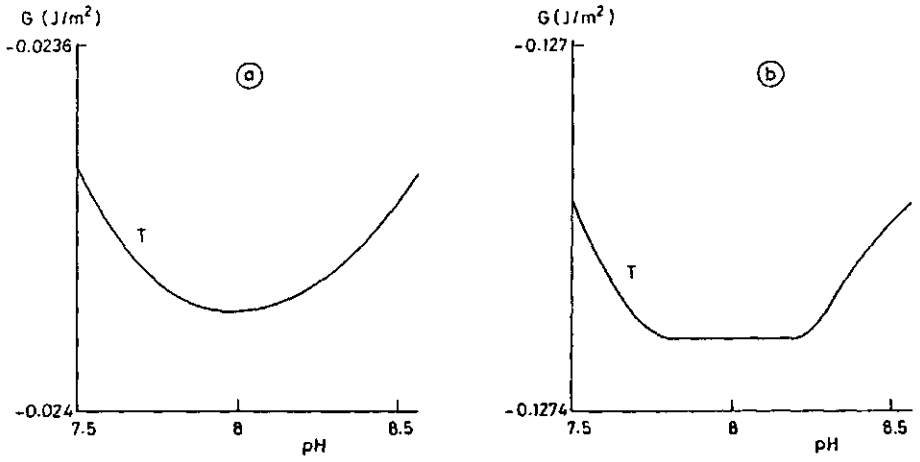


FIGURE 4.8 Expanded view of net free enthalpies of interaction. a: first computation, b: second computation. Symbols as in fig. 4.5.

## 4.6 REFERENCES

1. T.W. Healy, (1980) *Pure. Appl. Chem.* 52, 1207
2. B.W. Ninham, V.A. Parsegian (1973) *J. Theor. Biol.* 38, 101
3. V.A. Parsegian, D. Gingell (1972) *Biophys. J.* 12, 1192
4. D.C. Prieve, E. Ruckenstein (1980) *J. Colloid Interface Sci.* 73(2), 539
5. E. Ruckenstein (1978) *J. Colloid Interface Sci.* 66(3), 531
6. E. Ruckenstein, D.G. Kalthold (1981) in: B. Hallstrom, D.B. Lund, C. Traghardh (Eds) "Fundamentals and Applications of Surface Phenomena Associated with Fouling and Cleaning in Food Processing", p115. Reprocentralen, Lund, Sweden.
7. M.J. Scully (1986) *Biophysical Chemistry* 24, 33
8. J.Th.G. Overbeek (1952) in: H.R. Kruyt Ed. *Colloid Science*, chapters 4 and 6, Elsevier Publishing Company, Amsterdam-Houston-New York-London.
9. I.M. Metcalfe (1985), Ph.D. Thesis, Melbourne.
10. J.O'M. Bockris, A.K.N. Reddy (1970) "Modern electrochemistry, part II", Plenum Press, New York.
11. R.O. James (1981) in: M.A. Anderson, A.J. Rubin Eds. "Adsorption of Inorganics at Solid-Liquid Interfaces", chapter 6, Ann Arbor Science Publishers Inc., Ann Arbor
12. R.O. James, J.A. Parks (1982), *Surface and Colloid Sci.* 12, 119
13. I.H. Harding, T.W. Healy (1982) *J. Colloid Interface Sci.* 107(2), 382
14. T.W. Healy, L.R. White (1978) *Advan. Colloid Interface Sci.* 9, 303
15. B.H. Bijsterbosch, J. Lyklema (1978) *Advan. Colloid Interface Sci.* 7, 147
16. L.G.J. Fokkink (1987), Ph.D. Thesis, Wageningen.
17. C. Tanford (1962) *Advan. Protein Chem.* 17, 69
18. S. Levine, A.L. Smith (1971) *Discussions of the Faraday Society* 52, 290

## CHAPTER 5

## CHARGE REGULATION IN PROTEIN ADSORPTION

## 5.1 INTRODUCTION

## 5.1.1 GENERAL

In this chapter, the theory on charge regulation, developed in the previous chapters, is applied to an experiment. The system consists of particles of the insoluble salt silver iodide (AgI) as the adsorbent and the protein Bovine Serum Albumin (BSA) as the adsorbate. The experiment involves a series of pH-static titrations of AgI precipitates which are partially coated with protein. The system allows for independent control of the charge on the solid (through adjustment of the iodide concentration in the solution) and that on the adsorbed protein (through adjustment of the pH).

## 5.1.2 PROPERTIES OF AGI

Some relevant characteristics of AgI are briefly discussed below. For an extensive review of the electrochemistry of AgI see (1).

The Galvani potential difference  $\phi$  between the bulk phase of the solid AgI and the bulk phase of the solution is not influenced by a change in the composition of the interface at constant  $\text{Ag}^+$  ion activity. Apart from a constant, the Galvani potential can be measured with a AgI electrode (a Pt electrode coated with a thick layer of AgI), even if the surface of the electrode (or a dispersed AgI particle) is covered with protein. The relation between  $\phi$  and the  $\text{Ag}^+$  ion activity is given by Nernst's law,

$$\phi = \psi_0 + \chi' = 0.05816 \text{ pAg} + E \quad (\text{V}) \quad [1]$$

where  $\psi_0$  is the Volta potential (resulting from the accumulation of free charges in the interface),  $\chi'$  is the chi potential (due to the orientation of dipoles and polarisation of molecules in the interface), pAg is defined as

minus the logarithm of the  $\text{Ag}^+$  ion activity and  $E$  is a constant depending on the type of reference electrode. The difference of the Galvani potential with respect to the Galvani potential of bare AgI at the point of zero charge ( $p\text{Ag}_0 = 5.67$  (1)) can be calculated from,

$$\Delta\phi = \psi_0 + \chi = 0.05816 (p\text{Ag} - p\text{Ag}_0) \quad [2]$$

$$\chi \equiv \chi'(p\text{Ag}) - \chi'(p\text{Ag}_0)$$

The silver and iodide ion activities are connected through the solubility product  $S$  of AgI, which is extremely low in an aqueous environment. In 0.1 M  $\text{KNO}_3$ ,  $20^\circ \text{C}$ ,  $pS$  is given by,

$$pS = p\text{Ag} + p\text{I} = 16.07 \quad [3]$$

The Galvani potential difference  $\Delta\phi$  can be unambiguously measured, but one needs a model to separately estimate the Volta potential and chi potential. There are indications that there is a significant charge accumulation in the outer layers of the AgI crystals (5), in particular due to Frenkel defects. Furthermore, the chi potential is probably not independent of the Volta potential (4) because the orientation of the (water) dipoles in the interface is not fixed. These effects do not interfere with the thermodynamic analysis (section 5.4.1), but the model analysis (section 5.4.2) is dependent on the actual values for the surface (Volta) potential. However, incorporation of any sophisticated model for the calculation of the Volta and chi potentials in our co-adsorption model (chapter 4) would complicate matters far beyond the perspective of the present study. As a first approximation we will therefore assume that the AgI charge is confined to the surface and that the chi potential does not depend on  $\phi$ . As will be shown in section 5.4.2, the adsorption of the protein has but little effect on the chi potential anyway.

Silveriodide crystals do not contain acid or base sites. As a consequence, titrations of bare AgI precipitates with  $\text{AgNO}_3$  or KI in a (concentrated)  $\text{KNO}_3$  solution should give results which are independent of the pH. In all our experiments we used a  $\text{KNO}_3$  concentration of 0.1 M, the pH was between pH 4 and pH 7. Indeed, we found no influence of the pH of the blank titration curves.

It is not an easy task to determine the specific surface area of a AgI precipitate. Four different methods have been proposed (1,2): (i) BET

analysis, (ii) determination of dye plateau adsorption, (iii) determination of negative adsorption of indifferent electrolyte, (iv) double layer capacitance measurements. The latter two methods give values that are two to four times higher than the former two methods. In spite of an extensive discussion there is as yet no consensus about which method should be preferred. In most of the electrochemical work (1) the capacitance surface area was used for the analysis of AgI titration curves. More recently the dye (or BET) surface area was applied in adsorption studies of oligo- and polyelectrolytes (3). From a comparison of the maximally adsorbed amount of BSA with typical values reported in literature, we will conclude (section 5.3.1) that also in our case the dye surface area is appropriate.

### 5.1.3 PROPERTIES OF BOVINE SERUM ALBUMIN

Some relevant properties of BSA are collected in table 5.1. The structure of the protein has been described by Brown et al.(6). The backbone is folded in such a way that three almost identical "domains" interact through (weak) ion pairs. Probably in each domain the alpha-helices are aligned in a parallel fashion so as to form hydrophobic niches suitable for the binding of fatty acids, hormones, bilirubines and other (apolar) substances. A BSA molecule contains 17 disulfide bonds and one free mercapto group. In order to stabilize the arrangement of the disulfide bonds, we blocked the sulfhydryl with iodoacetamide (section 5.2.1) prior to the use of the protein in the adsorption and titration experiments. The isoelectric and isoionic points are at  $\text{pH} = 4.7$  and  $\text{pH} = 5.6$  respectively. Chapter 2, section 2.5, contains a thermodynamic analysis of the ion binding properties of BSA.

TABLE 5.1: Properties of Bovine Serum Albumin

|                           |       |                     |
|---------------------------|-------|---------------------|
|                           | ref.  |                     |
| Molecular weight          | (6)   | 67000 (Dalton)      |
| number of residues        | (6)   | 581                 |
| $\alpha$ -helix           | (10)  | 65 %                |
| $\beta$ -sheet            | (10)  | 18%                 |
| Sulfur bridges            | (6)   | 17                  |
| Mercapto groups           | (6)   | 1                   |
| shape (unhydrated)        | (8)   | 2.7x2.7x11.6 (nm)   |
| (hydrated)                | (9)   | 4x4x14 (nm)         |
| Ionic composition:        | (7)   |                     |
|                           | pK    | number per molecule |
| $\alpha$ -carboxyl        | 4.75  | 1                   |
| $\beta, \gamma$ -carboxyl | 4.0   | 99                  |
| imidazole                 | 6.9   | 16                  |
| $\alpha$ -amino           | 7.75  | 1                   |
| $\epsilon$ -amino         | 9.8   | 57                  |
| phenole                   | 10.35 | 19                  |
| guanidine                 | >12   | 22                  |
| mercapto                  | nd    | 1                   |

## 5.2 EXPERIMENTAL

### 5.2.1 PREPARATION OF AGI AND BSA

Two batches of AgI precipitate (A and B) were prepared by slowly adding 2 l of 0.105 M  $\text{AgNO}_3$  to 2 l of 0.1 M KI. The specific surface areas of the precipitates were determined by measuring the plateau adsorption of Methylene Blue ( $2.78 \mu\text{mol}/\text{m}^2$ ) as described by Koopal (2). The two batches had slightly different specific surface areas,  $0.25 \text{ m}^2/\text{gram}$  for precipitate A and  $0.30 \text{ m}^2/\text{gram}$  for precipitate B. These values were used to calculate the adsorbed amounts per unit of area. The titration experiments and the BSA plateau adsorption experiments were carried out with precipitate B, the other

experiments with precipitate A. The capacitance surface area and the point of zero charge of precipitate B were determined by short titrations around  $pAg = 5.5$ , their values were  $0.88 \text{ m}^2/\text{gram}$  and  $pAg_0 = 5.76$  respectively. As the literature value for the point of zero charge ( $pAg_0 = 5.67$ , (1)) is well established and close to the value we obtained, we used the literature value to fix the vertical positions of the titration curves.

BSA was purchased from Sigma (type VI,  $\gamma$ -globuline-and fatty acid free). The mercapto contents of the commercial protein preparation was between 0.3 and 0.4 sulfhydryl groups per BSA molecule. We decided to purify the protein, using a slight adaption of the method of Janatova et al. (11). We passed a concentrated BSA solution (4 grams in 50 ml eluens) through a DEAE-Sepharose 6B column (diameter 5 cm, bed volume 200 ml) with a solution of 0.02 M sodium phosphate buffer in 0.08 M NaCl (pH 6.8) as the eluens (25 ml/hour). Janatova used a gradient of increasing salt concentration whereas we preferred to use a constant salt concentration. After passage of 300 ml eluens, we collected about 1 gram of protein dissolved in 200 ml of eluens. The mercapto contents of the purified BSA was between 0.85 and 0.88. The sulfhydryl groups were subsequently carboxyamidated with either normal or radioactive ( $C^{14}$ ) iodoacetamide. Next, the protein was desalinated on a G-25 column and a Dowex mixed-bed ion exchanger, lyophilised and stored at  $-20^\circ \text{C}$ . The extinction coefficient of the finally obtained freeze-dried and salt-free protein was  $E_{280} = 0.671 \text{ ml}/\text{gram}/\text{cm}$ . The yield of the purification was 20 to 25%.

### 5.2.2 ADSORPTION ISOTHERMS AND EXCHANGE EXPERIMENTS

Adsorbed amounts of BSA were obtained by depletion. Typically, 0-5 ml of protein solution (containing 0-3 mg of BSA in 0.1 M  $\text{KNO}_3$ ) were added to 5 ml of well dispersed AgI precipitate (containing 1.7 gr AgI in 0.1 M  $\text{KNO}_3$ ) in 10 ml Sybron/Nalge polycarbonate centrifuge tubes. After the total volumes of the tubes had been adjusted to 10 ml with a 0.1 M  $\text{KNO}_3$  solution, the tubes were stoppered with polyethylene caps and shaken for 10 seconds on a Whirl mixer. The tubes were then rotated end over end for 16 hours to ensure constant protein adsorption (more than 90% of the final protein adsorption was already reached in less than a quarter of an hour). Next, the tubes were centrifuged for 20 minutes at 20000 rpm in a Beckman JA-21 centrifuge equipped with a JA-21 rotor. The protein concentration in the supernatant was determined by measuring the absorbance at 280 nm.

The protein-protein exchange experiments with the radioactive protein were conducted similar to the above procedure, but for safety reasons we had to make some adjustments. First, 5 ml unlabeled BSA (2 mg/ml) was added to 25 ml of dispersed AgI precipitate (solid contents 0.37 gram/ml) in a 50 ml Schott/Duran flask. The mixture was then vigorously stirred for 16 hours using a magnetic stirrer. After the protein adsorption had been determined, a small amount of radioactively labeled BSA (BSA<sup>\*</sup>) was added, less than 5% of the total amount of protein already present, and the stirring was continued. At selected time intervals 0.5 ml aliquots were taken from the dispersion and centrifuged in a top desk centrifuge in 1 ml polyethylene vials. The concentration of BSA<sup>\*</sup> in the supernatant was determined with a scintillation counter. From the adsorption ( $\Gamma$ ) and bulk concentration ( $c$ ) of BSA and BSA<sup>\*</sup>, the protein exchange ratio (PER) was calculated by

$$\text{PER} = \frac{\Gamma_{\text{BSA}^*}}{\Gamma_{\text{BSA}}} \cdot \frac{c_{\text{BSA}}}{c_{\text{BSA}^*}} \quad [4]$$

### 5.2.3 TITRATION EXPERIMENTS

The titration experiments were conducted in such a way that the charge of the AgI precipitate and the proton charge of the adsorbed BSA could simultaneously be measured.

The cell we used is sketched in fig. 5.1. The titrations were carried out in a thermostated (20<sup>o</sup> C) Schott titration vessel (maximum volume 150 ml). The vessel was equipped with four AgI electrodes fitted in one holder, a Schott pH glass electrode and a van Laar salt-bridge (resistance 700 kohm) connected to a reference vessel containing a Schott Ag/AgCl reference electrode. The electrode potentials were measured with a multichannel voltage meter (HP 3497A Data Acquisition/Control Unit) after they had been converted to low impedance signals with a home-built impedance transformer. The titrants (AgNO<sub>3</sub>/KI, both 0.01 M in 0.1 M KNO<sub>3</sub> and HNO<sub>3</sub>/KOH both 0.025 M in 0.1 M KNO<sub>3</sub>) were added with automated burets (Metrohm 655 Dosimat) through small teflon tubings. The titration vessel was continuously flushed with carbondioxide-free nitrogen gas. The homogenization of the (very) concentrated dispersion was achieved by stirring vigorously at the bottom and at the top of the vessel.

The experiments were automated by means of a HP 85 microcomputer. Every five minutes, the computer program collected the data from the electrodes, averaged

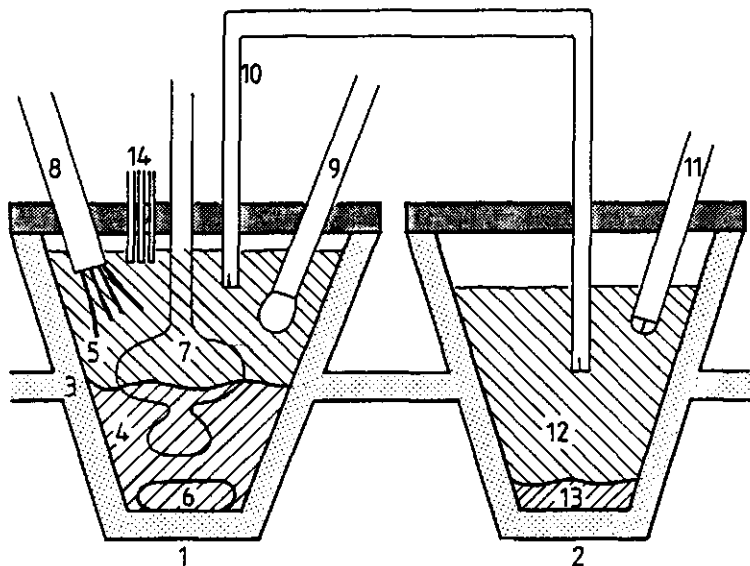


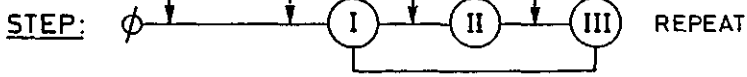
FIGURE 5.1. The cell used for the titration experiments. 1. titration vessel, 2. reference vessel, 3. water jacket, 4. AgI precipitate, 5. supernatant, 6. stirrer (bottom), 7. stirrer (top), 8. AgI electrode, 9. pH glass electrode, 10. salt-bridge, 11. Ag/AgCl reference electrode, 12. saturated KCl solution, 13. precipitated KCl, 14. titrant inlet.

the signals from the four independent AgI electrodes, decided whether equilibrium had set in (tolerated drifts 0.001 pH/min and 0.001 pAg/min, tolerated spread between the AgI electrodes 0.02 pAg), and ordered the burets to add small aliquots of titrant (0.01-0.1 ml) if necessary. The final titration curves were calculated from the raw data with a Simula program on a DEC-10 mainframe computer.

## AgI titration with pH stat

### ACTION:

ADD      ADJUST      ADD      ADJUST  
 BSA      pH              KI              pH  
 (~ 2 mg)    (~ 0.1 ml)    (~ 0.1 ml)    (~ 0.1 ml)



### CALCULATE:

$$\begin{array}{ccc}
 \sigma_A^I & & \sigma_A^{II} \approx \sigma_A^{III} \\
 \sigma_H^I & \approx & \sigma_H^{II} \quad \sigma_H^{III} \\
 pAg^I & & pAg^{II} \quad pAg^{III} \\
 pH^I & & pH^{II} \quad pH^{III}
 \end{array}$$

$$\sigma_A = F (\Gamma_{AgNO_3} - \Gamma_{KI}) \quad \sigma_H = F (\Gamma_{HNO_3} - \Gamma_{KOH})$$

$$pH^I \approx pH^{III} \approx pH \text{ stat}$$

### VISUALIZE:

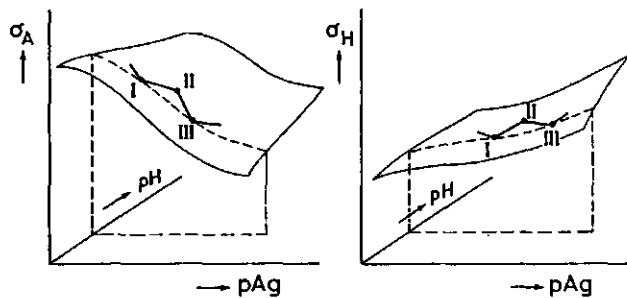


FIGURE 5.2. Scheme of the titration procedure.

The titration scheme is outlined in fig. 5.2. To the titration vessel containing 28-30 grams of AgI precipitate dispersed in 100 ml 0.1 M  $\text{KNO}_3$  at a  $p\text{Ag} \approx 5.5$  and  $\text{pH} = \text{pH}_{\text{stat}}$ , about 2 mg BSA dissolved in 1 ml 0.1 M  $\text{KNO}_3$  was added. The pH of the protein solution was also at the  $\text{pH}_{\text{stat}}$  value. Due to the adsorption of the protein, both the  $p\text{Ag}$  and the pH shifted from their initial values. After the pH was adjusted to the  $\text{pH}_{\text{stat}}$  value by adding  $\text{HNO}_3$  or  $\text{KOH}$ , a titration cycle (I,II,III) was repeated nine times. First KI was added (step I to II), after equilibration the pH was again adjusted to the previous  $\text{pH}_{\text{stat}}$  value (step II to III). The AgI ( $\sigma_A$ ) and proton ( $\sigma_H$ ) surface charge densities were calculated from the known amounts of titrants added and the measured  $p\text{Ag}$  and pH, using the specific surface area as determined from the Methylene Blue adsorption. A mathematical visualization of the titration scheme is also given in fig. 5.2. When the protein is adsorbed on the AgI precipitate, both the charge of the AgI and the proton charge of the protein are dependent on the  $p\text{Ag}$  and the pH.

At  $p\text{Ag} \approx 8$  the equilibration time was 1-2 hours, the total procedure for one curve took 6-8 hours. The total scheme was repeated several times with increasing loads of BSA.

To ensure that the  $\text{Ag}^+$  or  $\text{I}^-$  complexation with the (adsorbed) protein would be negligible, we conducted a series of  $\text{Ag}^+$  and  $\text{I}^-$  ion binding experiments according to the above titration scheme. In these experiments, the titration vessel contained 100 mg of BSA but no AgI precipitate. The results for  $\text{Ag}^+$  are given in fig. 5.3. We find that above  $\text{pH} = 7$  and below  $p\text{Ag} = 5$  the  $\text{Ag}^+$  ion complexation is substantial. Probably complexation takes place through the amino containing residues of BSA (12). The binding of iodide ions was below the detection limit. In the pH and  $p\text{Ag}$  range we used for the AgI titrations with adsorbed protein ( $\text{pH} < 7$ ,  $p\text{Ag} > 5.5$ ) the  $\text{Ag}^+$  ion binding by the protein can safely be neglected.

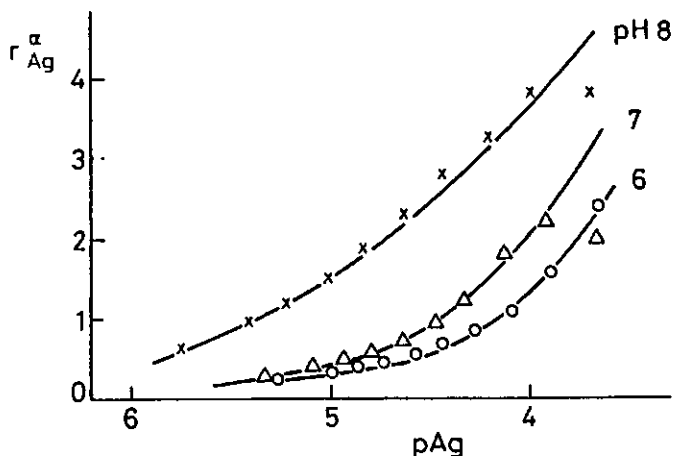


FIGURE 5.3. Binding of  $\text{Ag}^+$  ions to BSA in 0.1 M  $\text{KNO}_3$ . The pH is indicated.  $r_{\text{Ag}}^\alpha$  = mol of silver ions bound per mol of protein.

### 5.3 RESULTS

#### 5.3.1 ADSORPTION AND EXCHANGE EXPERIMENTS

The dependence of the adsorption of BSA ( $\Gamma_p$ ) on the bulk concentration ( $c_p$ ) is represented in fig 5.4a. The high affinity character of the adsorption is clearly demonstrated. Up to a value of 1-1.5  $\text{mg/m}^2$  the bulk concentration is virtually zero (less than 0.001  $\text{mg/ml}$ ), even when the protein and the AgI precipitate have the same sign of charge.

In these experiments the initial pH ( $\text{pH}_{\text{init.}}$ ) and pAg ( $\text{pAg}_{\text{init.}}$ ) of the AgI dispersion, the protein solution and the 0.1 M  $\text{KNO}_3$  solution were brought to the same value prior to mixing. The differences between the equilibrium pH and  $\text{pH}_{\text{init.}}$  and between the equilibrium pAg and  $\text{pAg}_{\text{init.}}$  are plotted in fig. 5.4b and fig 5.4c respectively.

The magnitudes of the pAg and pH shifts are of course dependent on the buffering capacities of the system for the  $\text{Ag}^+$ ,  $\text{I}^-$ ,  $\text{H}^+$  and  $\text{OH}^-$  ions, and therefore on the total amount of protein and AgI present. Indeed, the pH shifts decrease when the amount of protein (adsorbed plus non-adsorbed) increase. Although the pAg shifts are considerable, the AgI charge does not change much because of the large amount of precipitate.

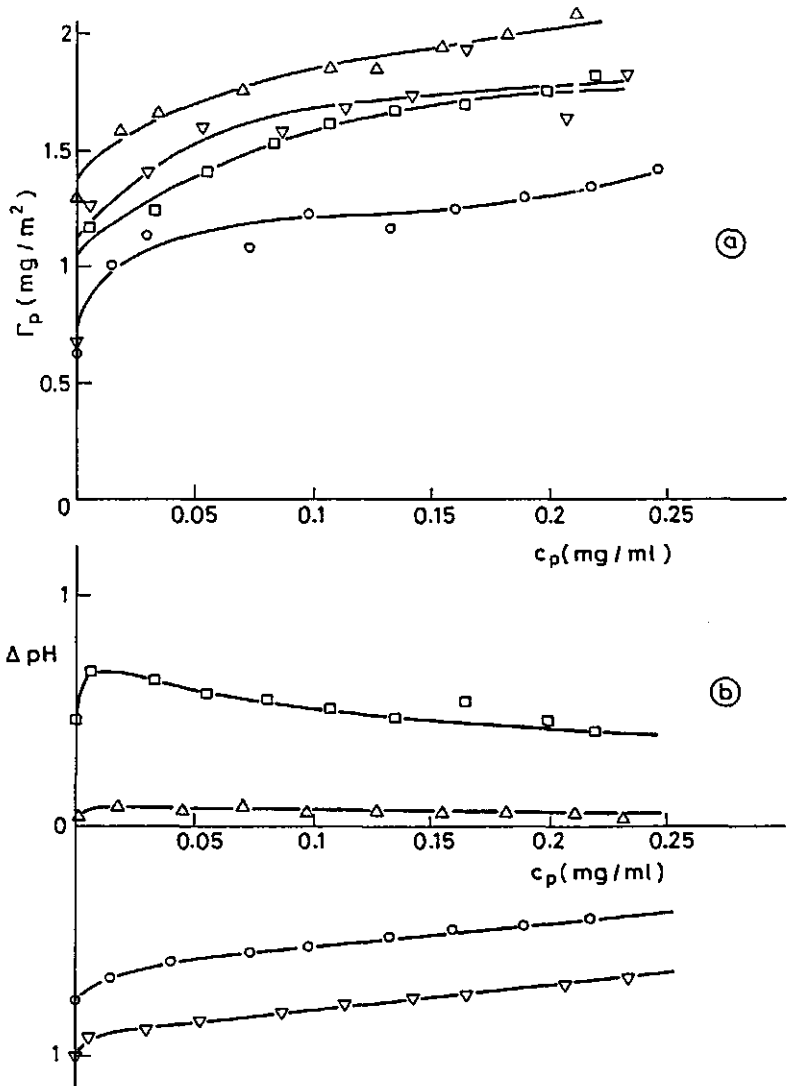


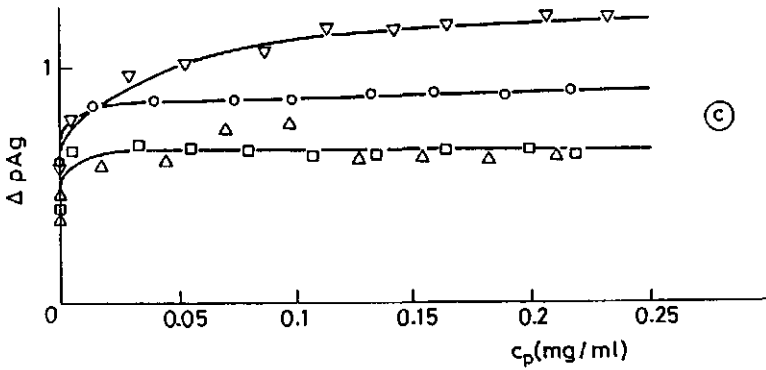
FIGURE 5.4. Adsorption of BSA on AgI in 0.1 M  $KNO_3$ .

| $pH_{init.}$ | $pAg_{init.}$ | symbol        |
|--------------|---------------|---------------|
| 7            | 6.07          | ( $\nabla$ )  |
| 7            | 10.07         | ( $\circ$ )   |
| 5            | 6.07          | ( $\Delta$ )  |
| 5            | 10.07         | ( $\square$ ) |

(a) Adsorbed amount of BSA ( $\Gamma_p$ ) vs. equilibrium concentration ( $c_p$ )

(b)  $\Delta pH = pH - pH_{init.}$

$$(c) \Delta pAg = pAg - pAg_{init.}$$



The  $pAg$  shifts for high and low  $pAg_{init.}$  (at constant  $pH_{init.}$ ) are similar. This indicates that the electrical capacitance of the AgI-liquid interface is only little influenced by the protein adsorption, an effect we will observe more directly in the shape of the AgI titration curves (section 5.3.2).

When the protein charge is fairly negative prior to adsorption ( $pH_{init.} = 7$ ) and the AgI charge is also negative but low ( $pAg_{init.} = 6.07$ ), the adsorbing protein, strangely enough, eject protons into the solution (the pH drops). On the other hand, when the AgI charge is more negative ( $pAg_{init.} = 10.07$ ), or the protein is initially almost uncharged ( $pH_{init.} = 5$ ) the adsorbing protein takes up protons from the solution (the pH rises).

In accordance with expectation, the Galvani potential of the AgI crystals becomes more negative upon adsorption of negatively charged BSA (the  $pAg$  shifts upwards), and the more so if the protein is initially more negative.

The titration experiments confirm all of these findings (section 5.3.2). An explanation of the most important effects will be given in terms of the co-adsorption model (chapter 4) in section 5.4.2.

In fig. 5.5 the plateau values of adsorption are represented for different values of the equilibrium pH and  $pAg$ . The plateau values were determined at constant total amount of protein in the system. Consequently, the bulk concentration varies a little with the adsorbed amount (between 0.11 and 0.2 mg/ml). The plateau value curves show that at  $pH = 4$  the adsorption is maximal at about  $1.8\text{--}2.3 \text{ mg/m}^2$ .

To the left of the isoelectric point (i.e.p) of the protein, the adsorption increases with decreasing Galvani potential, far to the right it is the other

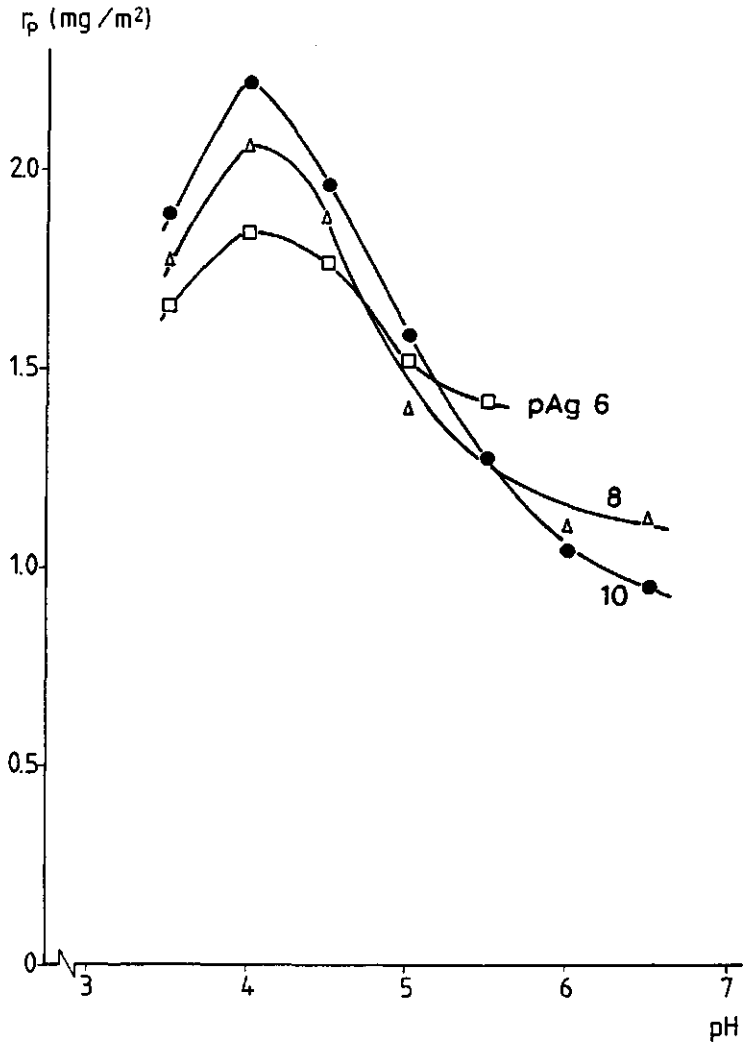


FIGURE 5.5. Plateau adsorption of BSA on AgI in 0.1 M KNO<sub>3</sub>. The pAg is indicated.  $c_p = 0.11 - 0.2$  mg/ml.

way around. This is probably due to the reversal of electrostatic interactions: below the i.e.p the affinity of the protein for the negative surface is higher than above the i.e.p and the more so if the surface potential is more negative (see however section 5.4.1 and below).

In literature it is well documented that the adsorption of BSA (or its human analogue Human Plasma Albumin) is maximal at, or close to, the isoelectric point (13,14,15,16). Our results confirm this. In addition, the maximum value corresponds well with values reported for a range of other surfaces. For sorbents like homo- and co-polymer latices (15,16), haemetite sol,  $\text{SiO}_2$  sol, polyoxymethylene crystals, polystyrene latices etc. (13,14) the maximum plateau value lies in the range of 2 to 3  $\text{mg/m}^2$ . We conclude that our results are not too "AgI" specific, and furthermore that the dye specific surface area we used is indeed appropriate.

An explanation of the value of the (plateau) adsorption is an intricate matter (17,18,19). Factors that favour the affinity of BSA for AgI (and hence would result in high adsorption if protein-protein repulsion forces were absent in the adsorbed layer) are a low protein stability and a positive protein charge. Both factors increase with decreasing pH. Factors that promote repulsion between adsorbed BSA molecules (and hence a low adsorption) are again a low protein stability (denaturation is accompanied by an increasing steric lateral repulsion as unfolded adsorbed BSA molecules occupy a larger portion of the surface) and a high protein charge. These factors are minimal around the isoelectric point. Obviously, the pH at which the attractions and repulsions balance does need not to be exactly at the isoelectric point.

Anticipating the thermodynamic analysis of section 5.4.1., the Gibbs energy of adsorption at pAg 6 and low surface coverage is similar for pH 4, pH 5 and pH 6. This would mean that the shape of the adsorption curve at pAg 6 (fig 5.5) reflects the variation of the BSA-BSA repulsion with the pH most clearly. To our surprise, we find that the increase of the repulsion cannot account for more than 10 to 20 percent of the decrease in plateau adsorption. If we then furthermore assume that the BSA molecule retains most of its shape when adsorbed at the isoelectric point as is commonly accepted (17,18,19), we must conclude that any structural alterations (which certainly will occur) do not lead to a gross unfolding of the adsorbed molecule. However, this may not be the full explanation. One of the findings of the thermodynamic analysis is that the Gibbs energy of adsorption at pAg 10, pH 4 is similar to that at pAg 6, pH 4 whereas the plateau adsorption at pAg 10, pH 4 is significantly larger

than the adsorption at pAg 6, pH 4. A further discussion will be postponed until sections 5.4.1 and 5.4.2.

We also studied the reversibility of the BSA adsorption by BSA<sup>\*</sup>-BSA exchange experiments. The results are represented in fig 5.6. We find that 30-40% of the protein exchanges within one minute and that 60-70% of the protein exchanges slowly in a few hours. After 12 hours, the exchange ratio reaches the value of 100%, indicating that the adsorption is at least reversible with respect to protein exchange. Neither the rates of exchange nor the final values of the exchange ratio do depend much on the pH. Perhaps the second exchange step is due to a heterogeneous population of adsorbed BSA molecules. As we have carefully purified the protein, the heterogeneity may be induced by the adsorption process but it is difficult to see how.

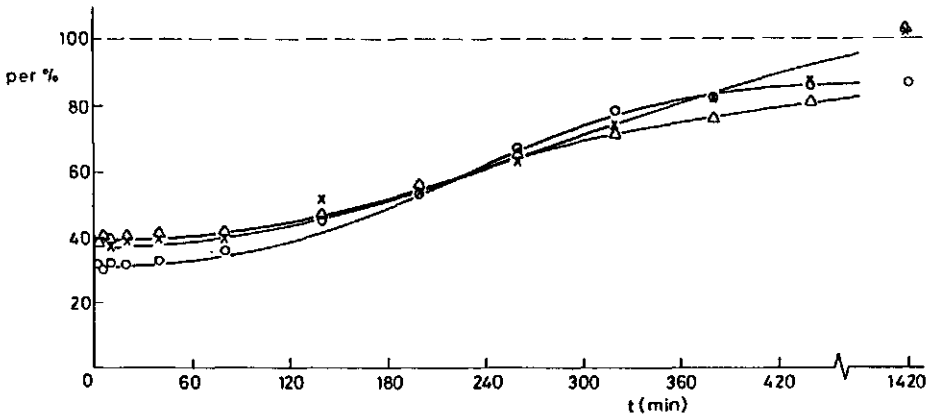


FIGURE 5.6. Protein Exchange Ratio (PER) vs. exchange time. 0.01 M KNO<sub>3</sub>, pAg 10.

pH 6,  $c_p = 0.08$  mg/ml (○) ; pH 5,  $c_p = 0.07$  mg/ml (×) ;  
 pH 4,  $c_p = 0.03$  mg/ml (Δ)

## 5.3.2 TITRATION EXPERIMENTS

Titration curves obtained at different pHstat values in 0.1 M  $\text{KNO}_3$  are represented in fig.5.7 (pHstat = 4), fig. 5.8 (pHstat = 5) and fig. 5.9 (pHstat = 6). Every titration experiment yielded six types of curves, each obtained at three different loads of BSA (apart from the blanks). Figs. 5.7-5.9, a and b, give the AgI charge density ( $\sigma_A = \sigma_A^{\text{III}}$ ) and proton charge density ( $\sigma_H = \sigma_H^{\text{III}}$ ) versus the pAg at constant pH. Figs. 5.7-5.9, c and e, give the change in the AgI charge density ( $\Delta\sigma_A = \sigma_A^{\text{III}} - \sigma_A^{\text{II}}$ ) and pAg ( $\Delta\text{pAg} = \text{pAg}^{\text{III}} - \text{pAg}^{\text{II}}$ ) when the system is titrated with  $\text{HNO}_3$ . Figs. 5.7-5.9, d and f, give the change in proton charge density ( $\Delta\sigma_H = \sigma_H^{\text{II}} - \sigma_H^{\text{I}}$ ) and pH ( $\Delta\text{pH} = \text{pH}^{\text{II}} - \text{pH}^{\text{I}}$ ) when the system is titrated with KI. The curves at constant pH (figs.5.7-5.9, a and b) will be discussed in detail below and in the next two sections. Due to the small specific surface areas of the precipitates, the measured effects in the pHstat cycle (figs.5.7-5.9, c through f) are not accurate enough for a quantitative analysis (although they will be used for a statistical test to verify the thermodynamic theory in section 5.4.1), and are therefore discussed briefly in a qualitative sense only.

In the titration experiments, the adsorption of BSA was below the plateau level at every pH. As BSA adsorbs with high affinity, the influence of non-adsorbed protein on the titrations is negligible.

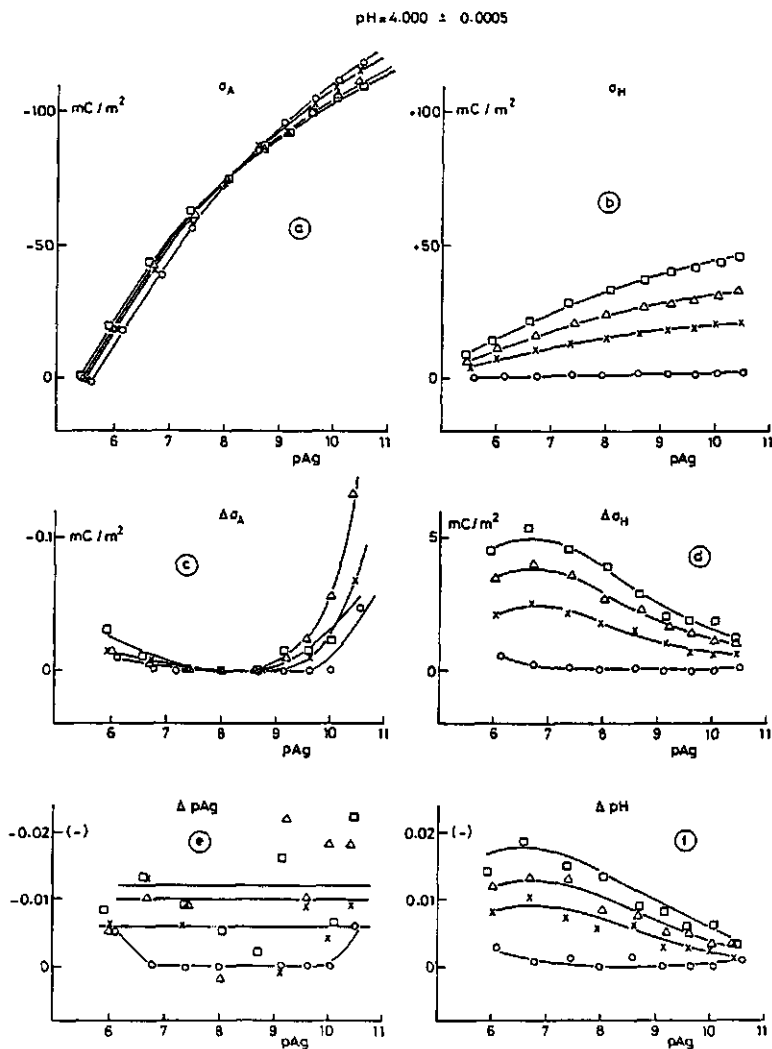


FIGURE 5.7. Titration curves of BSA adsorbed on AgI

0.1 M  $\text{KNO}_3$ ,  $\text{pH}_{\text{stat}} = 4$ .

blank (o);  $\Gamma_p$  ( $\text{mg}/\text{m}^2$ ) = 0.47 (x); 0.93 ( $\Delta$ ); 1.4 ( $\square$ ).

$$(a) \sigma_A \equiv \sigma_A^{III}, (b) \sigma_H \equiv \sigma_H^{III}, (c) \Delta\sigma_A \equiv \sigma_A^{III} - \sigma_A^{II},$$

$$(d) \Delta\sigma_H \equiv \sigma_H^{II} - \sigma_H^I, (e) \Delta\text{pAg} \equiv \text{pAg}^{III} - \text{pAg}^{II}, (f) \Delta\text{pH} \equiv \text{pH}^{II} - \text{pH}^I$$

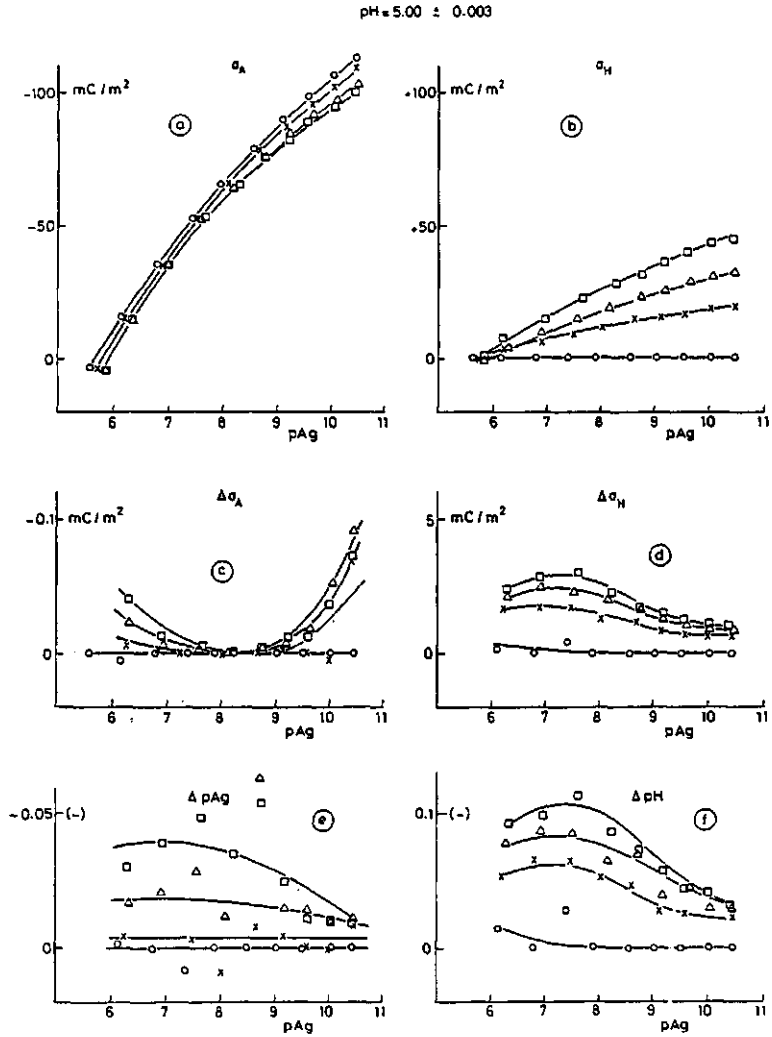


FIGURE 5.8. Titration curves of BSA adsorbed on AgI.

0.1 M  $\text{KNO}_3$ ,  $\text{pH}_{\text{stat}} = 5$ .

symbols and adsorbed amounts as in fig. 5.7

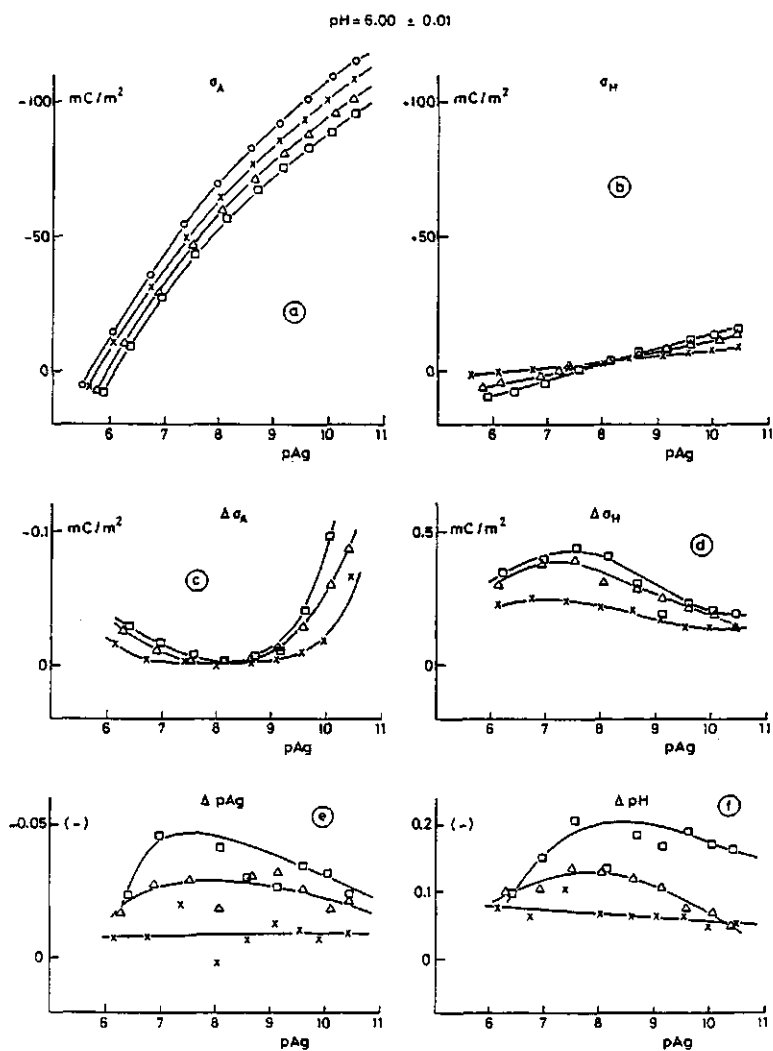


FIGURE 5.9. Titration curves of BSA adsorbed on AgI

0.1 M  $\text{KNO}_3$ ,  $\text{pH}_{\text{stat}} = 6$

blank (o) ;  $\Gamma_p$  ( $\text{mg/m}^2$ ) = 0.33 (x); 0.67 ( $\Delta$ ); 1.0 ( $\square$ ).  $\sigma_H$  for the blank was below the detection limits. Other symbols as in fig. 5.7

The blank curves of the AgI charge density  $\sigma_A$  at different pH are identical, illustrating the absence of base/acid sites on the AgI surfaces. The shapes of the blank curves are in good agreement with published titration curves of bare AgI precipitates in 0.1 M  $\text{KNO}_3$  (1). However, as we chose to use the dye surface area ( $0.30 \text{ m}^2/\text{gram}$ ) rather than the capacitance surface area ( $0.88 \text{ m}^2/\text{gram}$ ), the magnitude of  $\sigma_A(\text{pAg})$  is larger than the literature value by a factor of about three.

The slope of the  $\sigma_A(\text{pAg})$  curve is not much altered upon the adsorption of BSA, except at pH 4 above pAg 8.5. Stated otherwise, the differential electric capacitance of the interface is only little influenced by adsorbed BSA, an effect we also deduced from the observed pAg shifts in the adsorption experiments.

The  $\sigma_A(\text{pAg})$  curves measured in the presence of adsorbed BSA are shifted with respect to the blanks. Under conditions where BSA prior to adsorption is negative (above pH 4.7), the entire curves are shifted to a more negative Galvani potential, in agreement with the changes in pAg we found in the adsorption experiments. When the protein is initially positive (pH 4), the curves shift to a more positive Galvani potential only if  $\sigma_A$  is not too negative.

A comparison with literature data on the influence of various types of adsorbates (1,2,3,20) on the  $\sigma_A(\text{pAg})$  curve, learns that the BSA-AgI system behaves exceptional. In the case of adsorption of mono-alcohols (20), polyvinylalcohols (2), tetraalkylammonium nitrate salts (4), oligo- and polypeptides (3) it is found that generally (i) the point of zero charge shifts to the left and (ii) the slope of the curve decreases. Feature (i) is explained by a displacement of surface bound water molecules by the adsorbate. As a water molecule directs its negative side to the bare AgI surface (1), adsorption of organic molecules with a low dipole moment results in an upward shift of the chi potential. The maximum shift of 240 mV (1,20) is attained for molecules adsorbing with their hydrophobic moieties directed towards the surface. Feature (ii) is interpreted in terms of a decrease in the electrical capacitance of the Stern layer. The Stern layer of the bare AgI-water interface has a (relative) dielectric permittivity ( $\epsilon_S$ ) of about 5-10 and a thickness ( $d_S$ ) of about 0.2-0.5 nm. An (apolar) adsorbate will typically cause a decrease in  $\epsilon_S$  and an increase in  $d_S$ , and hence a decrease in the Stern capacitance ( $\epsilon_S/d_S$ ). Both feature (i) and (ii) are in first approximation linearly correlated to the surface concentration of the adsorbate. As a

consequence,  $\sigma_A(\text{pAg})$  curves obtained at different loads of adsorbate show a common intersection point which is not at the point of zero charge.

In our case we find a common intersection point only in the pH 4 titration curve. The thickness of an adsorbed protein molecule is certainly larger than  $d_S$ , by at least a factor of five. The dielectric permittivity of a protein body is probably similar to, or smaller than,  $\epsilon_S$ . Why then don't we find a decrease in the capacitance? In section 5.4.2 we will give evidence that this is due to the charge adaptability of the protein molecule. At pH 5, pH 6 (and pH 4 upto pAg 8.5) the protein adjusts its charge so easily that any change in surface charge is compensated by an opposite shift in the protein charge. In addition, the value of the electric capacitance of the contact layer between a protein molecule and the AgI surface is similar to that of the Stern capacitance of the blank: it is rather this layer that should be compared with the Stern layer on bare AgI.

In connection with the above, we note that the protein molecule probably does not displace water molecules from the surface to a great extent. The shift in the point of zero charge in the pH 5 curve, when prior to adsorption the protein is (almost) uncharged, is just too small. It could be that polar amino acid residues with a high dipole moment displace the water molecules without affecting the  $\chi$  potential, but we consider this unlikely.

The  $\sigma_H(\text{pAg})$  curves show that the adsorbed protein molecules take up extra protons when the AgI surface is titrated to a more negative potential. It is tempting to ascribe the co-adsorption of the protons to pure electrostatic effects; some dissociated acid/base residues of the protein will act as counter-charges for the surface. Hence, if the surface is brought to a more negative potential, the acid/base equilibria shift such that the number of bound protons increases.

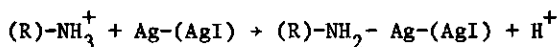
However, the titration curves reveal that non-electrostatic interactions also influence the proton titration. This can be inferred most clearly from the value of  $\sigma_H$  at  $\text{pAg}_0$  (= 5.67), where the bare AgI surface is uncharged. If for this pAg value the electrostatic interactions were also dominant, the protein charge would have been reduced upon adsorption. We then would have found a negative  $\sigma_H(\text{pAg}_0)$  at pH 4 (where the protein is initially positive) and a positive  $\sigma_H(\text{pAg}_0)$  at pH 6 (where the protein is initially negative). In contrast, we find a positive  $\sigma_H(\text{pAg}_0)$  at pH 4 and a negative  $\sigma_H(\text{pAg}_0)$  at pH 6.

Perhaps the shift in the apparent pK values at pH 4 is a result of

structural alterations of the protein rather than some specific interaction of the acid/base residues with the surface. The relatively low values for the pK's of the carboxylic groups in a free (non-adsorbed) BSA molecule (see table 5.1) have been attributed to the formation of weak ion pairs between the carboxylic and amino groups (7). If the protein molecule alters its structure upon adsorption, this will result in a disruption of some of the ion pairs and consequently an increase in the pK values of the carboxylic groups (and hence a positive  $\sigma_H(\text{pAg}_0)$ ). It is well known (4,7) that BSA becomes increasingly unstable at acid pH, below pH 4 it gradually expands and alters its structure.

An alternative explanation for the positive  $\sigma_H(\text{pAg}_0)$  at pH 4, is that a BSA molecule has an asymmetric charge distribution and faces its negative side towards the surface. Norde and Lyklema concluded that this occurs when Human Serum Albumin adsorbs on polystyrene latices (21-25). However, if this is also true in our case it is difficult to see why the shift in the point of zero charge in the pH 5 curve is so small.

At pH 6 we find a negative  $\sigma_H(\text{pAg}_0)$ . The  $\text{Ag}^+$  binding experiment (fig. 5.3) indicates that some acid/base residues, probably those containing amino groups, interact strongly with silver ions. If those same residues interact specifically with silver atoms incorporated in the AgI matrix, for example via



the pK of the base would decrease (and hence  $\sigma_H(\text{pAg}_0)$  would be negative). Likely candidates for such an interaction are the imidazole side groups of the histidines and the amino side groups of the lysines.

More insight can be gained if we express  $\sigma_A$  and  $\sigma_H$  in terms of the co-adsorption ratios  $\Delta r$  introduced in chapter 3. The co-adsorption ratios are related to the binding ratios ( $r$ ) in the adsorbed ( $\sigma$ ) and non-adsorbed ( $\alpha$ ) state through

$$r_I^\sigma \equiv r_{\text{KI}}^\sigma - r_{\text{AgNO}_3}^\sigma \quad [5]$$

$$r_I^\alpha \equiv r_{\text{KI}}^\alpha - r_{\text{AgNO}_3}^\alpha$$

$$r_H^\sigma \equiv r_{\text{HNO}_3}^\sigma - r_{\text{KOH}}^\sigma$$

$$r_H^\alpha \equiv r_{\text{HNO}_3}^\alpha - r_{\text{KOH}}^\alpha$$

$$\Delta r_I \equiv r_I^\sigma - r_I^\alpha$$

$$\Delta r_H \equiv r_H^\sigma - r_H^\alpha$$

For our system,  $r_I^\alpha$ ,  $r_{\text{KOH}}^\alpha$  and  $r_{\text{KOH}}^\sigma$  can be neglected. Note that we cannot discriminate between adsorption of iodide ions or expulsion of silver ions. Consequently,  $\Delta r_I$  may be positive or negative. For simplicity, we henceforth speak of iodide (co-) adsorption where we mean iodide minus silver (co-) adsorption.

The relations between the co-adsorption ratios and the charge densities are given by,

$$\Delta r_I = \frac{1}{F\Gamma_p} [ \sigma_A - \sigma_A^0 ] \quad [6]$$

$$\Delta r_H = \frac{\sigma_H}{F\Gamma_p}$$

where  $\sigma_A^0$  is the charge density of bare AgI (the blank), measured at the same pH and pAg as  $\sigma_A$ . The calculated co-adsorption ratios are plotted in fig. 5.10 versus the Galvani potential. We find that the iodide co-adsorption is fairly constant when the protein is negative or almost uncharged prior to adsorption. At pH 6 and pH 5 the AgI crystals expel on the average roughly 10 respectively 6 iodide ions per adsorbed protein into the solution. (We repeat that a negative  $\Delta r_I$  may also be understood as an uptake of  $\text{Ag}^+$  ions). When the protein is initially positive (at pH 4) the iodide co-adsorption ratio changes from about +7 at low AgI charge density to about -3 at high AgI charge density. The latter negative co-adsorption is extraordinary. Although a BSA molecule is at pH 4 initially positive, and it takes up even more protons upon adsorption, the AgI crystals respond to the adsorption by ejecting negative charge!

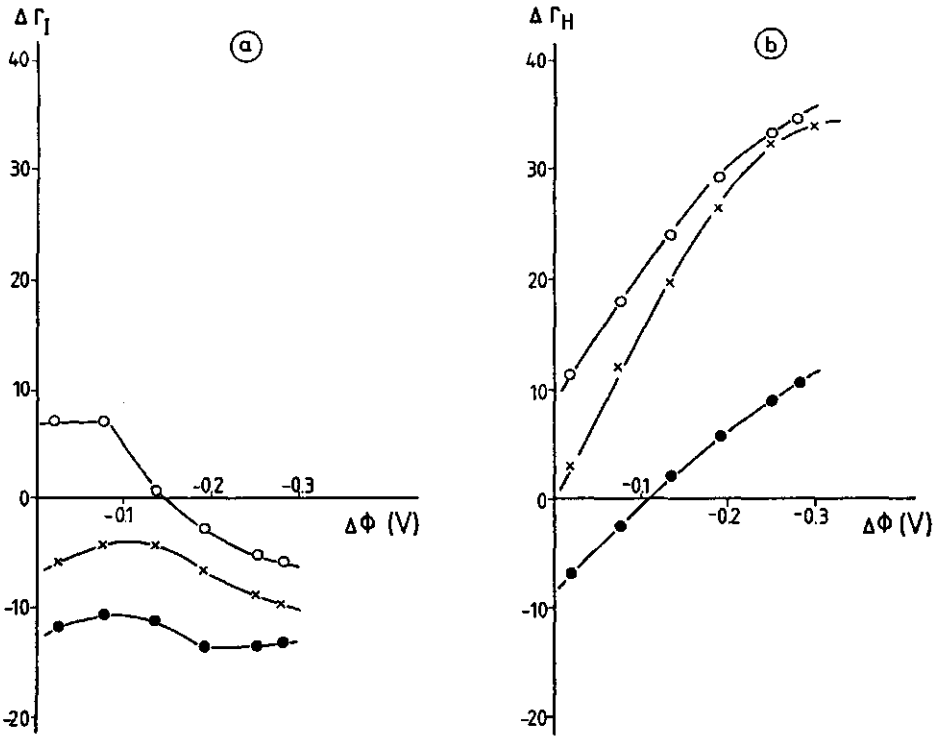


FIGURE 5.10. Co-adsorption ratio of iodide ions minus that of silver ions ( $\Delta r_I$ ) and co-adsorption ratio of protons ( $\Delta r_H$ ). Calculated for  $\Gamma_p$  ( $\text{mg}/\text{m}^2$ ) = 0.93 (pH 4, pH 5); 1.0 (pH 6). pH 4 (o); pH 5 (x); pH 6 (●).

Figs. 5.7, 5.8 and 5.9, c through f, reflect the intricate titrations in the pHstat cycle. The effects are small, but can be understood qualitatively in view of the above discussion. When the precipitates are titrated with KI (step I to II of the pHstat cycle), an adsorbed BSA molecule takes up protons from the solution (curves  $\Delta\sigma_H(\text{pAg})$ ), thereby increasing the pH (curves  $\Delta\text{pH}(\text{pAg})$ ). The proton charge and pH shifts are connected through the buffering capacity of the system for the pH which is higher at pH 4 (smaller pH shift) than at pH 6 (larger pH shift). When titrated with  $\text{HNO}_3$  (step II to III), the AgI crystals take up iodide ions from the solution (curves  $\Delta\sigma_A(\text{pAg})$ ), thereby decreasing the pAg (curves  $\Delta\text{pAg}(\text{pAg})$ ). The shift in AgI charge is very small around the stoichiometric point ( $\text{pAg} = \text{pI} = 8$ ) and is larger (but still small with respect to the increment in  $\sigma_A$  between step I to II) at higher and lower pAg.

A measure of the proton buffering capacity of adsorbed BSA at constant Galvani potential  $B^\sigma$  can be obtained from

$$B^\sigma \equiv - \left( \frac{dr_H^\sigma}{dpH} \right)_{\Delta\phi} \approx - \frac{1}{F\Gamma_p} \cdot \frac{[\sigma_H^{III} - \sigma_H^{II}]}{[pH^{III} - pH^{II}]} \quad [7]$$

The buffering capacity of free, non-adsorbed BSA ( $B^\alpha$ ) is defined by

$$B^\alpha \equiv - \left( \frac{dr_H^\alpha}{dpH} \right) \quad [8]$$

The proton buffering capacities were calculated for a BSA adsorption of 0.93 mg/m<sup>2</sup> (pH 4, pH 5) and 1.0 mg/m<sup>2</sup> (pH 6), see fig. 5.11a. The spread in the points is very large for the pH 4 curve because of the small amount of protein and the huge blank corrections. For comparison, the proton buffering capacity of free BSA as calculated from the titration data of Tanford (see chapter 2) is plotted in fig 5.11b as function of the the pH. We find that the buffering capacity of adsorbed protein increases in concert with an increase in proton charge, just as it is the case for free BSA.

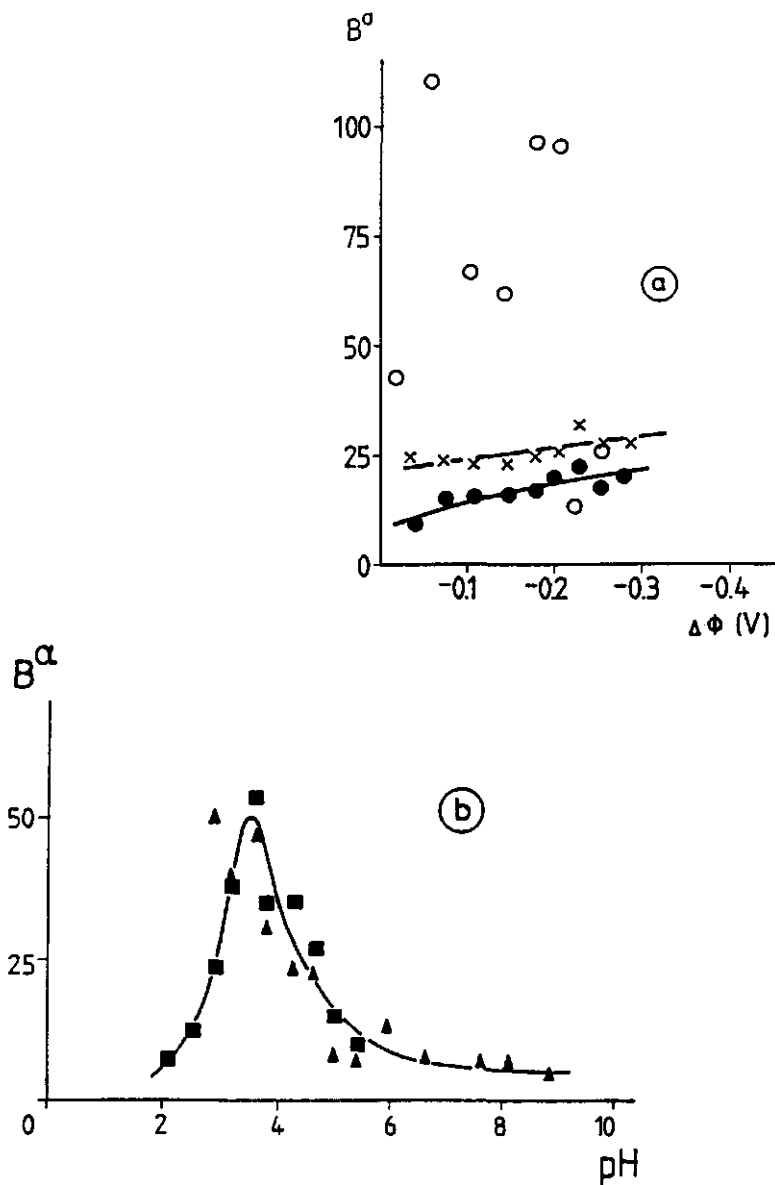


FIGURE 5.11. Proton buffering capacity of adsorbed (a) and free BSA (b).

(a) symbols as in fig. 5.10

(b)  $c_{KCl}$  (M) = 0.15 (■) ; 0.03 (▲).  $B^a$  calculated from proton titration curves obtained by Tanford (?).

## 5.4 DISCUSSION

## 5.4.1 THERMODYNAMIC ANALYSIS

In this section we analyse our results according to the classical thermodynamic approach for the AgI system (1) and with the phenomenological co-adsorption relations derived in chapter 3.

To start with the former, at constant temperature, the Gibbs adsorption equation for the system under study is given by

$$d\gamma = 2.303 \frac{RT}{F} \sigma_A dpAg + 2.303 \frac{RT}{F} \sigma_H dpH - \Gamma_p d\mu_p \quad [9]$$

where  $\gamma$  is the surface tension of the AgI-solution interface and  $\mu_p$  is the chemical potential of BSA. As the adsorbed amount of BSA in our experiments does not change with the pAg, the following transformation is more useful

$$d(\gamma - 2.303 \frac{RT}{F} \sigma_A pAg + \Gamma_p \mu_p) = - 2.303 \frac{RT}{F} pAg d\sigma_A + 2.303 \frac{RT}{F} \sigma_H dpH + \mu_p d\Gamma_p \quad [10]$$

From eq. [10] we derive the Maxwell relation

$$\left(\frac{\delta\sigma_H}{\delta\sigma_A}\right)_{pH} = - \left(\frac{\delta pAg}{\delta pH}\right)_{\sigma_A} \quad [11]$$

Both sides of Maxwell relation [11] can be expressed in the shifts in charges and ion activities in the pHstat cycle so that it can be experimentally verified.

The left hand side of eq.[11] (the charge exchange ratio) is equal to the ratio of the slopes of the  $\sigma_A(pAg)$  and  $\sigma_H(pAg)$  curves,

$$\left(\frac{\delta\sigma_H}{\delta\sigma_A}\right)_{pH} = \frac{(\sigma_H^{III} - \sigma_H^I)}{(\sigma_A^{III} - \sigma_A^I)} \quad [12]$$

As the amount of protein adsorption is constant, the pAg of the system is a function of the charge of the interface and the pH only

$$pAg = pAg(\sigma_A, pH) \quad (\Gamma_p \text{ constant}) \quad [13]$$

in differential form,

$$dpAg = \left(\frac{\delta pAg}{\delta pH}\right)_{\sigma_A} dpH + \left(\frac{\delta pAg}{\delta \sigma_A}\right)_{pH} d\sigma_A \quad [14]$$

The second differential coefficient in eq. [14] is equal to the reciprocal of the slope of the  $\sigma_A(pAg)$  curve,

$$\left(\frac{\delta pAg}{\delta \sigma_A}\right)_{pH} = \frac{(pAg^{III} - pAg^I)}{(\sigma_A^{III} - \sigma_A^I)} \quad [15]$$

As the titration steps of the pHstat cycle are small, we may linearly integrate eq. [14] to give

$$pAg^{III} - pAg^{II} = \left(\frac{\delta pAg}{\delta pH}\right)_{\sigma_A} (pH^{III} - pH^{II}) + \left(\frac{\delta pAg}{\delta \sigma_A}\right)_{pH} (\sigma_A^{III} - \sigma_A^{II}) \quad [16]$$

Combining eqs. [11]-[16], we can rewrite the Maxwell relation as a (Gibbs) check which must hold for every pHstat cycle

$$g = \left\{ \frac{(pAg^{III} - pAg^{II})}{(pH^{III} - pH^{II})} - CF \right\} \cdot \frac{(\sigma_H^{III} - \sigma_H^I)}{(\sigma_A^{III} - \sigma_A^I)} \stackrel{?}{=} -1 \quad [17]$$

$$CF \equiv \frac{(pAg^{III} - pAg^I)}{(\sigma_A^{III} - \sigma_A^I)} \cdot \frac{(\sigma_A^{III} - \sigma_A^{II})}{(pH^{III} - pH^{II})}$$

where we introduced the Gibbs test ratio  $g$ .  $CF$  accounts for the small shift in surface charge when the system is titrated with  $HNO_3$  (step II to III). As  $CF$  was less than 1 % of the ratio of the  $pAg$  and  $pH$  shifts in all cases, we neglected it in the calculations. In passing we note that the value of  $g$  is invariant with respect to the choice of the specific surface area. The experiments were not accurate enough to test relation [17] for every pHstat cycle separately. Therefore we performed a statistical analysis on more than 200 measured cycles. The results of the calculations are shown in fig 5.12. The histogram has a clear optimum around -1 (mean value -0.96), which substantiates the internal consistency of the experiments.

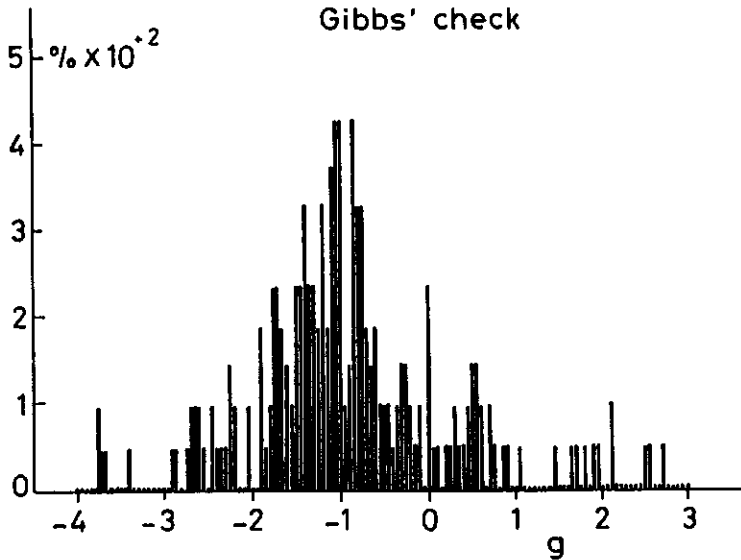


FIGURE 5.12. Frequency distribution of Gibbs check  $g$ . Calculated from 261 measured pHstat cycles, 41 cycles gave values for  $g$  higher than 3 or lower than -4.

An alternative thermodynamic analysis proceeds from the Gibbs co-adsorption equation (see chapter 3, eq. [3])

$$d(\gamma - \gamma^0) = -RT \Gamma_p \{ \Delta r_I dpAg - \Delta r_H dpH + \ln x_p \} \quad [18]$$

where  $\gamma^0$  is the surface tension of the uncovered AgI surface-solution interface and  $x_p$  is the mole fraction of protein in the solution. From the co-adsorption equation we derive (see table 3.1)

$$\left( \frac{\delta \Delta r_H}{\delta \Delta r_I} \right)_{pH} = \left( \frac{\delta pAg}{\delta pH} \right) \Delta r_I \quad [19]$$

Using the relations between charge densities and co-adsorption ratios (eq.[6]), eq.[19] is re-written as

$$- \left( \frac{\delta \sigma_H}{\delta \sigma_A} \right)_{pH} = \left( \frac{\delta pAg}{\delta pH} \right) \Delta r_I = \left( \frac{\delta pAg}{\delta pH} \right) \sigma_A \quad [20]$$

where we assumed that  $(\delta p_{Ag}/\delta pH)_{\sigma_A}$  for the blank is zero. Equation [20] is nothing else than the Maxwell relation [11] which we have already proven to be valid.

The fact that the Gibbs check holds, does not necessarily imply that the protein adsorption itself is in equilibrium. It might be that the protein molecules are irreversibly attached to the surface while the co-adsorptions of the small ions adjust reversibly to a change in surface potential or pH. However, we now present a second consistency check which demonstrates that the protein adsorption is reversible also. Let us consider the Maxwell relation (table 3.1)

$$\left(\frac{\delta \Delta r_H}{\delta p_{Ag}}\right)_{pH} = - \left(\frac{\delta \Delta r_I}{\delta pH}\right)_{pAg} \quad [21]$$

This equation relates the co-adsorption ratios, measured in different titration experiments. If we can verify its validity, we have shown that the order in which we added the various substances (protein, acid/base, KI), did not affect the results.

---

TABLE 5.2: Check of  $\left(\frac{\delta \Delta r_H}{\delta p_{Ag}}\right)_{pH} = - \left(\frac{\delta \Delta r_I}{\delta pH}\right)_{pAg}$

---

Points calculated from fig. 5.10 for  $pH = 5$

| $pAg$ | $\Delta \phi$ (V) | $\left(\frac{\delta \Delta r_H}{\delta p_{Ag}}\right)_{pH}$ (-) | $- \left(\frac{\delta \Delta r_I}{\delta pH}\right)_{pAg}$ (-) |
|-------|-------------------|---|--|
| 6     | -0.019            | 9.0   | 9.4  |
| 7     | -0.077            | 8.2   | 8.9  |
| 8     | -0.136            | 7.0   | 6.0  |
| 9     | -0.194            | 6.5   | 5.4  |
| 10    | -0.252            | 5.3   | 4.2  |
| 10.5  | -0.281            | 2.9   | 3.7  |

---

We estimated the right hand side differential of eq.[21] for every point in the  $\Delta r_I(\text{pAg}, \text{pH} = 5)$  curve (fig. 5.10) through

$$\left(\frac{\delta \Delta r_I}{\delta \text{pH}}\right)_{\text{pAg}} (\text{pH} = 5) \approx \frac{1}{2} [\Delta r_I(\text{pH} = 6) - \Delta r_I(\text{pH} = 4)]_{\text{pAg}} \quad [22]$$

As we measured the co-adsorption for three different pH values only, we were not able to use similar estimates for the  $\Delta r_I(\text{pAg}, \text{pH} = 4)$  and  $\Delta r_I(\text{pAg}, \text{pH} = 6)$  curves. The left hand side differential of eq.[21] was calculated from the slope of the  $\Delta r_H(\text{pAg}, \text{pH} = 5)$  curve. The results are listed in table 5.2. We find that the correlation coefficient between the values of the two differential coefficients is 0.92, not too bad.

Having established the thermodynamic consistency of all the experiments, we can now use the co-adsorption relations to calculate the Gibbs energy of adsorption (see eq.[5] of chapter 3). If we arbitrarily choose the adsorption at pAg 6, pH 6 as the reference point we have

$$\Delta G_{\text{ads.}}^{\ddagger} = \Delta G_{\text{ads.}}^{\ddagger*} + 2.303 \int_{\text{pAg}=6}^{\text{pAg}} \int_{\text{pH}=6}^{\text{pH}} [\Delta r_I \text{d pAg} - \Delta r_H \text{d pH}] \quad (\text{RT}) \quad [23]$$

where  $\Delta G_{\text{ads.}}^{\ddagger}$  and  $\Delta G_{\text{ads.}}^{\ddagger*}$  are the adsorption Gibbs energies at arbitrary pAg, pH and at pAg 6, pH 6 respectively. Note that the validity of eq.[21] implies that the value of the integral is independent of the path of integration. The difference between  $\Delta G_{\text{ads.}}^{\ddagger}$  and  $\Delta G_{\text{ads.}}^{\ddagger*}$  is plotted in fig. 5.13. We find that the affinity of a BSA molecule for the AgI surface decreases when the protein is initially negative and the (negative) AgI charge density decreases, in accordance with what we would expect. Again, the pH 4 curve displays a peculiar phenomenon. The affinity of a positive BSA molecule for a highly charged negative AgI surface is lower than the affinity of the same molecule for a less negative AgI surface!

In chapter 4 we presented model calculations of the interactions between a weak acid surface and a surface covered with strong base sites. The maximal negative charge density of the acid surface was higher than the maximal positive charge density of the base surface. One of our findings was that the interaction Gibbs energy was minimal at a pH where the charges of the free surfaces were equal in magnitude but opposite in sign such that the net proton co-adsorption was zero. At high pH, the acid surface was more negative than the base surface was positive and protons were co-adsorbed. At low pH the acid surface was not negative enough and protons were co-desorbed.

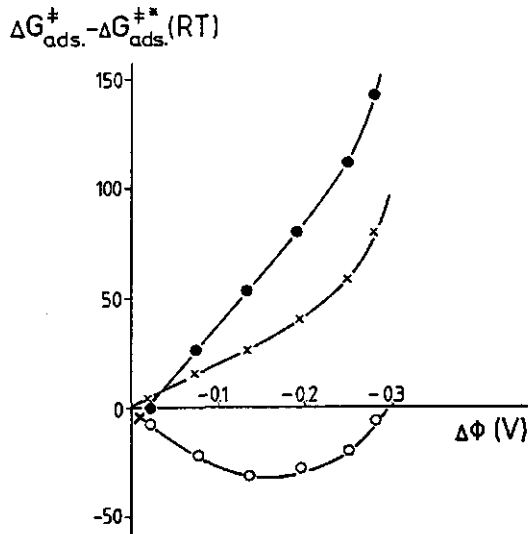


FIGURE 5.13. Gibbs energy of adsorption relative to that at pH 6, pAg 6. Calculated from the points in fig. 5.10, using eq.[23].

pH = 4 ( $\circ$ ) ; 5 ( $\times$ ) ; 6 ( $\bullet$ ).

Qualitatively, this resembles the interactions between BSA and AgI at pH 4. Below pAg 8.5 iodide ions are co-adsorbed, above pAg 8.5 iodide ions are co-desorbed so that the Gibbs energy of adsorption is minimal at pAg 8.5. The resemblance suggests that above pAg 8.5 the bare AgI surface is so negative that the protein cannot easily adjust its charge. As a result, in addition to a small induction in the co-adsorption of protons with increasing pAg, the surface itself diminishes its charge (with respect to the blank).

As the equilibrium protein concentration in the Henry region of adsorption (see section 5.3.1) was below our detection limit of 0.001 mg/ml under all circumstances, we are unable to calculate the absolute values of the Gibbs energies of adsorption. However, from the lower limit of the Henry constant in the  $pH_{init.} = 7$ ,  $pAg_{init} = 10$  adsorption curve (calculated to be  $1.33 \cdot 10^{11}$ , for the definition of the Henry constant see chapter 3 eq.[4]) we can estimate the upper limit of the integration constant through,

$$\Delta G_{ads}^{\ddagger*} (RT) < -\ln(1.33 \cdot 10^{11}) - 140 = -170$$

[24]

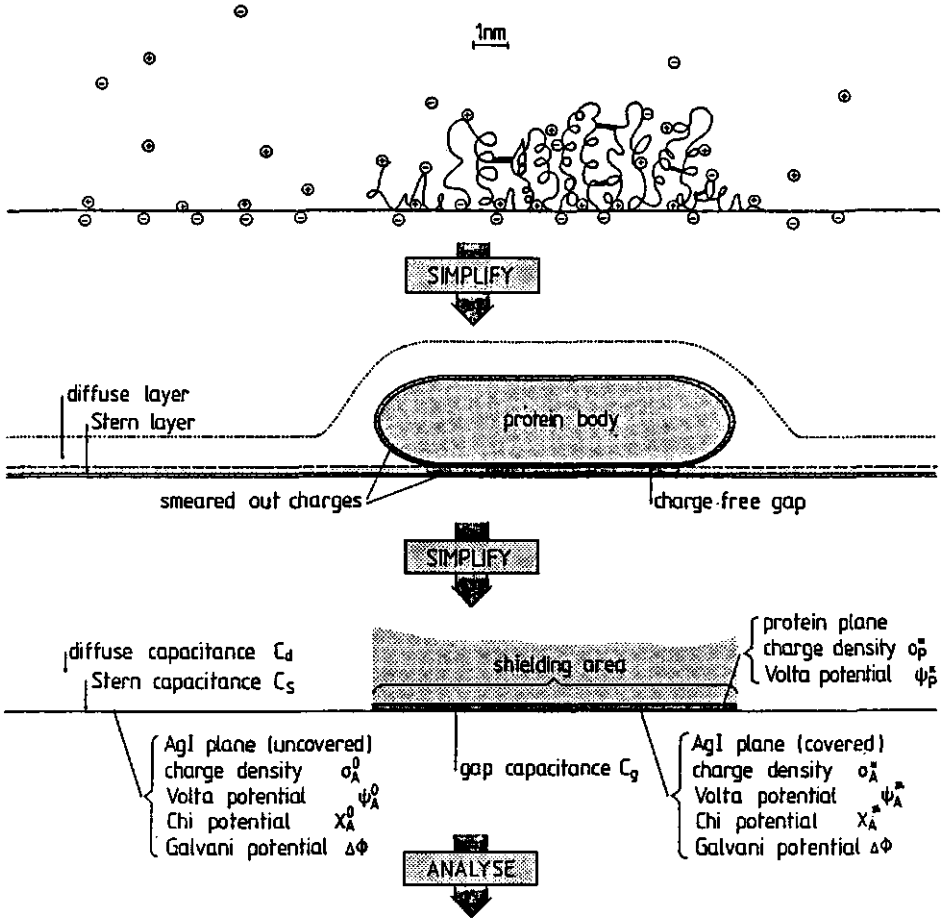
The resulting upper limits for the Gibbs energies of adsorption are truly gigantic. It should be realized that a change in the Gibbs energy of adsorption of only 2.3 RT units changes the equilibrium bulk BSA concentration at constant adsorbed amount of BSA by an order of magnitude. To give an impression: when we take the bulk BSA concentration at pAg 10, pH 6 as 0.001 mg/ml (= 14.9 nM), then the bulk concentration at pAg 8.5, pH 4 should be about 55 molecules per cubic lightyear. A very low concentration indeed.

How can we explain the enormous adsorption Gibbs energies? As negative BSA adsorbs with a high affinity on negative AgI, other than electrostatic interactions must be present, e.g hydrophobic interactions and interactions stemming from structural alterations of the protein (17,18,19). From the observation that the  $\chi$  potential and the capacitance are not much affected by the adsorbed protein, we concluded that surface attached water molecules are not displaced to a great extent. Hence the hydrophobic factor may be small, but it is impossible to estimate its magnitude. On the other hand, if structural rearrangements involve one extra degree of freedom for all the amino acid residues in the protein, they would contribute some 400 RT units to the Gibbs energy of adsorption. Also the contribution of specific interactions between the amino groups and the AgI surface may be appreciable. For example, if the pK of a lysine group shifts five units downwards, then the interaction of thirty of such groups with the surface results in a decrease of the adsorption Gibbs energy by about 450 RT.

#### 5.4.2 MODEL ANALYSIS

In this section we will analyse our results with the co-adsorption model as presented in chapter 4. According to the model, the charge densities on two surfaces in close proximity are equal in magnitude but opposite in sign. In the case of adsorbed BSA (for a schematic drawing see fig. 5.14) the titration properties of the solution side of the molecule may, in principle, also be affected by the surface potential. However, if the thickness of the protein body (unfolded or not) is larger than, say, 2 nm and if its (relative) dielectric permittivity is lower than, say, 2-10, the body acts as an insulator and shields the surface to such an extent that the net charge of the contact region on the surface side is zero. Under these circumstances the potential on the solution side of the protein will be independent of the surface potential.

## Ion binding model for BSA adsorption on AgI



$$\begin{aligned}
 \text{shielding efficiency } \phi^S &\equiv \text{shielding area} / \text{total area} \\
 \text{mean AgI charge density } \sigma_A &= (1 - \phi^S)\sigma_A^0 + \phi^S\sigma_A^* \\
 \text{mean protein charge density } \sigma_p &= \phi^S\sigma_p^0 \\
 \text{constant Galvani potential } \Delta\Phi &= \psi_A^0 + X_A^0 = \psi_A^* + X_A^* \\
 \text{capacitance relation (gap)} C_g &= \partial\sigma_A^* / (\psi_A^* - \psi_p^0) = \partial\sigma_p^0 / \partial(\psi_p^0 - \psi_A^*)
 \end{aligned}$$

FIGURE 5.14. Schematic drawing of adsorbed BSA. Includes outline of the model analysis.

Some years ago, Norde (21-25) conducted a series of electrophoretic mobility measurements of polystyrene latex particles saturated with adsorbed Human Serum Albumin. Indeed, between pH 4 and 8 the zeta potential was similar to that of the protein prior to adsorption. Therefore, as a first approximation we only consider the charges and potentials in the contact layer between surface and protein.

In order to suit the BSA-AgI system, we slightly adapt the parent co-adsorption model.

The first modification is that we use a differential gap capacitance  $C_g$  rather than an integral gap capacitance.  $C_g$  is defined by

$$C_g \equiv \left( \frac{\delta \sigma_{AgI}^*}{\delta(\psi_A^* - \psi_P^*)} \right) = \left( \frac{\delta \sigma_P^*}{\delta(\psi_P^* - \psi_A^*)} \right) \quad [25]$$

where  $\psi_A^*$ ,  $\psi_P^*$  and  $\sigma_{AgI}^*$ ,  $\sigma_P^*$  are the Volta potentials and charge densities of the AgI surface and protein in the contact region.  $\psi_A^*$  is related to the Volta potential of the uncovered part of the AgI surface  $\psi_A^0$  through the Galvani potential which must be constant over the entire AgI surface

$$\Delta\phi = \psi_A^* + \chi_A^* = \psi_A^0 + \chi_A^0 \quad [26]$$

As before,  $\Delta\phi \equiv \phi(pAg) - \phi(pAg_0)$ . We assume that the difference between the chi potentials  $\chi_A^*$  and  $\chi_A^0$  is constant, probably they have similar values (section 5.3.2).

A second modification is that we lump all the charges ( $\sigma_S^*$ ) stemming from co-adsorbing electrolyte ions ( $K^+$  and  $NO_3^-$ ) together and confine them to binding sites on the protein. Separately taking salt adsorption on the AgI surface into account does not contribute essentially to the discussion but complicates the mathematics. We then have

$$\sigma_{AgI}^* = \sigma_A^* \quad [27]$$

$$\sigma_P^* = \sigma_H^* + \sigma_S^*$$

and due to the net zero charge of the contact region

$$\sigma_S^* = -(\sigma_A^* + \sigma_H^*) \quad [28]$$

The measured charge densities ( $\sigma_A$  and  $\sigma_H$ ) are related to those of the uncovered AgI surface ( $\sigma_A^0$ ) and on the free protein ( $\sigma_H^0$ ) through

$$\sigma_A = (1 - \theta^S) \sigma_A^0 + \theta^S \sigma_A^* \quad [29]$$

$$\sigma_H = \theta^S (\sigma_H^* - \sigma_H^0)$$

where  $\theta^S$  is the 'dielectric shielding efficiency'. It is defined as

$$\theta^S \equiv a_S \Gamma_p \quad [30]$$

where  $a_S$  is the area of the contact region per protein molecule. The area a BSA molecule occupies on the surface if it adsorbs side-on with unperturbed structure,  $a_p$ , is somewhere between 30 and 52 nm<sup>2</sup>. The lower and upper value are calculated from the unhydrated and hydrated dimensions of native BSA respectively (see table 5.1). For two reasons we expect  $a_S$  to be larger than  $a_p$ . The first is that structural rearrangements will flatten the molecule somewhat so that more residues are close to the surface. Second, acid/base residues on the lateral sides of the adsorbed protein body will also be affected by the surface potential, although to a lesser extent than those in the contact layer.

The number of acid/base sites on the protein in the contact region is limited, and so the intrinsic capacitance  $C_1$  of the adsorbed protein may be small (see table 4.1, compare with table 5.1). As we do not exactly know what the densities and the degrees of titration of the acid/base residues in the contact region are, it is difficult to make an estimate of the value of  $C_1$ . If for sake of argument we assume that the protein retains its native structure upon adsorption, we find that the upper value of  $C_1$  is 1 to 1.5 F/m<sup>2</sup> (when half of the  $\beta, \gamma$ -carboxyl groups are titrated). Unfolding or titration of residues on the lateral sides of the protein would probably result in an higher value of  $C_1$ .

We recall that  $C_1$  is a measure of the electrochemical adaptability of the protein. If  $C_1$  is large, the protein adjusts its charge at (almost) constant potential. An infinitesimal shift in  $\psi_p^*$  is then enough to keep  $\sigma_p^*$  in balance with  $\sigma_A^*$ . If  $C_1$  is zero, the protein interacts with constant charge.

Combination of eqs.[25-30] results in a relation between the total capacitance  $C \equiv (\delta\sigma_A/\delta\Delta\phi)_{pH}$ , the blank capacitance  $C_0$  and the effective

capacitance of the contact region  $C_R$

$$C = (1-\theta^S) C_0 + \theta^S C_R \quad [31]$$

The capacitance of the blank is related to the diffuse double layer capacitance  $C_D$  and the Stern capacitance  $C_S$  via

$$C_0 = \frac{C_D C_S}{(C_D + C_S)} \quad [32]$$

In 0.1 M  $KNO_3$ ,  $C_D$  is 0.7 F/m<sup>2</sup> around the point of zero charge,  $C_S$  is then about 4 F/m<sup>2</sup>. Note that if we would have used the capacitance specific surface area (0.88 m<sup>2</sup>/gram) instead of the dye specific surface area (0.30 m<sup>2</sup>/gram), the value of  $C_S$  would have been 0.7 F/m<sup>2</sup>. The commonly accepted value for  $C_S$  for AgI (1) (also using the capacitance surface area) is about 0.3 F/m<sup>2</sup>. Nevertheless, we decided to use the specific surface obtained from Methylene Blue adsorption as argued before. At higher surface potentials  $C_S$  is smaller, perhaps due to dielectric saturation in the water layer close to the surface (1).

$C_R$  is related to the intrinsic and gap capacitance via

$$C_R = \frac{C_1 C_g}{(C_1 + C_g)} \quad [33]$$

In the bio-electrochemical literature (26,27), the double layer capacitances of electrodes in the presence of adsorbed protein are often described with an equation morphologically identical to [31].  $C_R$  is then replaced by the capacitance under 'full' saturation  $C_\infty$  and  $\theta^S$  is interpreted as the 'degree of coverage'. However, until now there was no satisfactory theory which could predict the value of  $C_\infty$ . Sometimes the assumption has been made that it is zero (28) without any justification whatsoever. From eq.[33] we deduce that  $C_R$  may well have appreciable values, and furthermore that its value depends on the surface potential and pH (through  $C_1$ ). It is only in special cases that it is close to zero, as we shall show below.

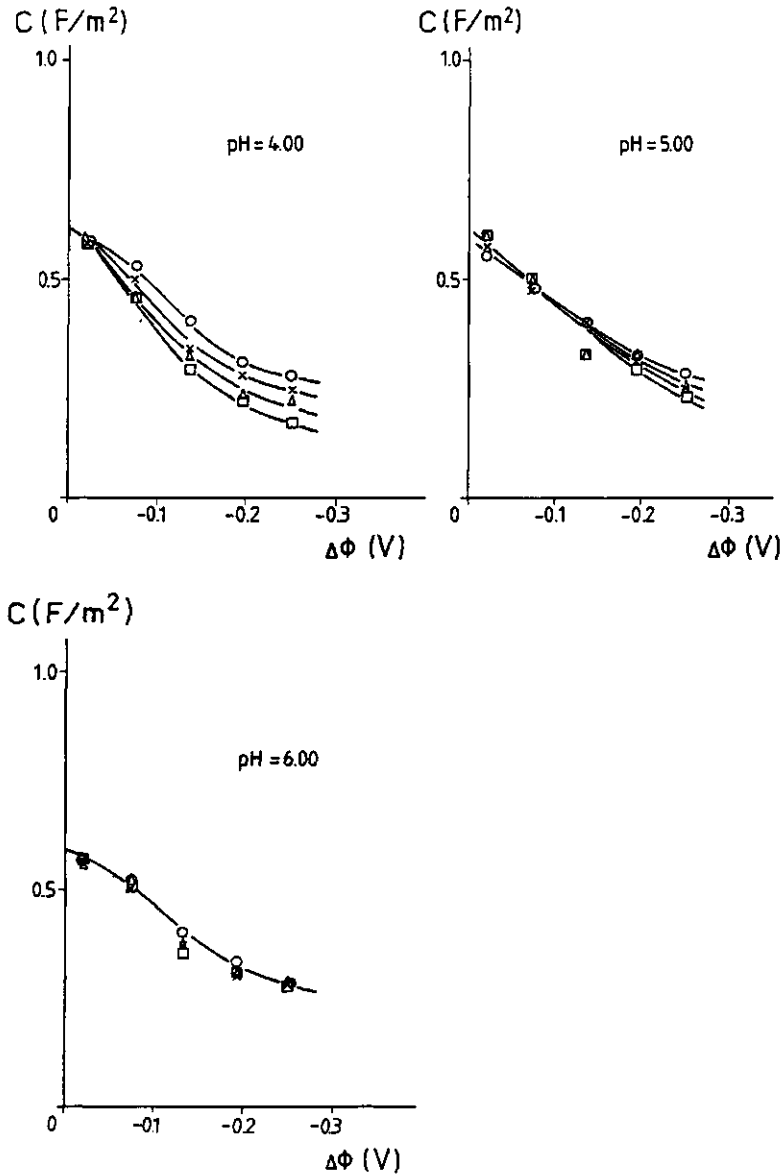


FIGURE 5.15. Electric capacitance vs. Galvani potential.

pH 4, pH 5: blank (o) ;  $\Gamma_p$  ( $mg/m^2$ ) = 0.47 (x) ; 0.93 ( $\Delta$ ) ; 1.4 ( $\square$ )  
 pH 6: blank (o) ;  $\Gamma_p$  ( $mg/m^2$ ) = 0.33 (x) ; 0.67 ( $\Delta$ ) 1.0 ( $\square$ )

The values of  $C$  are plotted in fig. 5.15. We find that the capacitance is not much affected by the protein adsorption (except in the pH 4 curves), as we already noted in section 5.3.2. In terms of the co-adsorption model, this suggests that  $C_i \approx C_0$  and  $C_g \approx C_s$ . These approximate equalities should not be stressed too far; as we have five capacitances of which only three are known, it is not possible to calculate  $C_i$  and  $C_g$  separately. However, as the value of  $C_i$  is not unrealistic, we assume that  $C_g$  and  $C_s$  do not deviate by more than a factor of two to three. Even if we allow for this uncertainty in  $C_g$ , its high value indicates that the gap still contains some water, something we already concluded from the fact that the shift in chi potential was only minor.

The co-adsorption model allows two independent estimates of  $a_g$ , the area of the contact region. The first is obtained from the values of the charge exchange ratio  $(\delta\sigma_H / \delta\sigma_A)_{pH}$ . It is related to the capacitances and the shielding efficiency by

$$\left(\frac{\delta\sigma_H}{\delta\sigma_A}\right)_{pH} = -\frac{\theta^S}{(1+f_S)} \cdot \frac{C_R}{C} \quad [34]$$

where  $f_S$  is a measure of the co-adsorption of electrolyte. It is defined as

$$f_S \equiv \left(\frac{d\sigma_S^*}{d\sigma_H^*}\right) \quad [35]$$

If we insert  $C_R \approx C_0 \approx C$  we have

$$\left(\frac{\delta\sigma_H}{\delta\sigma_A}\right)_{pH} \approx -\frac{\theta^S}{(1+f_S)} = -\frac{a_s \Gamma_p}{(1+f_S)} \quad [36]$$

The charge exchange ratios are plotted in fig 5.16. We find that they increase with increasing amount of protein as predicted by eq. [36]. There seems to be some dependency on the Galvani potential, but the scatter is really too large to be conclusive. A mean value of  $a_g/(1+f_S)$  is obtained from a statistical analysis of all the points in fig. 5.16. In fig. 5.17 the results are plotted in the form of the frequency distribution of the charge exchange ratios. We find that  $a_g/(1+f_S)$  is always between 20 and 45 nm<sup>2</sup>, averaging around 35 nm<sup>2</sup>. The value of  $f_S$  cannot be calculated independently, but it seems improbable that  $f_S$  is higher than +1 (more likely,  $f_S$  is negative!). If we take  $f_S = 1$  in order to obtain an upper limit estimate for  $a_g$ , we find that the maximum average value is about 70 nm<sup>2</sup>. As the (maximal) value of  $a_g$  is not too far apart from that of  $a_p$ , the results indicate that the structural rearrangements

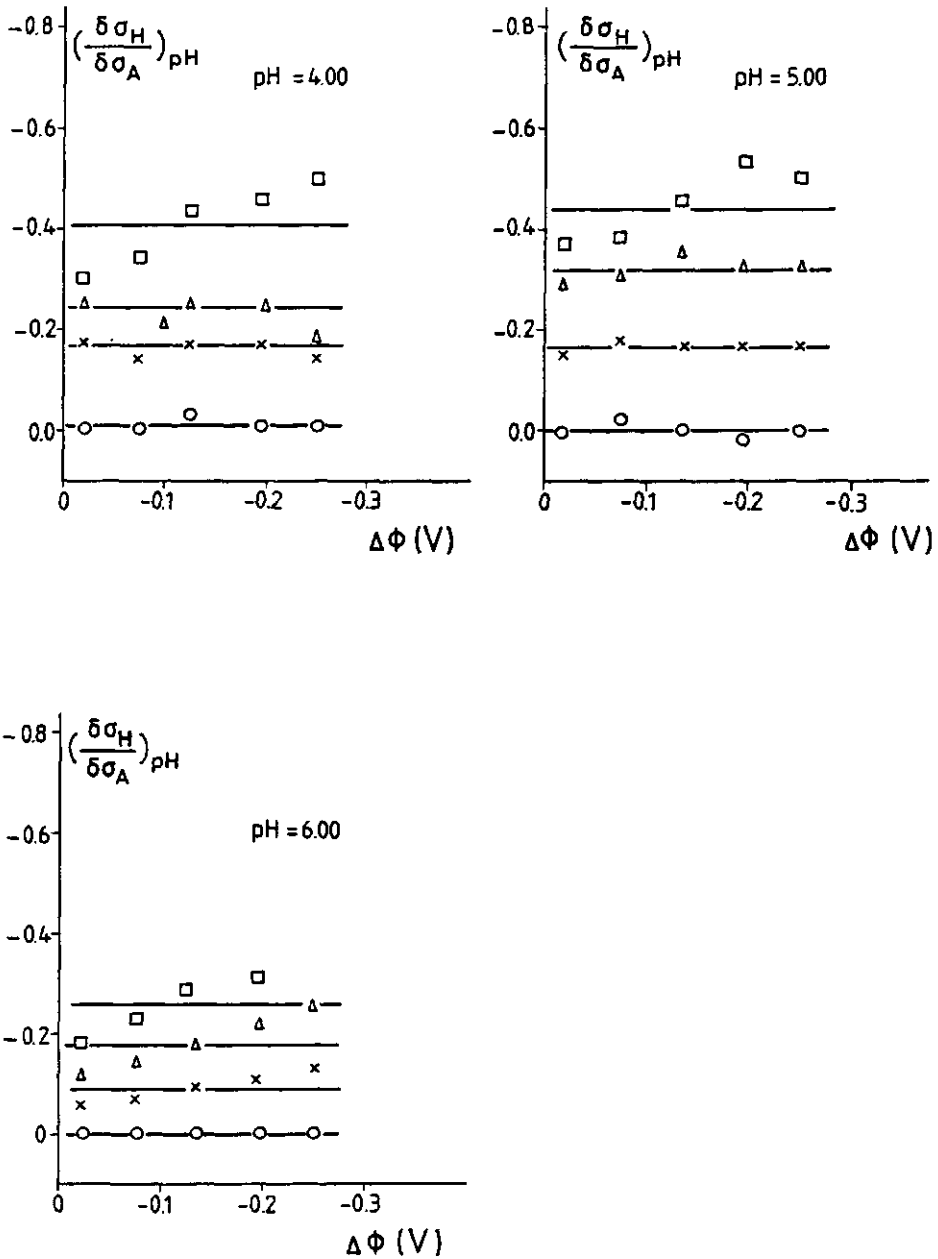


FIGURE 5.18. Charge exchange ratio vs. Galvani potential.

pH 4, pH 5: blank (o) ;  $\Gamma_p$  (mg/m<sup>2</sup>) = 0.47 (x) ; 0.93 ( $\Delta$ ) ; 1.4 ( $\square$ ).

pH 6 : blank (o) ;  $\Gamma_p$  (mg/m<sup>2</sup>) = 0.33 (x) ; 0.87 ( $\Delta$ ) ; 1.0 ( $\square$ )

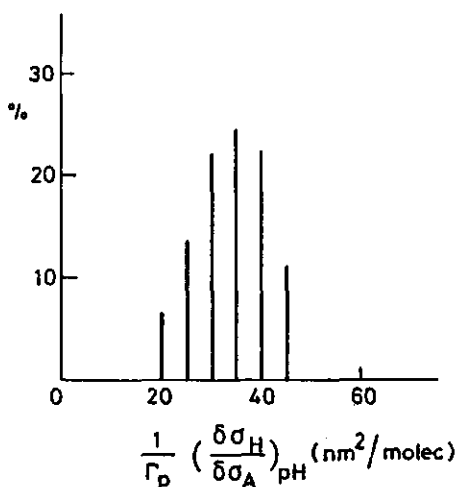


FIGURE 5.17. Frequency distribution of charge exchange ratio per adsorbed BSA molecule (calculated from the points in fig. 5.16).

do not lead to gross unfolding, especially if we take into account that titration of the lateral sides also makes the protein 'look larger'.

A second estimate of  $a_s$  is obtained from the pH 4 capacitance curves. As argued in the previous section, the drop in capacitance and the concomitant co-desorption of iodide ions is a consequence of a lesser charge adaptability of the protein. Stated otherwise, above pAg 7-9 the protein increasingly resists taking up more protons because all the acid/base residues in contact with the surface are reaching their endpoints of titration. In principle, this should be accompanied by a severe drop in the intrinsic capacitance. Perhaps the low values of the proton buffering capacity  $B^\sigma$  above pAg 9 (see fig. 5.11, the pH 4 curve) are an indication of a low value of  $C_1$ . For native BSA, the intrinsic capacitance is between 0.05-0.1 F/m<sup>2</sup> when the degrees of titration of the carboxylic groups are 0.01. Such a low value of  $C_1$  would make  $C_R$  very small with respect to  $C_0$ . In that case an estimate of the shielding efficiency, and therefore of  $a_s$ , can be obtained from the relative decrease in the capacitance per adsorbed protein molecule. Slightly rewriting eq.[31] we have

$$(1 - C_R/C_0) a_s = \frac{1}{\Gamma_p} (C_0 - C)/C_0 \quad [37]$$

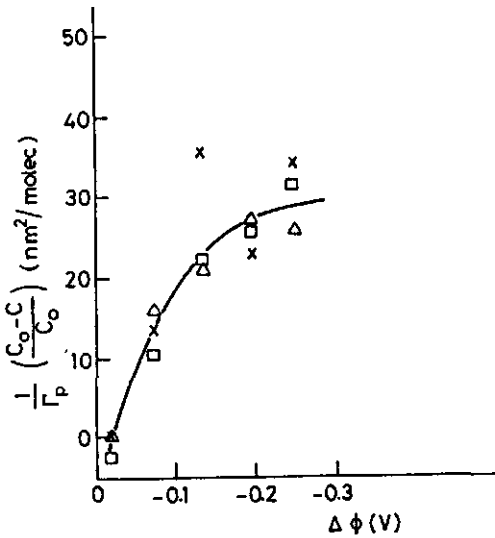


FIGURE 5.18. Relative capacitance decrease per adsorbed BSA molecule at pH 4.  $\Gamma_p$  (mg/m<sup>2</sup>) = 0.47 (x); 0.83 ( $\Delta$ ); 1.4 ( $\square$ ).

In fig.5.18 the right hand side of eq.[37] is plotted versus the Galvani potential. We find that above pAg 7 - 9 the curve levels off to a value between 25 and 35 nm<sup>2</sup>. This must be considered as a lower limit estimate of  $a_s$  since the factor  $C_R/C_0$  is perhaps not entirely negligible. But even so, if  $C_R/C_0$  would be 0.5 (which is unlikely in view of the above mentioned arguments) this second estimate of  $a_s$  would still indicate that gross unfolding does not occur. A conclusion we already drew from the first estimate.

## 5.5 REFERENCES

1. B.H. Bijsterbosch, J. Lyklema (1978) *Advan. Colloid Interface Sci.* 9, 147
2. L.K. Koopal (1978), Ph.D thesis, Agricultural University, Wageningen
3. H.A, van der Schee (1984), Ph.D thesis, Agricultural University, Wageningen
4. A. de Keizer (1981), Ph.D thesis, Agricultural University, Wageningen
5. E.R. Honig (1969) *Trans. Far. Soc.* 65, 2248
6. J.R. Brown, P. Shockley (1982) *Lipid-Protein Interactions* 1, 26
7. C. Tanford, S.A. Swanson, W.S. Shore (1955) *J. Am. Chem. Soc.* 77, 6421
8. C.L. Ridiford, B.R. Jennings (1966) *Biochem. Biophys. Acta* 126, 71
9. P.G. Squire, P. Moser, C.T. O'Konski (1968) *Biochem. J.* 7, 426
10. R.G. Reed, R.C. Feldhoft, O.L. Clute, T. Peters Jr. (1975) *Biochemistry* 14, 21
11. J. Janatova, J.K. Fuller, M.J. Hunter (1968) *J. Biol. Chem.* 243(13), 3612
12. J. Steinhardt, S. Beychock (1964) in "The Proteins", vol. II, ch. 8 ed. J. Neurath, Academic Press, New York, London
13. T. Suzuwa, H. Shirihama, T. Fujimoto (1982) *J. Colloid Interface Sci.* 86(1), 144
14. H. Shirihama, T. Suzuwa (1985) *Coll. & Polym. Sci.* 263, 141
15. W. Norde, F. Macritchie, G. Nowicka, J. Lyklema (1986) *J. Colloid Interface Sci.* 112(2), 447
16. P.G. Koutsoukos, C.A. Mumme-Young, W. Norde, J. Lyklema (1982) *Colloids Surfaces* 5, 93
17. J. Lyklema (1984) *Colloids Surfaces* 10, 33
18. W. Norde (1986) *Advan. Coll. Interf. Sci.* 25, 267
19. W. Norde, J.G.E.M. Fraaye, J. Lyklema (1987), ACS Symposium Series, accepted
20. B. H. Bijsterbosch, J. Lyklema (1965) *J. Colloid. Sci.* 20, 665
21. W. Norde, J. Lyklema (1978) *J. Colloid Interface Sci.* 66, 257
22. W. Norde, J. Lyklema (1978) *J. Colloid Interface Sci.* 66, 266
23. W. Norde, J. Lyklema (1978) *J. Colloid Interface Sci.* 66, 277
24. W. Norde, J. Lyklema (1978) *J. Colloid Interface Sci.* 66, 285
25. W. Norde, J. Lyklema (1978) *J. Colloid Interface Sci.* 66, 295
26. B. Ivarsson, I. Lundstrom (1985) *CRC Critical Reviews in Biocompatibility*

2, 1

27. E. F. Bowden, T. M. Hawkrige, H.N. Blount (1985) in "Comprehensive Treatise of Electrochemistry", vol. 10, Bioelectrochemistry, eds. S. Srinivasan, Y.A. Chiznadzhev, J.O'M. Bockris, B.E. Conway, E. Yeager, Plenum Press, New York, London
28. F. Scheller, M. Jünchen, H.-J. Prümke (1975) Biopolymers 14, 1553

### SUMMARY

The subject of this thesis is protein partition between an aqueous salt solution and a surface or an apolar liquid and the concomitant co-partition of small ions. The extent of co-partitioning determines the charge regulation in the protein partitioning process.

Chapters 2 and 3 deal with phenomenological relations between the partition coefficient of the protein and the extent of the co-partition. The method of analysis is illustrated by some worked-out examples, using data taken either from literature or from chapter 5. The examples include proton titration curves, ion exchange chromatography, adsorption on colloidal particles and solubilization in reverse micelles. An important conclusion is that the partition process is subject to a rule, similar to the principle of Le Chatelier for chemical equilibria: if upon protein partitioning ions are expelled into the water phase, an increase of the ionic concentrations results in a decrease of the protein partition coefficient and conversely.

A theory which allows for the prediction and molecular interpretation of the charge regulations is presented in chapter 4. The model describes the electrochemistry of a protein molecule through site binding of ions on a rigid surface. Although this is a considerably simplified picture of a real protein molecule, some aspects of the theory may be of general validity. One of them is the notion of the electrochemical adaptability of a charged colloidal particle, as measured by its intrinsic capacitance. In the case of a high intrinsic capacitance, a change in electrostatic interactions results in a large charge regulation whilst the surface potential remains almost constant. On the other hand, if the intrinsic capacitance is low, the particle resists externally imposed shifts in charge but does adapt its surface potential.

Chapter 5 contains an experimental study towards understanding the mechanism of charge-regulation in protein adsorption. The system consists of crystals of the insoluble salt silver iodide as the adsorbent and the protein Bovine Serum Albumin as the adsorbate. By using a combined iodide and proton titration technique, the charges of the surface and the protein can be measured independently. We find that a negative surface induces a positive shift in the charge of the adsorbed protein. Opposed to intuitive expectation, the reverse is not always true: when the charge of the protein charge is maximally positive, adsorption renders the silver iodide surface less negative.

The anomalous charge regulation is explained in terms of the intrinsic

capacitance of the adsorbed protein. The maximally positive protein cannot adapt its charge, and so the silver iodide surface is forced to adjust its charge completely to that of the protein. As the contact layer between adsorbed protein and the silver iodide crystal is electroneutral under almost all circumstances, the silver iodide surface must be as negative as the protein is positive. Hence, if the charge of the surface before adsorption is more negative than this value, adsorption of the protein is accompanied by a desorption of negative charge.

The experimental results are well understood in view of the developed phenomenological theory and model analysis. Two thermodynamic relations are successfully verified, indicating the internal consistency of the various experiments. Application of the model gives two independent estimates of the size of the adsorbed protein. It is concluded that the protein does not substantially modify its native structure upon adsorption.

### SAMENVATTING

In tal van biologische en kunstmatige processen speelt de verdeling van eiwit over twee macroscopische fasen een grote rol. Meestal bestaat één fase uit een waterige oplossing, de samenstelling van de tweede fase kan daarentegen zeer gevarieerd zijn. Bij de reversibele hechting van transporteiwitten aan bio-membranen bestaat de tweede fase bijvoorbeeld uit een flexibel aggregaat van kleine fosfolipiden. Maar ook macromoleculen kunnen als tweede fase fungeren, zoals bij de complexvorming tussen histoneiwit en polynucleïnezuur of de assemblage van virussen. Twee belangrijke toepassingen van twee-fase systemen treffen we aan in de biotechnologie: technieken om eiwitten te zuiveren zijn vaak gebaseerd op preferente adsorptie aan een rigide oppervlak, of preferente solubilisatie in een tweede, niet met water mengbare, vloeistof.

De wisselwerkingen van het eiwit met zijn omgeving in elk der twee fasen bepaalt de mate waarin de verdeling plaatsvindt. Als het eiwit bijvoorbeeld een apolair karakter heeft, zal het de neiging hebben de waterige oplossing te ontvluchten naar een minder hydrofiele tweede fase. Een ander type wisselwerking is gerelateerd aan de stijfheid in de eiwitstructuur. In de regel is het zo, dat eiwit een voorkeur heeft voor de fase waarin zijn structuur het meest wanordelijk is. Voor eiwitten met een labiele structuur kan deze factor dominant zijn, voor stabiele eiwitten is ze minder van belang.

In dit proefschrift wordt vooral aandacht besteed aan een derde belangrijke wisselwerking, namelijk de electrostatische. Kleine ionen dragen bij tot een zo gunstig mogelijke electrostatische wisselwerking tussen eiwit en omgeving. Aangezien de aard van de wisselwerking van fase tot fase verschilt zal er een ladingsregulering plaatsvinden waardoor verdeling van eiwit altijd samengaat met een herverdeling van kleine ionen.

In hoofdstukken 2 en 3 wordt thermodynamica gebruikt om uitdrukkingen af te leiden die kwantitatief het verband aangeven tussen de verdelingscoëfficiënten van het eiwit en de ionen. De analyse is geheel fenomenologisch; er worden geen of nauwelijks veronderstellingen gemaakt over de moleculaire eigenschappen van het systeem. Dit is geen gering voordeel omdat de gevonden relaties daarmee algemeen geldig zijn. De theorie wordt dan ook gebruikt om de gemeenschappelijke noemer in ogenschijnlijk zeer verschillende experimenten aan te tonen. Een belangrijke conclusie is dat de verdeling in veel gevallen onderworpen is aan een verschuivings wet zoals die door Le Chatelier

geformuleerd is voor scheikundige evenwichten.

Een nadeel van de fenomenologische theorie is haar gering voorspellend vermogen. In hoofdstuk 4 wordt een model analyse gepresenteerd waarmee dat in principe wel mogelijk is. In het model wordt een eiwitmolekuul voorgesteld als een rigide oppervlak, bedekt met zure en basische groepen. Dit is een aanzienlijke vereenvoudiging van de werkelijkheid, maar de theorie bezit toch een aantal waardevolle aspecten. Het blijkt dat de electrostatische wisselwerkingen geïnterpreteerd kunnen worden met zogenaamde intrinsieke capaciteiten. De intrinsieke capaciteit van een geladen colloïdaal deeltje is een maat voor haar electrochemisch aanpassingsvermogen. Verandering in omgeving resulteert bij een hoge waarde voor de intrinsieke capaciteit in grote ladings verschuivingen bij nagenoeg constante oppervlaktepotentiaal. Bij een lage waarde voor de intrinsieke capaciteit biedt het deeltje sterke weerstand tegen extern opgelegde veranderingen in haar lading en verschuift de oppervlakte potentiaal juist.

Een experimenteel onderzoek naar het mechanisme van de ladingsregulatie wordt beschreven in hoofdstuk 5. Het betreft de adsorptie van een runderbloed eiwit aan kleine kristalletjes van het onoplosbare zilverjodide zout. Met behulp van een gecombineerde zilverjodide en proton titratie kunnen tegelijk de lading van het geadsorbeerde eiwit en de oppervlaktelading van het zilverjodide worden bepaald. De resultaten laten zien dat naarmate het zilverjodide oppervlak negatiever wordt, de lading van het geadsorbeerde eiwit in positieve richting opschuift. Op haar beurt induceert een negatieve eiwitlading een positievere oppervlaktelading op het zilverjodide. Het omgekeerde is echter niet in alle gevallen waar: als het eiwit maximaal positief is stoot het zilverjodide oppervlak bij adsorptie juist negatieve lading uit, een onverwacht verschijnsel.

De anomale ladingsregulering wordt verklaard in termen van de intrinsieke capaciteit van het geadsorbeerde eiwit. Het maximaal positieve eiwit kan zijn lading maar moeilijk veranderen en heeft dus een lage intrinsieke capaciteit. Daardoor is het zilverjodide oppervlak gedwongen zijn lading volledig aan te passen aan die van het eiwit. Omdat het grensgebiedje tussen geadsorbeerd eiwit en zilverjodide oppervlak onder alle omstandigheden praktisch electroneutraal is, wordt het zilverjodide oppervlak dan even negatief als het eiwit positief is. Als nu de lading van het oppervlak vóór adsorptie negatiever is dan deze waarde gaat adsorptie van positief eiwit gepaard met desorptie van negatieve ionen.

De experimentele resultaten laten zich goed beschrijven met de fenomenologische theorie en de modelanalyse. Twee thermodynamische relaties kunnen met succes worden getoetst op hun geldigheid waardoor de interne consistentie van de verschillende experimenten bewezen is. Toepassing van het model levert twee schattingen voor de grootte van het geadsorbeerde eiwitmolekuul. Ondanks de vele benaderingen komen ze redelijk met elkaar overeen. Ze tonen aan dat het eiwit zijn structuur bij adsorptie grotendeels behoudt.

**LEVENSLLOOP**

Johannes Gerardus Elisabeth Maria Fraaije werd op 26 juni 1956 in Ammerzoden geboren. Na zijn middelbare schoolopleiding bezocht hij vanaf 1975 de Landbouwhogeschool te Wageningen. Het doctoraalexamen, met Fysische chemie en Moleculaire Fysica als hoofdvakken en Wiskunde als bijvak, werd in januari 1983 afgelegd. Van februari 1983 tot augustus 1987 was hij werkzaam bij de vakgroep Fysische en Kolloïdchemie van de Landbouwuniversiteit, tot februari 1987 in dienst van de organisatie voor Zuiver Wetenschappelijk Onderzoek, daarna voor de Landbouwuniversiteit. Vanaf 1 oktober 1987 werkt hij in tijdelijke dienst op de afdeling Physique de la Matière Condensée van het Collège de France te Parijs.

## DANKWOORD

Na ontelbare zweetdruppels, eindeloze depressies, gefrustreerde verwensingen en wanhopige worstelingen met onwillige apparatuur is eindelijk mijn proefschrift af. Wat mij nog rest is het schrijven van een dankwoord, een plicht die ik graag op me neem.

Beste Hans Lyklema, ik heb je in het laatste jaar leren kennen als een intelligent maar vooral ook integer mens. Ik realiseer me dat zonder jouw geestelijke duw-en trekstoten tijdens de eindsprint dit proefschrift er niet was gekomen.

Beste Willem Norde, door allerlei oorzaken hebben we niet veel samengewerkt in de afgelopen periode. Ik vind het jammer dat het zo gelopen is, ik weet dat jij dat ook vindt. Je bent bereid geweest verschillende versies van mijn proefschrift in status nascendi van kommentaar te voorzien, daarnaast heb je bijgedragen aan het oplossen van de nodige logistieke problemen, daarvoor mijn dank.

Beste gevoelige Thecla, volhouder Erik, koelbloedige Jan-Willem, snelle Roel, no-nonsens Erik-Jan, intelligente Marinette, jonge Jaap, vrolijke Frank, ik heb jullie als doctoraal studenten langer of korter onder mijn hoede gehad. De kwalificaties die ik jullie heb geven schieten natuurlijk tekort, maar ze zijn eerlijk en positief bedoeld. In mijn proefschrift komt jullie werk slechts tersluiks aan bod; het leek me beter jullie boeiende resultaten op een andere plaats in de de openbaarheid te brengen. Mijn grote dank voor alles wat ik van jullie heb geleerd.

Beste collega Eduard, jij hebt het wonderbaarlijke vermogen om een bedroefde schildknaap in een oogwenk te veranderen in een glanzende ridder. Ik herinner me de keren dat we diep in de nacht over de dijk dwaalden, en oeverloos discussieerden over de peilloze diepte van de vrouwelijke ziel. Ik herinner me ook nog een disco waar we het wel eens even zouden maken. Mooi niet dus. Affijn, misschien kunnen we het in een kroeg aan de Seine nog eens proberen.

Beste Frans, ik ken niemand met zo'n combinatie van flonkerende kraaloogjes en goedmoedige slimheid als jij. Als collega en overbuurman heb je mij ingewijd in de geheimen van de DEC en Simula. Ik hoop voor je dat je in de nabije toekomst het klavier van je mooie piano even goed leert bespelen als het toetsenbord van je terminal. Zet die dan maar uit: een terminal mag nóóit een eindstation zijn.

Beste Riet Hilhorst, Willem van Berkel (beide van Biochemie), Mathijs Dekker

(van Proceskunde), Jaap Visser en Harry Kester (beide van Erfelijkheidsleer), jullie zijn zo vriendelijk geweest om gegevens en/of apparatuur af te staan waarmee ik het verband tussen toegepaste en fundamentele wetenschap duidelijk kon maken. Er komt zeker nog een vervolg, "for the profit of us all, and for science".

En dan zijn er nog talloze mensen die hun technische of administratieve vaardigheden hebben aangewend om mijn onderzoek te voorspoedigen. Maarten Bakkenes zag kans om naast zijn drukke onderwijstaak de lastige uitwisselings-experimenten met enthousiasme uit te voeren. Anton Korteweg heeft in zeer korte tijd maar met grote precisie de adsorptie-isothermen opgemeten. Hennie van Beek ("Nou, vooruit dan maar") en Louis Verhagen hebben mijn snel wisselende ideeën zonder mankeren gestalte gegeven in de meest vreemde constructies. Ronald Wegh en Rob Vullings zorgden voor de onontbeerlijke elektronische schakels tussen de natte pot en het droge papier. Ben Spee en Willem van Maanen regelden nauwgezet de immer aanzwellende stroom van glaswerk en chemicaliën. Bert Bouwman was altijd bereid om mij de nukken van de tekstverwerker uit te leggen. Hij speelde ook op meer dan één manier de goedheiligman door zonder tegen te sputteren mijn voorraad potloden, pennen, archiefmappen etc., etc., aan te vullen. José Zeevat heeft met groot plichtsbesef in haar vakantie het schamele engels van de tekst verbeterd, de nog resterende fouten zijn natuurlijk voor mijn rekening. Wil Kleijne heeft niet rechtstreeks meegewerkt aan de totstandkoming van mijn proefschrift, maar onze con fuoco beleefde avondjes met drank, kaas en muziek vormden uiterst plezierige intermezzi. De artistieke gaven van Gerrit Buurman en Anneke Hoekstra komen tot uiting in de figuren en schemas.

Beste Martin Cohen Stuart, Ben Bonekamp en Jos Keurentjes, onze gezamenlijke avonturen met de platvis hebben mij ervan doordrongen dat een wetenschappelijk teamverband pas percoleert als de overlap tussen de individuele gedachten een kritische drempelwaarde overschrijdt. Dat besef hoop ik nog lange tijd met me mee te dragen.

In de laatste fase van mijn onderzoek heb ik getracht het gedrag van optisch transparante elektroden te doorgronden. De benodigde spectroscopische apparatuur werd met naastenliefde ter beschikking gesteld door de vakgroep Moleculaire Fysica. Hoewel de eerste resultaten bemoedigend waren, bleek al gauw dat de zaak veel ingewikkelder in elkaar zat dan ik eerst dacht. Niettemin mijn dank aan Prof. Schaafsma, Arie van Hoek en Jaap Krüse voor de getoonde interesse.